

**GEOMORPHOLOGY OF THE NORTHEAST PLANNING AREA,  
NATIONAL PETROLEUM RESERVE—ALASKA, 2002**

FINAL REPORT

Prepared for

**ConocoPhillips Alaska, Inc.**  
P.O. Box 100360  
Anchorage, AK 99510

And

**Anadarko Petroleum Corporation**  
3201 C Street, Suite 603  
Anchorage, AK 99503

Prepared by

M. Torre Jorgenson,  
Erik. R. Pullman,

**ABR, Inc.—Environmental Research & Services**  
PO Box 80410  
Fairbanks, AK 99708

and

Yuri L. Shur

**Dept. of Civil Engineering**  
University of Alaska  
PO Box 755900  
Fairbanks, AK 99775

April 2003



*Printed on recycled paper.*

## EXECUTIVE SUMMARY

Permafrost development on the Arctic Coastal Plain in northern Alaska greatly affects the distribution of ground ice, engineering properties of the soil, ecological conditions at the ground surface, lake-basin development, and response of the terrain to human activities. Of particular interest for assessing potential impacts from oil development in the National Petroleum Reserve-Alaska (NPROA) are the identification of terrain relationships for predicting the nature and distribution of ground ice across the landscape and the evaluation of disturbance effects on permafrost. Accordingly, this study was designed to determine the nature and abundance of ground ice at multiple spatial scales to develop terrain relationships for predicting ice distribution, to assess the rates of landscape change and develop a conceptual model of how ground ice changes during the evolution of the landscape, and to estimate the amount of thaw settlement likely to occur after disturbance. The study focuses primarily on permafrost dynamics associated with lake-basin development because lacustrine processes, as opposed to eolian, fluvial or marine processes, are currently the dominant geomorphic processes in the study area.

### NATURE AND DISTRIBUTION OF GROUND ICE

Classification of materials near the ground surface (<3 m) was done at multiple spatial scales, and included ice structures (microstructures caused by ice segregation), lithofacies (textural-structural assemblages in a stratigraphic profile), and terrain units (depositional and morphological units across the landscape). Eight primary ice structures were identified, including pore, lenticular, vein, layered, reticulate, ataxitic, organic-matrix, and solid ice. Soil materials were classified into 12 lithofacies, the most common of which included: (1) massive organics in the active layer of all terrain types except eolian inactive sand, (2) massive turbated fines with organics just below the active layer, and (3) gravelly massive turbated fines found at 1–3 meters depth at most coring locations. A total of 25 terrestrial terrain units and 9 waterbodies classes were identified, including one colluvial, two eolian, 11 fluvial, seven lacustrine, and two alluvial-marine, and two marine deposits.

When comparing relationships among ice structures, lithofacies, and terrain units using data from 31 cores (2–3 m), there were strong relationships that can be used to partition the variability in distribution of ice across the landscape. Large differences were found in the frequency of occurrence of the various ice structures among lithofacies: pore ice was nearly always associated with massive, inclined, and layered sands; lenticular and ataxitic ice were most frequently associated with massive and layered fines, organic matrix ice was usually found in massive and layered organics and limnic fines. Reticulate ice was broadly distributed among fine and organic lithofacies.

Important differences were observed in the volume of segregated ice among ice structures, lithofacies, and surface terrain units. Among ice structures, mean ice volumes determined from laboratory analysis were highest for layered ice (77%) and organic-matrix ice (73%), intermediate for reticulate ice (71%), ataxitic ice (70%), and veined ice (69%), and lowest for lenticular ice (59%) and pore ice (45%). Among lithofacies, the mean volume of segregated ice was highest in massive organics (78%), intermediate in fines with organics (72%) and layered organics (68%), and lowest in massive sands (43%), layered fines (43%), and layered sands (40%). Among terrain units, mean ice volumes were highest in alluvial-marine deposits (71%) and ice-rich thaw basin centers (66%), intermediate in ice-rich thaw basin margins (62%) and ice-poor thaw basin centers (59%), and lowest in ice-poor thaw basin margins (48%) and eolian inactive sand (45%).

### LANDSCAPE CHANGE

Photogrammetric analysis of waterbody changes in three small study regions was used to evaluate shoreline erosion from 1945–1955 to 2001. Overall, 0.74% of the total land area was lost to shoreline erosion during the period (46–56 yr) for which data were available. The average annual erosion rate for the three study areas was 0.04% of the total land area. Average rates of shoreline retreat were very slow (0.02 m/yr), even for large, deep lakes (0.08 m/yr). The maximum observed rate of shoreline retreat was 0.8 m/yr. Deep lakes (mean 26.1% of area) were much more prevalent

than shallow lakes (mean 6.6%), and shallow lakes typically are small (<5 ha).

Recent degradation of ice wedges was evident from both field observations and photogrammetric analysis. Field observations at nine polygonal troughs found indicators (e.g. water in pits, drowned tussocks) that indicate the degradation has been recent, although coring indicated that degradation did not occur in 2001. Photogrammetric analysis of waterbody characteristics found the extent of flooding in upland areas was 1.7% in 1945 only, 4.3% in 2001 only, and 0.1% in both years. In lowland areas, flooding covered 16.2% of the area in 1945 only, 3.5% in 2001 only, and 2.7% in both years. Overall, flooding covered 13.7% of the terrestrial area (larger waterbodies excluded) in 1945 only, 3.8% in 2001 only, and 2.2% in both years. We attributed the increase in newly flooded areas (3.8%) in 2001 (a dry year) not present in 1945 (wet year) to be the result of thermokarst. The low percent of areas flooded in both years indicates the thermokarst has caused a redistribution of water from round flooded polygon centers to linear degrading troughs.

Our examination of the development of lake basins, based on topographic profiles, soil and ground ice surveys, stratigraphic analysis, radiocarbon dating, photogrammetric analysis, and regional comparisons, revealed that lake evolution on the coastal plain was much more complex and less cyclic than suggested by previous investigations. Our revised conceptual model for the portion of the Arctic Coastal Plain underlain by extensive sand sheets includes (1) initial flooding of primary lakes, (2) lateral expansion and sorting and redistribution of lacustrine sediments, (3) lake drainage, (4) differential ice aggradation in silty centers and sandy margins (5) formation of secondary thaw lakes and infilling ponds, and (6) basin stabilization.

## **THERMOKARST POTENTIAL AND TERRAIN SENSITIVITY**

We developed estimates of potential thaw settlement following disturbance in various terrain units, based on (1) volumes of excess segregated ice, (2) volumes of wedge ice, and (3) the equilibrium active layer depth following surface

disturbance (active-layer readjustment). Based on an active-layer readjustment to 0.8 m, which is typical of non-flooded highly disturbed surfaces, mean ( $\pm$  SD) thaw settlement is calculated to be  $0.51 \pm 0.40$  m in alluvial-marine deposits,  $0.27 \pm 0.29$  m in ice-rich thaw basins centers,  $0.19 \pm 0.23$  m in ice-rich thaw basin margins,  $0.22$  m in ice-poor thaw basin centers,  $0.04 \pm 0.05$  m in ice-poor thaw basin margins, and  $0.10 \pm 0.07$  m in eolian inactive sand. Based on data from the literature and our field observations, we estimated that all wedge ice in the top 2 m would be lost, leaving a highly polygonized surface. The expected loss of volume due to thawing of ice wedges is about 20% for old alluvial-marine deposits, 15% for ice-rich thaw basins with well-developed, low-centered polygons, and negligible for ice-poor thaw basins.

Based on the differences in the potential for thaw settlement among terrain units, we developed a conceptual model of terrain responses to severe disturbances associated with scraping of the surface or complete removal of the vegetative cover. For example, on alluvial-marine deposits where the volumes of segregated ice and wedge ice near the surface are high, thermokarst will create highly irregular micro-topography with deep and shallow troughs, and prominent high-centered polygons above the water-filled troughs. In contrast, in ice-poor thaw basins, where segregated ice volumes are much lower and wedge ice is negligible, thermokarst will create uniform, very shallow ponds as the surface settles below the water table.

## TABLE OF CONTENTS

Executive Summary .....	i
List of Figures.....	iii
List of Tables .....	v
Acknowledgments .....	v
Introduction.....	1
Methods .....	2
Nature and Distribution of Ground Ice .....	2
Field Surveys .....	2
Classification and Mapping .....	4
Landscape Change .....	5
Lakeshore Erosion .....	5
Ice Wedge Degradation .....	5
Thaw Settlement and Terrain Sensitivity.....	6
Results and Discussion .....	7
Nature and Abundance of Ground Ice .....	7
Classification and Mapping .....	7
Soil Properties.....	16
Landscape Change .....	32
Lakeshore Erosion .....	32
Ice Wedge Degradation .....	37
Conceptual Model of the Evolution of Lakes and Drained Basins.....	46
Thaw Settlement and Terrain Sensitivity.....	57
Thaw Settlement .....	57
Conceptual Model of Thermokarst Development .....	59
Implications for Land Management.....	61
Conclusions.....	62
Literature Cited.....	63

## LIST OF FIGURES

Figure 1. Soil sampling locations in the Northeast Planning Area, NPRA, 2002.....	3
Figure 2. Composite core profiles illustrating stratigraphy and ice structures associated with the four dominant terrain units in the Northeast Planning Area, NPRA, 2002.....	9
Figure 3. Photographs of simple ice structures found in permafrost in the Northeast Planning Area, NPRA, 2002.....	12
Figure 4. Aerial photographs of dominant terrain units on the coastal plain in the Northeast Planning Area, NPRA, 2002.....	17
Figure 5. Distribution of terrain units in the Northeast Planning Area, NPRA, 2002 .....	19
Figure 6. Soil stratigraphy along a terrain sequence in the eastern portion of the Northeast Planning Area, NPRA, 2002 .....	21
Figure 7. Soil stratigraphy along a terrain sequence in the central portion of the Northeast Planning Area, NPRA, 2002 .....	22
Figure 8. Soil stratigraphy along a terrain sequence in the western portion of the Northeast Planning Area, NPRA, 2002.....	23

Figure 9.	Frequency of occurrence of ice structures by lithofacies and by surface terrain unit for profiles in the Northeast Planning Area, NPRA, 2002.....	24
Figure 10.	Frequency of occurrence of lithofacies by surface terrain unit for profiles in the Northeast Planning Area, NPRA, 2002.....	25
Figure 11.	Particle-size characteristics of dominant lithofacies, thickness of surface organics and cumulative organics by surface terrain unit, and thaw depths within the soil profiles, Northeast Planning Area, NPRA, 2002 .....	26
Figure 12.	Depth profiles of electrical conductivity and pH by surface terrain unit, Northeast Planning Area, NPRA, 2002.....	28
Figure 13.	Depth profiles of % carbon and carbon density by surface terrain unit, Northeast Planning Area, NPRA, 2002 .....	29
Figure 14.	Mean carbon stocks by surface terrain unit, Northeast Planning Area, NPRA, 2002 .....	30
Figure 15.	Mean volumetric ice contents grouped by primary ice structure, lithofacies, and surface terrain unit, Northeast Planning Area, NPRA, 2002 .....	31
Figure 16.	Depth profiles of volumetric ice and dry density by surface terrain unit, Northeast Planning Area, NPRA, 2002.....	33
Figure 17.	Mean accretion rates of surface materials by surface terrain unit, Northeast Planning Area, NPRA, 2002.....	34
Figure 18.	Map of changes in lake shorelines from 1948 to 2001, Northeast Planning Area, NPRA, 2002 .....	35
Figure 19.	Waterbody characteristics of eroding lakes in the Northeast Planning Area, NPRA, 2002...	36
Figure 20.	Views of ice wedges at bank exposures illustrating the thin layer of organic and mineral material over massive ice, and sediment deformation between ice wedges, Northeast Planning Area, NPRA, 2002.....	38
Figure 21.	Oblique aerial views and ground views at two sites illustrating degradation of ice wedges .....	39
Figure 22.	Changes in flooded areas in the west change study region 1945 and 2001 used to differentiate areas of thermokarst, Northeast Planning Area, NPRA, 2002.....	41
Figure 23.	Changes in flooded areas in the central change study region between 1945 and 2001 used to differentiate areas of thermokarst, Northeast Planning Area, NPRA, 2002.....	42
Figure 24.	Aerial photographs from 1945 and 200, maps of waterbodies classified by spectral classification, and a map of waterbody change for uplands in the west study region, Northeast Planning Area, NPRA, 2002 .....	43
Figure 25.	Aerial photographs from 1945 and 200, maps of waterbodies classified by spectral classification, and a map of waterbody change for lowlands in the central study region, Northeast Planning Area, NPRA, 2002 .....	44
Figure 26.	Summary of changes in flooded areas by terrain unit grouped by upland and lowland terrain unit, for the central and western map areas, Northeast Planning Area, NPRA, 2002 .....	45
Figure 27.	Mean annual air temperatures for Barrow Alaska, 1921–2002.....	47
Figure 28.	A conceptual model of lake-basin development on the Arctic Coastal Plain in the Northeast Planning Area, NPRA, 2002 .....	49
Figure 29.	Estimates of mean excess segregated ice volume and potential thaw settlement due to melting of segregated ice in each of six terrain units in the Northeast Planning Area, NPRA, 2002.....	58

Figure 30. Conceptual model of thermokarst development after disturbance of ice-rich permafrost on the dominant terrain units in the Northeast Planning Area, NPRA, 2002..... 60

**LIST OF TABLES**

Table 1. Classification and description of lithofacies observed in the Northeast Planning Area, NPRA, 2002..... 8

Table 2. Classification and description of ground ice observed in the Northeast Planning Area, NPRA, 2002..... 11

Table 3. Classification and description of terrain units observed in the Northeast Planning Area, NPRA, 2002..... 13

**ACKNOWLEDGMENTS**

This study was funded by ConocoPhillips Alaska, Inc., and managed by Caryn Rea, Environmental Studies Coordinator. We also would like to acknowledge the assistance of Dave Swanson, who helped in the field in 2001 and provided insightful discussions on soil processes, and J. J. Frost and Luke McDonough, who helped with the coring. Betty Anderson provided a technical review.



## INTRODUCTION

Permafrost development on the Arctic Coastal Plain in northern Alaska greatly affects the ecological conditions at the ground surface (Billings and Peterson 1980, Webber et al. 1980, Walker 1981), the engineering properties of the soil (Johnson 1981, Kreig and Reger 1982, McFadden and Bennet 1991), and the response of the terrain to human activities (Brown and Grave 1979, Webber and Ives 1978, Lawson 1986). Of particular interest for assessing potential impacts from oil development in the National Petroleum Reserve-Alaska (NPRA) are the identification of terrain relationships for predicting the nature and distribution of ground ice across the landscape, and the evaluation of how permafrost will respond to disturbance. Accordingly, this study was designed to (1) determine the nature and abundance of ground ice at multiple spatial scales to develop terrain relationships for predicting ice distribution, (2) assess the rates of landscape change, (3) develop a conceptual model of how ground ice changes affects the evolution of landscape, and (4) estimate the amount of thaw settlement likely to occur after disturbance as a measure of terrain sensitivity. The study focuses on permafrost modification associated with lake-basin development on the coastal plain portion of the NPRA Development Project Area because lacustrine processes, as opposed to fluvial or marine processes, are the dominant geomorphic processes in the study area.

While there is widespread recognition that the soils of the Arctic Coastal Plain have high ice contents, little information is available on the nature, distribution, and dynamics of ground ice. Kreig and Reger (1982) provided a comprehensive analysis of relationships between landforms and soil properties, but their data do not allow the prediction of ice distribution across the coastal plain. At Barrow, the volume of segregated ice in the surface soils often approached 80% (Brown 1968) and overall ice contents associated with segregated ice averaged 62% (Hinkel et al. 1996), but the relationships of ice contents to terrain characteristics were not examined. On the Mackenzie River Delta, pore and segregated ice constituted 80% and wedge ice 12–16% of total ice volume (Pollard and French 1980), and the

structure of the ice has been well documented (Murton and French 1994). Analyses of the nature and distribution of ground ice on the Colville River Delta showed that ice content was strongly related to ice structure, soil texture, and terrain unit (Jorgenson et al. 1997, Jorgenson and Shur 1998, Jorgenson et al. 1998). The mean total volume of segregated ice for the most ice-rich terrain unit, abandoned floodplains, was 79%. In a similar study of ground ice patterns and thermokarst potential in the Prudhoe Bay and Kuparuk oilfields, the mean volume of segregated ice in alluvial plain deposits was 76% (Burgess et al. 1998). The present study contributes to this growing body of information by quantifying differences in the structure and abundance of ground ice among terrain units on the coastal plain.

One of the most striking features of the Arctic Coastal Plain is the abundance, and recurring oriented pattern, of the lakes and drained basins. The abundance of lakes and drained basins has been attributed to a cycle of repeated thermokarst, lake drainage, and regeneration of ice-rich permafrost (Britton 1957, Tedrow 1969, Billings and Peterson 1980). Everett (1980) conceptualized six stages of thaw-lake development that included (1) original ice-rich elevated conditions, (2) initial thermokarst development along ice wedges, (3) coalescence into small ponds, (4) enlargement into large deep lakes, (5) complete or partial drainage resulting in flat basins, and (6) aggradation of ice, primarily through development of ice wedge polygons. In this study, we re-examine and revise this conceptual model by determining rates of thaw-lake enlargement, evaluating ice content at different stages of the cycle, and defining the process of ice aggradation in the final stages of the process.

While naturally occurring thermokarst is fundamental to ecological processes on the thaw-lake plains of the arctic lowlands (Britton 1957, Billings and Peterson 1980, Walker et al. 1980, Carter et al. 1987), human-induced thermokarst is a concern for land development in the Arctic because of the subsequent changes in hydrology, soils, and vegetation (Brown and Grave 1979, Jorgenson 1986, Lawson 1986, Walker et al. 1987). Of specific concern for oil development is the possibility of thermokarst as a result of off-road and seismic trail disturbances (Walker et al. 1987,

Emers and Jorgenson 1997), alteration of drainage patterns following road development, road dust, oil spill cleanups (Jorgenson et al. 1991, Jorgenson et al. 1992), closeout and rehabilitation of reserve pits (Burgess et al. 1999), and gravel removal after site abandonment (Jorgenson and Kidd 1991, Kidd et al. 1997). Thus, to develop land rehabilitation strategies that are site-specific and appropriate to the rapidly changing environmental conditions associated with thermokarst, it is essential to understand the nature and abundance of ground ice across the oilfields, and to relate ice characteristics to terrain characteristics at a level useful for land management. This study contributes to a better understanding of how to manage human activities on permafrost terrain by providing estimates of potential thaw settlement for the dominant terrain units and by outlining a conceptual model of terrain responses to disturbance.

To provide a framework for sampling and analyzing the spatial variability of ground ice across the landscape, and to identify the geographic scales most useful for interpretation and management, we used a hierarchical approach that incorporated regional, landscape, and local ecosystem scales. At the regional level, we used ecodistricts and ecosubdistricts (associations of terrain units and geomorphic processes) developed by Jorgenson et al. (1997) as the basis for allocating our sampling effort. At the landscape scale, we used terrain units (depositional units related to a specific geomorphic process) to stratify our sampling and as the basis for analysis. At the local ecosystem level (areas with relatively uniform soil stratigraphy and vegetation), we classified our samples (soil cores) by micro-scale characteristics such as ice structures and lithofacies (texture and structure) for use in analysis.

Specific objectives of this study were to:

1. determine the nature and abundance of ground ice at multiple spatial scales, in order to correlate terrain units with associated ice characteristics,
2. quantify the rates of landscape change (shoreline erosion and ice wedge degradation) and develop a conceptual model of the patterns and processes involved in lake basin development and;
3. estimate the potential thaw settlement of

the various terrain units and develop a conceptual model of thermokarst development after disturbance.

## **METHODS**

### **NATURE AND DISTRIBUTION OF GROUND ICE**

#### **FIELD SURVEYS**

Field surveys were conducted during 3–15 August 2001 and 1–16 August 2002. Data on soil stratigraphy were collected along transects (toposequences) within each of three predominant surficial geology deposits in the Northeast Planning Area, NPRA (Carter and Galloway 1985): alluvial-marine, alluvial terrace, and eolian inactive sand. Along each transect, 3–5 soil cores were collected (31 cores total) in terrain units that covered the entire gradient of landscape development from young thaw basins to the oldest and highest surfaces (Figure 1). The stratigraphy of the near-surface soil (i.e., the active layer) was described from soil pits to assess the depth of thaw, surface organic thickness, and mineral characteristics. For sampling frozen soils below the active layer, a 3-in.-diameter SIPRE corer with a portable power head was used to obtain 1–2.7 m cores. Seven profiles (three in 2001 and four in 2002) also were described from bank exposures after unfrozen material was removed with a shovel to expose undisturbed frozen sediments. Descriptions for each profile included the texture of each horizon, the depth of organic matter, depth of thaw, and visible ice volume and structure. In the field, soil texture was classified according to the Soil Conservation Service system (SSDS 1993).

Soil samples were taken every 20–30 cm from 31 core sections and 3 exposures, within soil horizon boundaries (total of 285 samples). Samples were analyzed for volumetric and gravimetric water content, electrical conductivity, and pH. Soil volume was determined by measuring core sample length at three points and the circumference of the core. EC was measured using an Orion model 290 EC meter and pH was determined using an Orion model 290 pH meter. Additional analyses for particle size and total carbon were performed on a

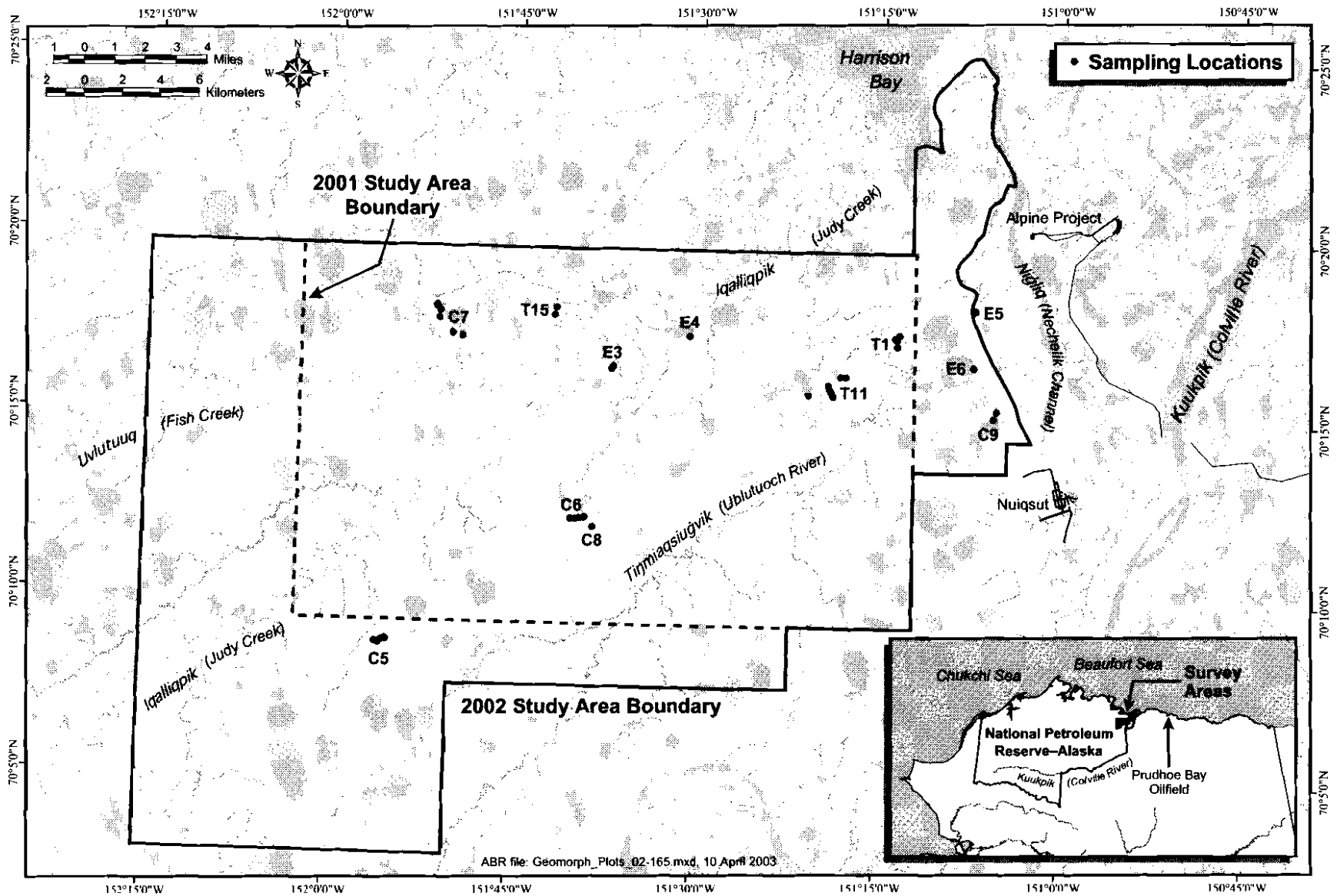


Figure 1. Soil sampling locations in the Northeast Planning Area, NPRA, 2002.

subset of soil samples by the Palmer Research Station Soils Laboratory (Palmer, AK).

To establish minimum ages for the older stratigraphic terrain units, one sample of basal organic material (sedge peat) was collected from each of six cores in 2001 and from active layer and basal material on four cores in 2002. Laboratory analyses were performed by Beta Analytic, Inc. (Coral Gables, FL). Dates in this report are presented as calibrated calendar ages, years before present (BP) (1950) and include the range associated with the 2 sigma error (Stuiver et al. 1998).

Total carbon stocks ( $\text{kg/m}^2$ ) were calculated for each core within the six terrain types sampled in this study. Carbon stocks for each core were derived by computing a carbon mass for each stratigraphic section within each core. Carbon mass was calculated using one of four methods, listing in descending order of precision: (1) direct measurements of both % carbon and dry soil density, (2) direct measurement of % carbon and dry density derived from a regression of dry density and soil carbon, (3) an estimate of % carbon based on lithofacies and direct measure of dry density, or (4) an estimate of both % carbon and dry density based on lithofacies. Total carbon stock means  $\pm$  SD were calculated for both the top one-meter and top two-meter intervals with each of six terrain units.

#### CLASSIFICATION AND MAPPING

The micro-scale soil textures and structures described from the field profiles were grouped into lithofacies (distinctive suites of sedimentary structures related to a particular depositional environment), and cryostructures (repeating patterns of ice distribution). Lithofacies and cryostructures of the cores described in the field were reviewed for consistency in the office using field descriptions and photographs of cores. Lithofacies were classified according to systems of facies analysis for fluvial deposits developed by Miall (1978, 1985) and Brierley (1991). We added several new classes to these systems to incorporate features specific to the permafrost environment. Ice structure (form, distribution, and volume of ice) was classified in the field in 2001 following a version of the system developed by Murton and French (1994), modified to better differentiate the

structures that we observed (Jorgenson et al. 1997). This classification system was developed during similar work in the Colville River Delta and Kuparuk Oilfield during 1995–1998.

During classification, primary ice structures were further subdivided by secondary characteristics, such as shape and size. Frequently, ice structures occurred in assemblages in which the individual structures were too small to differentiate; these were classified as composite structures. In total, 52 structures and composite structures were identified in the field. This number was too large for practical application, so we aggregated classes through a two-step process. First, we aggregated the non-composite structures into eight simple, primary structure types. Second, the composite types were grouped according to the most complex ice type (in descending order of complexity: solid > ataxitic > reticulate > vein > layered > lenticular > organic-matrix > pore) present in the composite structure. For example, a composite structure that contained ataxitic, reticulate, and layered ice was grouped with the ataxitic structure type. Vertical trending ice structures (vein, reticulate, ataxitic) were considered to be more advanced or complex than horizontal structures (pore, lenticular, layered).

The terrain-unit classification system that we used was adapted from the systems developed by Kreig and Reger (1982) and the Alaska Division of Geological and Geophysical Surveys for their engineering-geology mapping scheme. We modified the system to incorporate the surficial geology units mapped for the area by Carter and Galloway (1985). Because this study focused on permafrost development associated with lacustrine processes, the analysis was restricted to the following units: (1) alluvial-marine terrace, (2) alluvial terrace, (3) eolian inactive sand, (4) ice-rich thaw basin centers, (5) ice-rich thaw basin margins, and (6) ice-poor thaw basins. Alluvial-marine and alluvial terraces were combined for analysis, due to small sample sizes.

Terrain units were mapped by photo-interpretation of true color photography (1:14,000 scale), and by digitizing the units on-screen over a georectified orthophoto mosaic produced by AeroMap, Inc., Anchorage, AK.

## LANDSCAPE CHANGE

### LAKESHORE EROSION

In 2001, an analysis of change was performed for three small areas within the larger study area, to assess rates of shoreline erosion resulting from lacustrine processes. The three areas (1450 ha each) were selected to include three main terrain units (alluvial-marine terrace, alluvial terrace, and eolian inactive sands) (Figure 1). Aerial photographs from 1945 (NARL series, 1:45,000 scale) and from 1955 (USGS, 1:50,000 scale) were controlled to the 2001 orthophoto mosaic using stable features (e.g., polygon intersections, stable lake peninsulas) common to both the old and recent photography. Error assessments then were performed on the co-registered photos to determine the minimum size of change that could be recorded accurately. Five stable tundra features (polygonized tundra intersections) were selected (four on the area perimeter and one in the center) for each study area. The mean distance between the features on the two dates of photography was used to calculate a mean ( $\pm$  SD) positional error for each study area.

Lake shorelines then were digitized on the 1945 or 1955 controlled photos and compared with shorelines delineated from the 2001 orthophoto mosaic. Lakes were classified as deep ( $\geq 1.5$  m, no bottom features evident,) or shallow ( $< 1.5$  m, bottom features evident). This depth corresponds to the critical depth that allows a thaw bulb (talik) to develop beneath the lake. The extent of change was determined by superimposing the two lake shore layers and classifying the resulting features. Any area that was delineated within a waterbody on the 2001 photos but not on earlier photography was defined as eroded. The sum of the eroded areas was used to calculate the percent of the total area lost to erosion. Perimeter-weighted mean erosion rates were calculated for three lake classes: shallow lakes, deep lakes  $< 20$  ha, and deep lakes  $> 20$  ha. An overall average rate of lateral erosion was calculated by averaging all erosion rates, weighted by the perimeter of each lake.

### ICE WEDGE DEGRADATION

In 2002, an analysis of ice wedge degradation was performed in two of the three small study areas (central and west, 1450 ha each) defined in 2001.

The eastern study area (analyzed in the 2001 report) was not included in the 2002 analysis because the resolution of the 1955 photography was not sufficient for resolving small waterbodies (pits and polygon troughs) that were the subject of this study. Aerial photographs from 4 July 1945 (NARL series, 1:45,000 scale black and white) were georeferenced to the 14–15 July 2001 orthophoto mosaic using stable features (polygonized tundra intersections, stable lake peninsulas) common to both the old and recent photography. The ecological land survey (ELS) map was used to exclude non-terrestrial areas (lakes and streams) from the analysis.

Inundated tundra areas were determined using image-processing techniques to identify areas of “deep” ( $> 30$  cm) water that were typical of the thermokarst pits observed in the field. All image analysis was performed with Imagine 8.2 (ERDAS, Inc.). For the 1945 photography, the controlled digital image was balanced to account for systematic illumination variation across the photo. Water was differentiated by choosing the grayscale value that most commonly depicts the transition from wedge sedge meadow tundra (water  $< 10$  cm deep) to deeper water areas. All grayscale values in the digital image below this number were coded to 1, while all remaining areas were coded to 0. Threshold values for each image were chosen by examining the extent of water in all terrain types, but preference was given for a threshold value that most accurately delineated water bodies on Alluvial-marine Terrace and Eolian inactive sand deposits. In establishing a threshold, we intended to be conservative to bias toward differentiating deeper water to avoid including very shallow water on wet tundra.

Because the 2001 digital image consists of three separate bands (true-color image), waterbodies in terrestrial areas were identified using a two-step classification procedure. First, an unsupervised classification was done on the study area sections and each pixel was assigned up to five ranked classes. Second, a fuzzy classification was run to determine the pixel’s most likely class based on surrounding pixel values. The resulting set of classes then was evaluated manually to determine which classes represented deep water areas. For both years, water coverage was calculated for each terrain/surface form

combination by summing the pixel areas within each ELS region.

The classified images from both years were used to create a four-class image of each landscape change study region. Each pixel was classified as one of four types: unflooded (not flooded in 1945 or 2001), flooded in 1945, flooded in 2001, or flooded in both 1945 and 2001. Inundated areas were summarized by upland (well-drained) and lowland (poorly drained) areas by grouping surface form designations within terrain types. For example, within Alluvial-marine deposits, upland areas were defined as areas with high-centered, high-relief polygons (Phh) and areas of mixed thaw pits and polygons (Tm). These surface forms represent ice-rich areas where lacustrine processes or other disturbances have been absent for extended periods of time. The ice-rich nature of sediments and predominance of ice wedges make these areas the most sensitive to thermokarst. Areas of high-centered, low-relief polygons (Phl) also are common in swales in upland areas, but frequently are interspersed with low-centered polygons and wetter micro-sites. For the analysis, this surface form was grouped with lowland types.

**THAW SETTLEMENT AND TERRAIN SENSITIVITY**

Potential thaw settlement was estimated from the summation of thaw strain (defined as the decrease in volume a frozen soil sample undergoes when thawed) for individual soil horizons and the potential change in the active layer thickness caused by surface disturbance. Thaw strain is similar in concept to excess ice, which is that portion of the ice that exceeds the pore volume that the soil would have under natural unfrozen conditions. The additional potential surface subsidence due to thawing of wedge ice is computed independently (see below). Thaw strain was determined for each of the sampled terrain types (alluvial-marine and alluvial terrace combined, thaw basin, ice-poor margins, thaw basin, ice-rich margins, and ice-rich thaw basin centers).

When possible, thaw strain (% volume) for each permafrost sample was calculated with Crory's (1973) formula:

$$V_s = [(\gamma_{dt} - \gamma_{df}) / \gamma_{dt}] \times 100$$

where:

$V_s$  = Thaw strain (%)

$\gamma_{df}$  = Dry unit weight of initial frozen condition (g/cm<sup>3</sup>)

$\gamma_{dt}$  = Dry unit weight of thawed soil (g/cm<sup>3</sup>), based on mean for lithofacies

The use of this formula requires a dry unit weight (density) value for active layer material measured from each sampled lithofacies. Because many of the lithofacies we encountered were unique to the permafrost zone (due to cryoturbation of organic and mineral materials), the required dry density values could not be derived from measurements of active layer samples. The relative proportion of organic matter in a sample was found to be more important in determining dry density than particle size composition or texture of active layer samples. Therefore, we developed a regression equation relating dry density to total carbon (%) ( $n = 45, R^2 = 0.82$ ):

$$\gamma_{dt} = -0.4323 \ln(C) + 1.7101$$

where:

$\gamma_{dt}$  = Dry unit weight of thawed soil (g/cm<sup>3</sup>)

C = % total carbon

Thaw strain (synonymous with excess ice) then was calculated for the samples that were analyzed for percent total carbon. For permafrost samples, the dry density of the unfrozen soil was calculated from the regression and used to determine thaw strain. For permafrost samples with no determination of percent total carbon, percent thaw strain was determined from the regression of thaw strain to volumetric ice ( $n = 87, R^2 = 0.70$ ). This approach assumes that during consolidation of soil after thawing the dry density is close to that typically found in the active layer.

In previous investigations in the Colville River Delta (Jorgenson et al. 1997) and Kuparuk

and Prudhoe Bay oilfields (Burgess et al. 1999), visual estimates of excess ice content was well correlated with volumetric measures of excess ice. However, the correlation was poor for the NPRA data, presumably due to the high proportion of organic material in many of the cores. To estimate thaw settlement for each soil horizon, we assigned values from sampled sections to adjacent horizons based on similarity of lithofacies and visual ice content. The potential settlement (change in height) for each core was calculated by:

$$\Delta H = [(A_d - A_o) \times V_s] / (1 - V_s)$$

where:

$A_d$  = Equilibrium thaw depth of disturbed tundra

$A_o$  = Equilibrium thaw depth of background tundra

$V_s$  = Thaw strain (fraction),

Mean potential thaw settlement ( $\pm$  SD) for each terrain unit was calculated by averaging the  $V_s$  values determined for each core.

## RESULTS AND DISCUSSION

In presenting and discussing our results, we focus on the patterns of occurrence and processes in permafrost development that are responsible for the evolution of the landscape. First, we classify the types of ground ice and soil materials that occur in near-surface sediments at multiple spatial scales (lithofacies, ice structures, and surface terrain unit), and illustrate how these patterns are interrelated across representative toposequences. The classification of lithofacies and terrain units emphasizes differences in materials that are related to lacustrine, eolian, and marine deposits, and to permafrost aggradation and degradation. We evaluate these classes by comparing differences in soil properties (particle size, salinity, organic content, thaw depths, and ice volumes), with particular attention to ice characteristics. Second, we quantify the rates of lakeshore erosion and ice wedge degradation. Based on these results, we develop a conceptual model of the geomorphic evolution of the landscape in the eastern NPRA, which accounts for changes in sediment type,

organic matter content, and ice accumulation in the upper 3 meters of the soil. Finally, we evaluate the range of potential thaw settlement resulting from surface disturbance in various terrain units and discuss its implications for land management.

## NATURE AND ABUNDANCE OF GROUND ICE

### CLASSIFICATION AND MAPPING

#### Lithofacies

Sediments observed within the NPRA Study Area were classified by texture and structure into 11 lithofacies that reflect depositional environments (e.g., lacustrine, eolian deposits) and cryogenic processes (e.g., soil turbation) (Table 1). The most common lithofacies in near-surface sediments were (1) massive organics in the active layer on all terrain types except active eolian inactive sand deposits, (2) massive turbated fines with organics just below the active layer, and (3) massive turbated gravelly fines at 1–3 meters depth at most coring locations (Figure 2). Other common lithofacies included layered organics, massive fines with organics, and turbated sands with organics. We also interpreted the processes involved in development of the various lithofacies (Table 1).

#### Cryostructures

Eight primary ice structure types (based on continuity of ice patterns) were identified in the NPRA: pore, lenticular, vein, layered, reticulate, ataxitic, organic-matrix, and solid ice (Table 2, Figure 3). The same types of ice structure were identified in the Colville River Delta (Jorgenson et al. 1997) and the Kuparuk/Prudhoe Bay area (Burgess et al. 1999), indicating that they are widely distributed in arctic Alaska. Therefore, our classification system should be appropriate for describing the range of ice characteristics over a large area of the Arctic Coastal Plain.

#### Terrain Units

During field surveys, 25 terrestrial terrain units and 9 classes of waterbodies were identified (Table 3). One of the terrestrial terrain units were related to colluvial processes, 2 to eolian processes, 11 to fluvial processes, 7 to lacustrine processes, 2 to marine processes and 2 to alluvial-marine processes. Of principal interest for this study was

Table 1. Classification and description of lithofacies observed in the Northeast Planning Area, NPRA, 2002.

Lithofacies class (code)	Primary and secondary particle sizes	Sedimentary structures	Process
Sands-massive (Sm)	Medium-coarse sands	None visible, medium-coarse, light brown sands, may be pebbly	Eolian and marine deposition
Sand, layered (Sl)	Medium-coarse sands	Horizontally stratified layers	Planar bed flow (lower and upper flow regime) or eolian
Sands, inclined (Si)	Medium-coarse sands	Undifferentiated wavy-bedded, ripple, or crossbed stratified layers. Interpretation limited by small size of cores.	Eolian sand dunes
Gravelly Fines, massive, turbated (Fgmt)	Fine sands with 5–15% gravel	None visible, light brown with turbated, gleyed inclusions	Eolian and marine deposition
Sands with organics, turbated (Sot)	Medium sands with turbated peat inclusions	Disrupted inclusions or inclined bedding due to cryoturbation	Compression and displacement of material during freezing and thawing
Fines, massive (Fm)	Silts and fine sands	None visible	Eolian, riverine, and lacustrine deposits of silts and fine sands
Fines with organics, massive (Fom)	Silts and fine sands with well-decomposed organics	None visible	Soil formation in massive silts
Fines with organic inclusions, massive, turbated (Fomt)	Silts and fine sands with poorly decomposed organic inclusions	Disrupted organic and mineral inclusions	Compression and displacement of material during freezing and thawing
Fines, layered (Fl)	Silts and fine sands	Horizontally stratified layers	Lacustrine deposition in shallow thaw lakes
Fines with algae (Fa)	Benthic algal mat and other limnic material	None visible to horizontal lamination	Lacustrine sediments
Organic, massive (Om)	Undecomposed organics, includes trace silt or sand layers	None visible	Autochthonous organic matter, lacustrine or fluvial sedimentation is rare or lacking
Organic, layered (Ol)	Undecomposed organic and fine mineral layers	Horizontal bedding, some mineral redistribution in peat	Lacustrine or eolian deposition in autochthonous organic matter

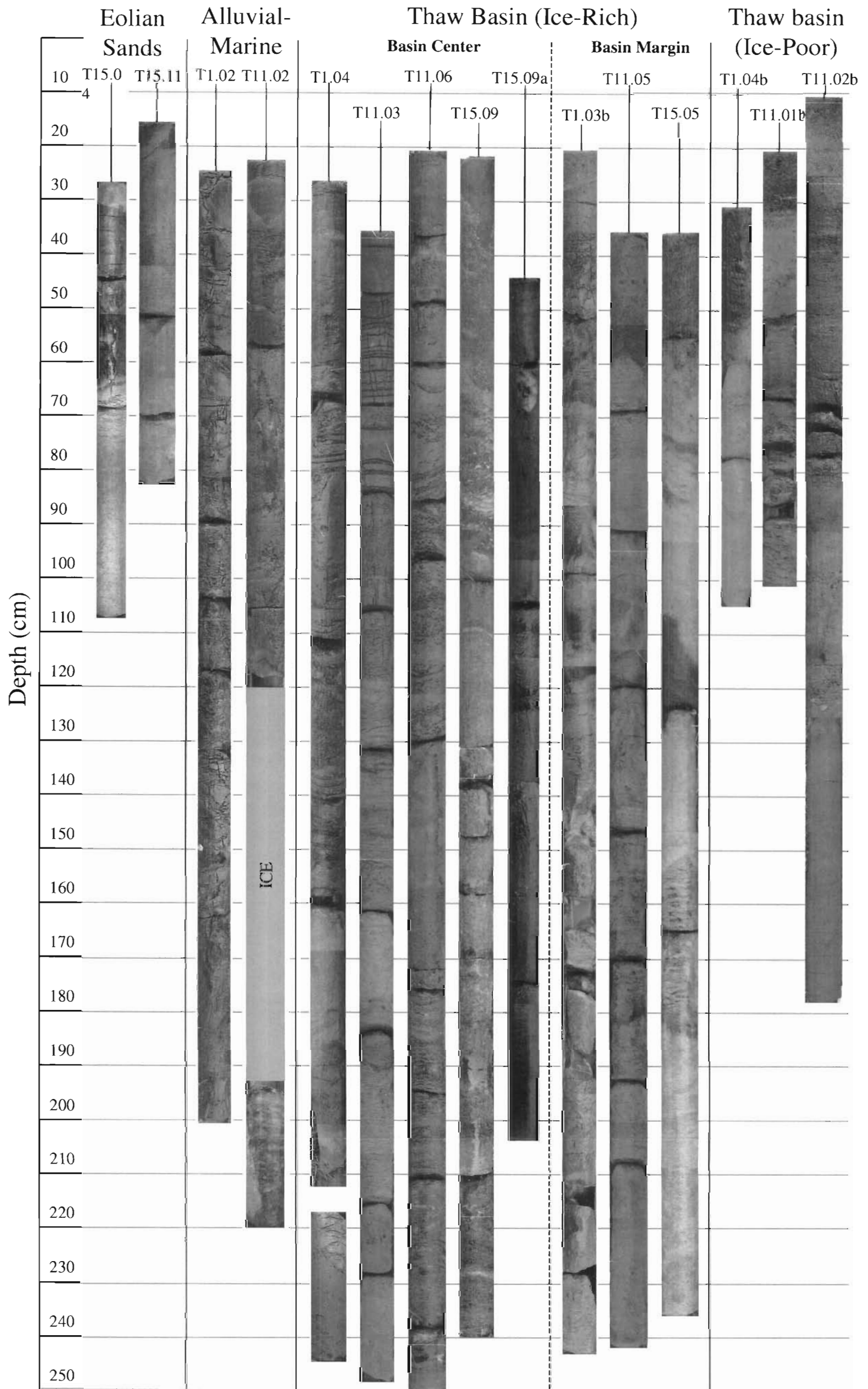


Figure 2. Composite core profiles illustrating stratigraphy and ice structure associated with four dominant terrain units in the NPRA Development Area, northern Alaska, 2001.

Table 2. Classification and description of ground ice observed in the Northeast Planning Area, NPRA, 2002.

Cryostructure	Definition
Pore	Ice in minute holes, or pores, within mineral soil matrix that has an almost structureless appearance. May be visible (without hand lens) or non-visible. Visual impression is that ice does not exceed original voids in soil. Forms where pore water freezes <i>in situ</i> .
Organic-matrix	Ice formed within organic matrix and has a structureless appearance. May be visible or non-visible. Mostly formed where pore water freezes <i>in situ</i> .
Lenticular	Lens-shaped, thin (generally <0.5 mm), short bodies of ice within a soil matrix. The orientation is generally normal to the freezing front and usually reflects the structure of the sediments.
Vein	Isolated, thin lens, needle-like, or sheet-like structures, or particles visible in the face of soil mass. Usually inclined and bisecting sedimentary structures. Differs from layered ice in that they are solitary and do not have a repeated, parallel pattern.
Layered	Laterally continuous bands of ice less than 10-cm thick. Usually parallel, repeating sequences that follow with sedimentary structure or are normal to freezing front. Thicker layers (> 10 cm) are described as solid ice.  Sparse: ice layers <5% of structure. Medium: ice layers 5–25% of structure. Dense: ice layers 25–50% of structure.
Reticulate	Net-like structure of ice veins surrounding fine-grained blocks of soil. Ice occupies up to 50% of surface area.  Trapezoidal: ice has distinct horizontal parallel veins with occasional diagonal, vertically oriented veins. Soil blocks have trapezoidal appearance due to fewer vertical veins than lattice-like ice. An incomplete form of lattice-like reticulate ice. Lattice-like: ice exhibits regular, rectangular, or square framework. Foliated: irregular horizontally dominated ice giving soil a platy structural appearance.
Ataxitic	Ice occupies 50–99% of cross-sectional area, giving the soil inclusions a suspended appearance.  Sparse: ice occupies 50–75% area, soil inclusions occupy 25–50% of area. Medium Inclusions: ice occupies 75–95% of area, soil inclusions occupy 5–25%. Dense Inclusions: ice occupies 96–99% of area, soil inclusions occupy 1–5%.
Solid	Ice (>10-cm thick) where soil inclusions occupy <1% of the cross-sectional area.  Sheet ice: Cloudy or dirty, horizontally bedded ice exhibiting indistinct to distinct stratification. Wedge Ice: V-shaped masses of vertically foliated or stratified ice resulting from infilling of frost fissures. Best identified when large exposures or cross-sections are visible.

the lacustrine terrain units associated with lake-basin development. These included ice-poor thaw basin margins, ice-poor thaw basin centers, ice-rich thaw basin margins, and ice-rich thaw basin centers (Figure 4). The study also focused on alluvial-marine deposits and alluvial terraces, which represent the terrain that has not been altered by lacustrine or riverine processes. For purposes of analysis in other sections of the report, alluvial terraces were combined with alluvial-marine deposits because of their similarity and the small

sample sizes for each. A map of the terrain units within the study area is provided in Figure 5.

During the course of the study our concepts of the genesis of lake basins have evolved based on the results of our analyses of soil stratigraphy. We originally classified the lacustrine deposits as thaw basin deposits to be consistent with earlier concepts of lake basin genesis and with our earlier mapping (Jorgenson et al. 1997) and that of others (Kreig and Reger 1982, Cater and Galloway 1985, Rawlinson 1993). We now conclude that most basins are not the result of thermokarst (see

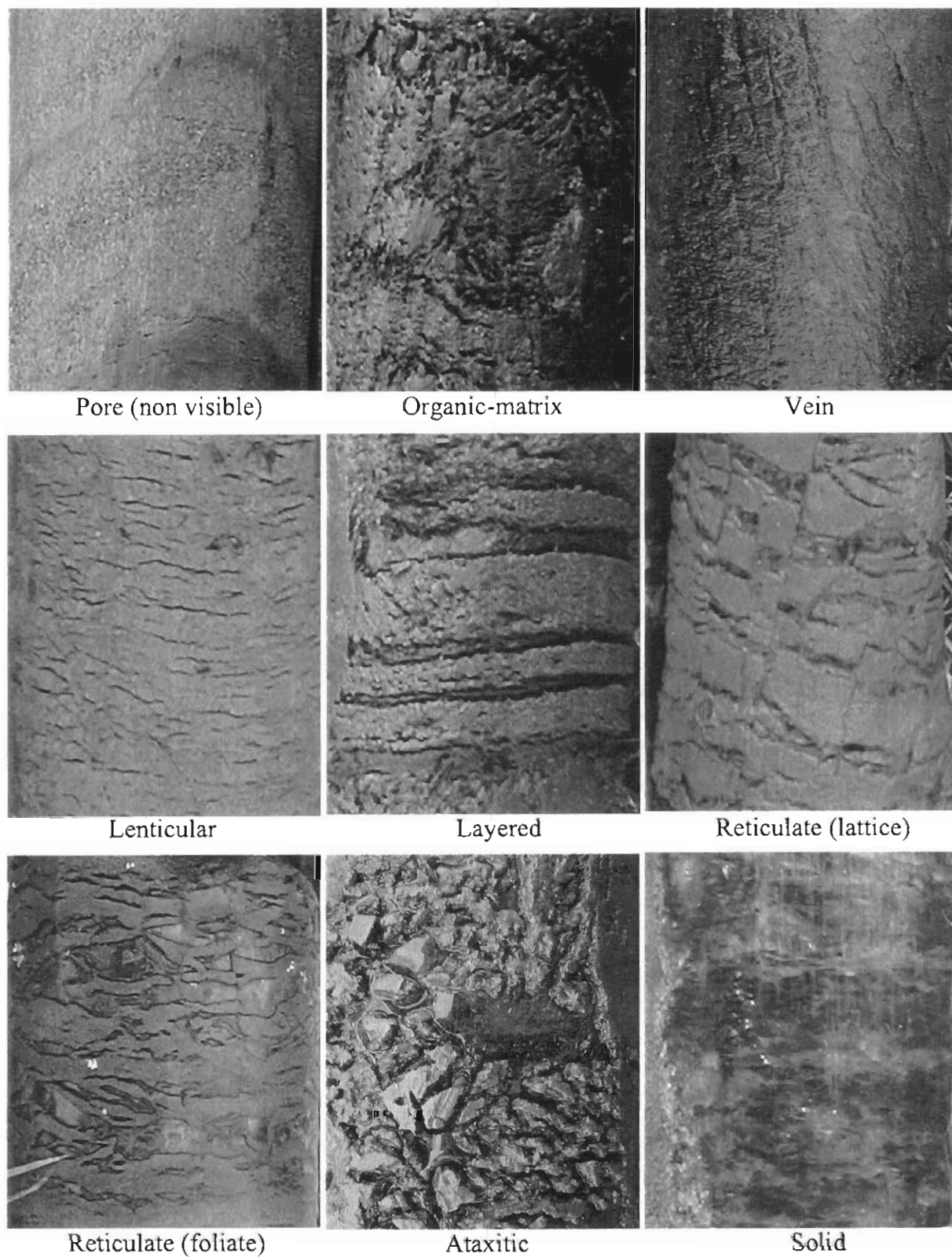


Figure 3. Photographs of simple ice structures found in permafrost in the Northeast Planning Area, NPRA, 2002.

Table 3. Classification and description of terrain units observed in the Northeast Planning Area, NPRA, 2002.

Unit	Description
Solifluction Deposit	Unconsolidated fine-grained, sandy, or gravelly material, resulting from mass movement of saturated materials. Usually associated with gelifluction processes at the base of slopes and in snowbeds.
Slump Deposit (not mapped)	A type of landslide deposit characterized by downward slipping of unconsolidated fine-grained to gravelly material moving as a unit. Slumps typically are associated with cutbanks along river channels. Areas with slumping often have minor amounts of other mass-wasting processes including debris sliding and falling.
Eolian Active Sand Deposit	Fine to very fine, well-sorted sand containing abundant quartz with minor dark minerals. Sand is stratified with large-scale cross bedding in places. Active dunes are barren or partially vegetated and are undergoing active accretion and deflation. Active dunes usually occur adjacent to exposed sandy channel deposits.
Eolian Inactive Sand Deposit	Fine to very fine, well-sorted sand containing abundant quartz with minor dark minerals. Sand is stratified with large-scale cross bedding in places. Often contains buried soils and peat beds in upper few meters. Inactive dunes are well vegetated, typically have thin to thick organic soil horizons at the surface, and are not subject to active scouring or movement. Inactive dunes occur both on the coastal plain and adjacent to river channels. While much of the Arctic Coastal Plain is covered by thin sand sheets, the sandy surface material is usually included as a component of the Alluvial Plain and Alluvial-Marine Deposits.
Delta Active Channel Deposits	Silty and sandy channel or lateral accretion deposits laid down from the bed load of a river in a deltaic setting under low water velocities. This unit includes point bars, lateral bars, mid-channel bars, unvegetated high-water channels, and broad sandbars exposed during low water. Generally, sediment texture becomes finer in a seaward direction along the distributaries. Organic matter, including driftwood, peat shreds, and other plant remains, usually is interbedded with the sediments. Only those riverbed deposits that are exposed at low water are mapped, but they also occur under rivers and cover deposits. Frequent flooding (every 1–2 yr) prevents the establishment of permanent vegetation
Delta Inactive Channel Deposits	Delta deposits in channels that are only flooded during periods of high flow. Because of river meandering, these “high-water” channels are no longer active during low-flow conditions. Generally, there is little indication of ice-wedge development, although a few older channels have begun to develop polygon rims. Very old channels with well-developed, low-centered polygons are not included in this unit.
Delta Active Overbank Deposits	Thin (10–50 cm) fine-grained, horizontally stratified cover deposits (primarily silt) that are laid down over sandier channel deposits during flood stages. Relatively frequent (every 3–4 yr) deposition prevents the development of a surface organic horizon. Supra-permafrost groundwater generally is absent or occurs only at the bottom of the active layer during mid-summer. This unit usually occurs on the upper portions of point and lateral bars and supports low and tall willow vegetation.
Delta Inactive Overbank Deposits	Fine-grained cover or vertical accretion deposits laid down over coarser channel deposits during floods. The surface layers are a sequence (20–60 cm thick) of interbedded organic and silt horizons, indicating occasional flood deposition. Under the organic horizons is a thick layer (0.3–2 m thick) of silty cover deposits overlying channel deposits. Surface forms range from nonpatterned to disjunct and low-density, low-centered polygons. Lenticular and reticulate forms of segregated ice, and massive ice in the form of ice wedges, are common.

Table 3. (Continued).

Unit	Description
Delta, Abandoned- floodplain Cover Deposit	Peat, silt, or fine sand (or mixtures or interbeds of all three), deposited in a deltaic overbank environment by fluvial, eolian, and organic processes. These deposits generally consist of an accumulation of peat 20–60 cm thick overlying cover and riverbed alluvium. Because these are older surfaces, eolian silt and sand may be common as distinct layers or as intermixed sediments. The surface layer, however, usually lacks interbedded silt layers associated with occasional flood deposition. Lenticular and reticulate forms of segregated ice, and massive ice in the form of ice wedges, are common in these deposits. The surface is characterized by high density, low-relief polygons and represents the oldest surface on the floodplain.
Meander Fine Active Channel Deposits	Sand and mud deposited as lateral accretion deposits in active river channels by fluvial processes. Occasional subrounded to rounded pebbles may be present. Frequent deposition and scouring from flooding usually restricts vegetation to sparse pioneering colonizers. The channel has a meandering configuration characterized by point bars.
Meander Fine Inactive Channel Deposits	Sand and mud deposited as lateral accretion deposits in inactive channels during periods of high flow. Because of river meandering, these “high-water” channels are no longer active during low-flow conditions. Generally, there is little indication of ice-wedge development, although a few older channels have begun to develop polygon rims. Very old channels with well-developed low-centered polygons are not included in this unit.
Meander Active Overbank Deposit	Thin (0.5–1 ft), fine-grained, cover deposits (primarily silt) that are laid down over sandy or gravelly riverbed deposits during flood stages. Deposition occurs sufficiently frequently (probably every 3–4 yr) to prevent the development of a surface organic horizon. This unit usually occurs on the upper portions of point and lateral bars and supports riverine willow vegetation.
Meander Inactive Overbank Deposits	Interbedded layers of peat and silty very fine sand material (0.5–2 ft thick), indicating a low frequency of flood deposition. Cover deposits below this layer generally consist of silt but may include pebbly silt and sand and usually are in sharp contact with underlying channel deposits. This unit has substantial segregated and massive ice, as indicated by the occurrence ice-wedge polygons.
Meander Abandoned Overbank Deposits	Sediments are a mixture of peat, silt, or fine sand. Surface organic horizon is free of fluvial deposits indicating that the terrain is no longer affected by riverine processes. Typically, these areas occupy the highest position on the floodplain, and represent the oldest local terrain. Abandoned floodplain deposits typically have at least 20 cm of surface organics over silt-loam or fine-sand alluvium. Low-centered polygons and small ponds are common.
Headwater Lowland Floodplain	Small streams and tributaries in lowland areas that are too small to be delineated apart from their associated floodplains. These low gradient streams carry little sediment and the floodplain generally is restricted to the immediate vicinity of the stream.
Alluvial Terrace	Old alluvial deposits, weathered or overlain with eolian and organic material (terrace D of Rawlinson 1993). Soils are cryoturbated loam or sandy loam, buried organics often are present. High-centered polygons are the most common surface form indicating high ice content of surface soils. Thaw basins also are common features.
Alluvial–marine Deposits	Composition is variable but generally consists of a sequence of eolian, alluvial, and marine deposits. Thickness of pebbly eolian sand is highly variable and sometimes absent. Underlying fluvial deposits include gravelly sand, silty sand, and organic silt, and occasionally have buried peat beds and logs. Stratified layers of marine gravelly sand, silty sand, silt, and minor clay occur in some locations beneath the fluvial deposits and commonly are fossiliferous. This unit is not subject to river flooding. Surface materials can be differentiated as sandy (Mps) or fine-grained (Mpf). This unit includes both the alluvial sand over marine silt and clay (Qam) and alluvial and eolian sand and marine sand and silt (QTas) units of Cater and Galloway (1985).

Table 3. (Continued).

Unit	Description
Loess (not mapped)	Wind-blown silt and very fine sand in homogeneous, nonstratified deposits. On the coastal plain in the study area, loess typically occurs as a layer too thin (<0.5 m) to map as a surficial material.
Thaw Basin Deposit, Ice- poor Centers	Lacustrine deposits formed by the draining of thermokarst lakes or other lakes. Soils of the basin center typically are fine-grained and organic-rich, with stratigraphy re-formed by subsidence. The presence of nonpatterned ground or disjunct polygonal rims indicates that ground ice content is low and that lake drainage has occurred recently. Ponds in these basins typically have irregular shorelines and are highly interconnected.
Thaw Basin Deposit, Ice- poor Margins	Lacustrine deposits formed by the draining of thermokarst lakes or other lakes. Soils of the basin margins typically are sandy with a thick surface organic horizon. The presence of nonpatterned ground or disjunct polygonal rims indicates that ground ice content is low and that lake drainage has occurred recently. Ponds in these basins typically have irregular shorelines and are highly interconnected.
Thaw Basin Deposit, Ice- Rich Centers	The sediments are similar to those of ice-poor thaw lake deposits but have much more ground ice, as indicated by the development of low-centered or high-centered polygons. The centers of basins usually have organic-rich silty sediments that have high potential for ice segregation and often are raised by ice aggradation. Surface morphology ranges from low-centered polygons at early stages of development to high-centered polygons on distinctly raised domes.
Thaw Basin Deposit, Ice- Rich Margins	The sediments are similar to those of ice-poor thaw lake deposits but have much more ground ice, as indicated by the development of low-centered or high-centered polygons. Waterbodies within these basins tend to be rectangular, to have smooth, regular shorelines, and to be poorly interconnected.
Thaw Basin Deposit, Ice- Rich Undifferentiated	Sediments similar to ice-rich, thaw lake deposits but having less ground ice with poorly developed low-centered or high-centered polygons. This type is used when the thaw lake centers and margins are poorly differentiated.
Thaw Basin Deposit, Pingo	Sediments similar to ice-rich, thaw basin centers but with much more ground ice indicated by a raised area of well-drained high-centered polygons.
Delta Thaw Basin, Ice-Poor	Deposits in thaw lakes within deltaic deposits. They usually are connected to a river or to nearshore water (tapped lake). Most connections occur when a meandering distributary cuts through a lake's bank; once connected, the lake is influenced by changes in river level. During breakup, large quantities of sediment-laden water flow into the lake, forming a lake delta at the point of breakthrough. Sediments generally consist of fine sands, silts, and clays, and typically are slightly saline.
Active Tidal Flat	Areas of nearly flat, barren mud or sand that are periodically inundated by tidal waters and undergoing active sedimentation. Tidal flats occur on seaward margins of deltaic estuaries, leeward portions of bays and inlets, and at mouths of rivers. Tidal flats frequently are associated with lagoons and estuaries and may vary widely in salinity, depending on how exposed the flat is to salt-water incursion and the rate of influx of fresh water. Although similar to delta riverbed/sandbar deposits, they are differentiated by their occurrence as triangular-shaped mudflats along the fringe of the delta.
Inactive Tidal Flat	Areas of nearly flat, barren mud or sand that are periodically inundated by tidal waters but sedimentation is infrequent allowing the build-up of organic material. The surface is vegetated with halophytic vegetation.

Conceptual Model of the Evolution of Lakes and Drained Basins) and that they should more appropriately be mapped simply as generic lacustrine deposits. To maintain consistency with previous mapping, however, we maintained the old terminology.

#### Relationships Among Terrain Components

The terrain components (lithofacies, ice structures, terrain units) generally occur in distinct associations across the landscape. Lithofacies and ice structures were classified by independent characteristics (sediment type versus ice structure) and the relationships between them reveal interrelated processes. However, both lithofacies and terrain units were based on sediment characteristics and lithofacies were used in the definition of terrain units. Thus, components at these two spatial scales are interrelated partly because of the way the components were defined. In the following section, we evaluate the interrelationships among lithofacies, ice structures, and terrain units by comparing variation at these three scales across topographic sequences.

Topographic sequences provide information on elevation, terrain units, surface forms, and vegetation at selected locations within the NPRA (Figures 6–8). Toposequences were oriented to cross both multiple drained-lake basins and the intervening terrain (Figure 1). Transect 1 (T1), located between Oil Lake and the Ublutuoeh River illustrates the topographic progression from ice-poor thaw basin, through ice-rich thaw basin, to the surrounding alluvial terrace (Figure 6). Transect 11 (T11), just west of the Ublutuoeh River, crosses ice-poor thaw basins, alluvial-marine deposits, and ice-rich thaw basin margins (Figure 7). Transect 15 (T15), located in the northwest quadrant of the NPRA Study Area, crosses eolian inactive sand, an ice-poor thaw basin, and an ice-rich thaw basin (Figure 8).

The profiles provide information for evaluating landscape evolution theories because they provide an estimate of the total amount of ice that would be required to be aggraded or degraded during thaw-lake development. Differences in relative elevation between the ice-poor basins and the adjacent old surface (alluvial terrace, alluvial-marine deposit, and eolian inactive sand) ranged from 2.5 to 2.7 m, indicating the amount of

ice that would have to be lost during degradation. The difference in relative elevation between ice-rich margins and ice-rich thaw basin centers ranged from 0.7 to 2.7 m, indicating the amount of ice that can accumulate (causing heaving of the surface) is highly variable.

Analysis of the data obtained from the cores revealed strong relationships among the distributions of ice structures, lithofacies, and terrain units. These relationships can be used effectively to partition the variation in ice structures across the landscape. The frequency of occurrence of most ice structures differed greatly among lithofacies. Pore ice was almost always associated with massive, inclined, and layered sands; lenticular and ataxitic ice were associated most frequently with massive and layered fines, and organic-matrix ice usually was found in massive and layered organics and limnic fines (Figure 9). In contrast, reticulate ice was broadly distributed among both fine and organic lithofacies.

The associations between ice structures and terrain units were more complex, due to the more complex stratigraphy of soil materials associated with the various terrain units (Figure 9). The simplest association was for eolian inactive sand, which was dominated by pore ice. In contrast, most ice structures were found in units other than eolian inactive sand but varied somewhat in their frequency. For example, lenticular and ataxitic ice were found most frequently in thaw basins, whereas vein ice was found most frequently in alluvial-marine deposits.

#### SOIL PROPERTIES

In the following analysis, we compare the physical and chemical properties (particle size, salinity, organic content, thaw depths, and ice volumes) of soils among lithofacies and terrain units. We also discuss landscape processes that contribute to the changes in physical and chemical characteristics of the soil.

Soil analysis was based on lithofacies classifications. The simplest associations between lithofacies and terrain units were seen in alluvial-marine deposits and eolian inactive sand (Figure 10). Eolian inactive sand was dominated by massive, inclined, and layered sand indicative of active dune processes. Alluvial-marine deposits

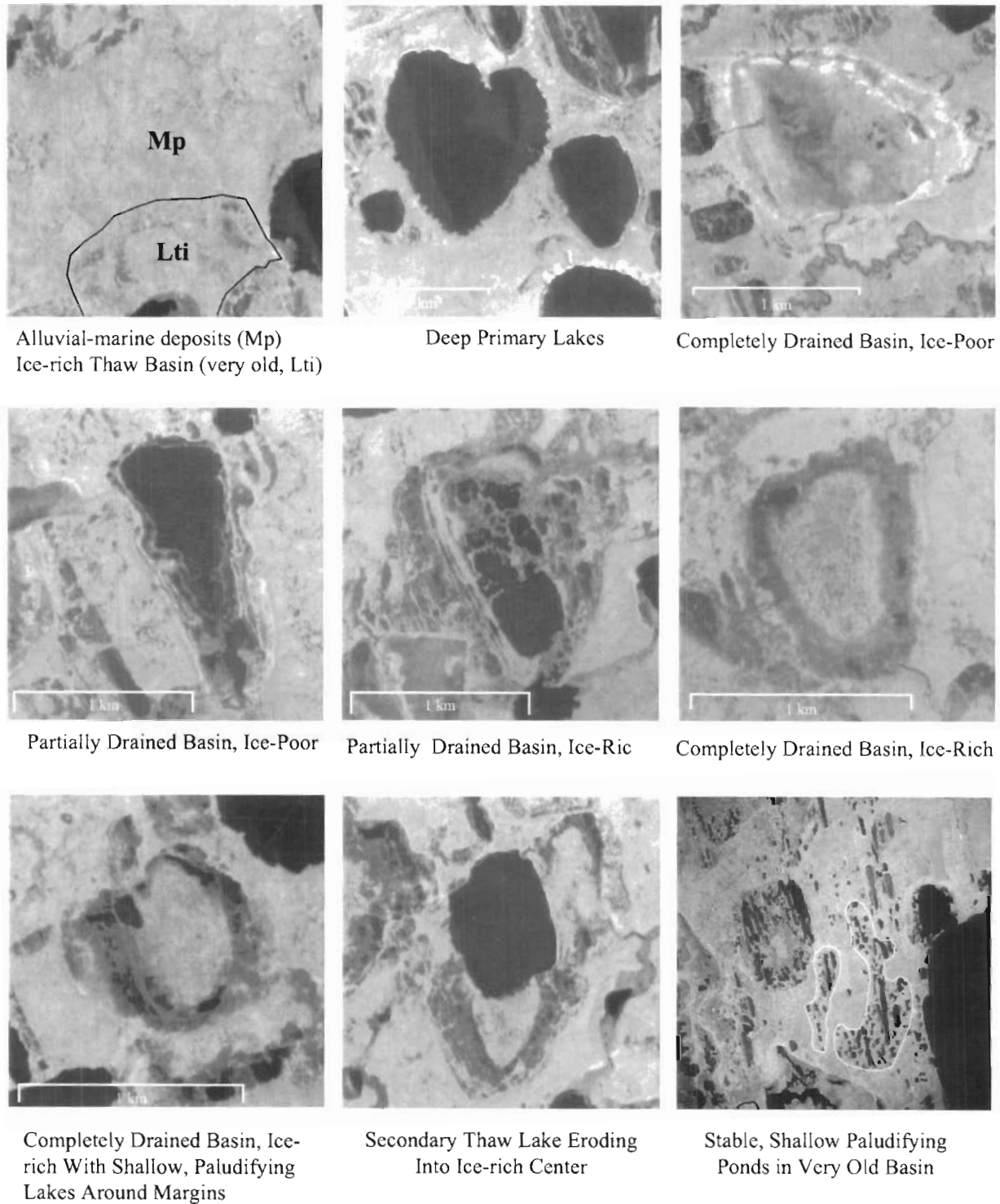
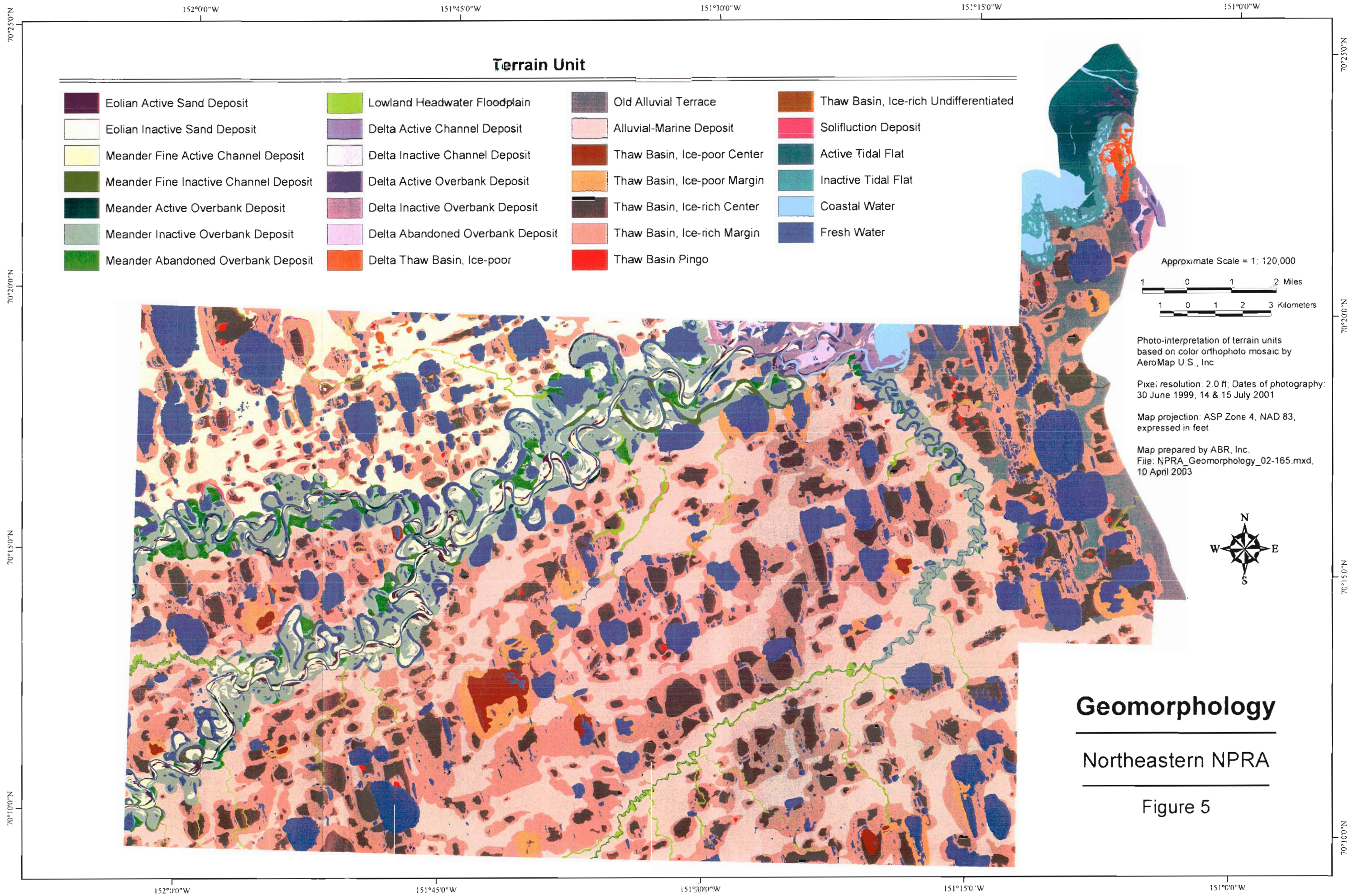


Figure 4. Aerial photographs of dominant terrain units on the coastal plain in the Northeast Planning Area, NPRA, 2002.



**Terrain Unit**

- |                                       |                                  |                             |                                       |
|---------------------------------------|----------------------------------|-----------------------------|---------------------------------------|
| Eolian Active Sand Deposit            | Lowland Headwater Floodplain     | Old Alluvial Terrace        | Thaw Basin, Ice-rich Undifferentiated |
| Eolian Inactive Sand Deposit          | Delta Active Channel Deposit     | Alluvial-Marine Deposit     | Solifluction Deposit                  |
| Meander Fine Active Channel Deposit   | Delta Inactive Channel Deposit   | Thaw Basin, Ice-poor Center | Active Tidal Flat                     |
| Meander Fine Inactive Channel Deposit | Delta Active Overbank Deposit    | Thaw Basin, Ice-poor Margin | Inactive Tidal Flat                   |
| Meander Active Overbank Deposit       | Delta Inactive Overbank Deposit  | Thaw Basin, Ice-rich Center | Coastal Water                         |
| Meander Inactive Overbank Deposit     | Delta Abandoned Overbank Deposit | Thaw Basin, Ice-rich Margin | Fresh Water                           |
| Meander Abandoned Overbank Deposit    | Delta Thaw Basin, Ice-poor       | Thaw Basin Pingo            |                                       |

Approximate Scale = 1: 120,000

1 0 1 2 Miles

1 0 1 2 3 Kilometers

Photo-interpretation of terrain units based on color orthophoto mosaic by AeroMap U.S., Inc

Pixel resolution: 2.0 ft; Dates of photography: 30 June 1999, 14 & 15 July 2001

Map projection: ASP Zone 4, NAD 83, expressed in feet

Map prepared by ABR, Inc.  
File: NPR\_A\_Geomorphology\_02-165.mxd, 10 April 2003



**Geomorphology**

---

Northeastern NPR

---

Figure 5

### FISH CREEK LOWER COASTAL PLAIN

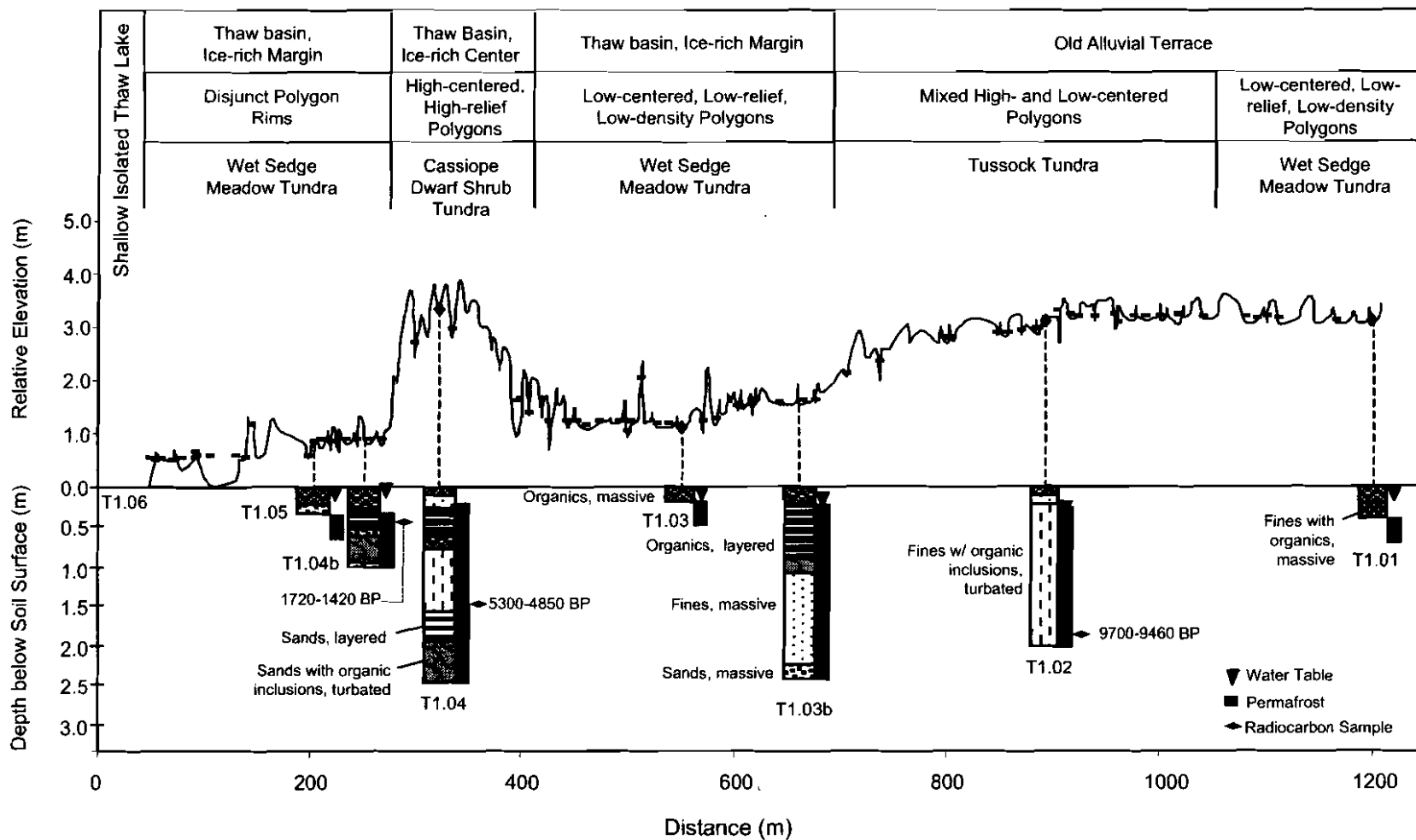


Figure 6. Soil stratigraphy along a terrain sequence (Transect 1) in the eastern portion of the Northeast Planning Area, NPRA, 2002.

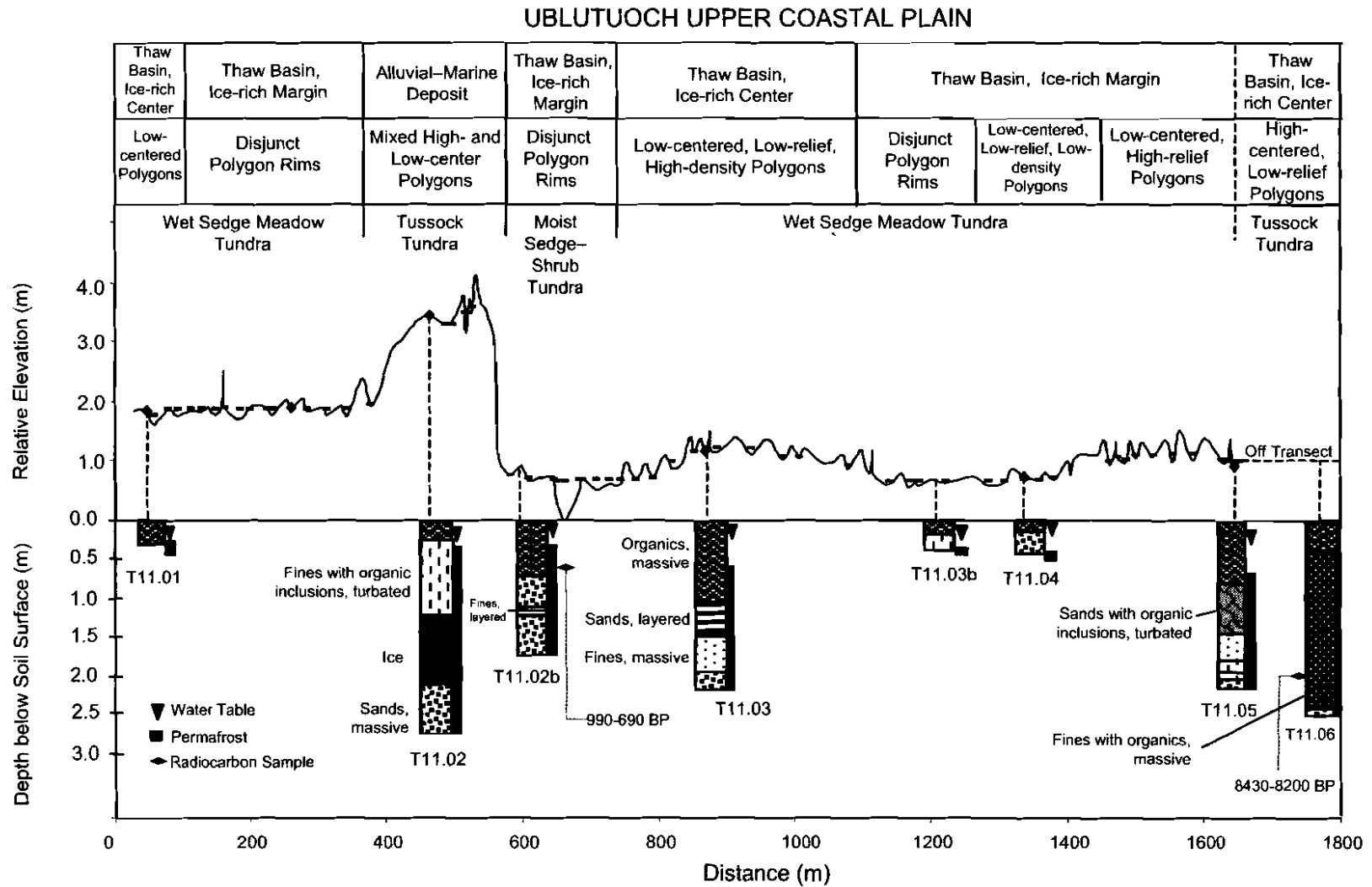


Figure 7. Soil stratigraphy along a terrain sequence (Transect 11) in the central portion of the Northeast Planning Area, NPRA, 2002.

IKPIKPUK UPPER COASTAL PLAIN

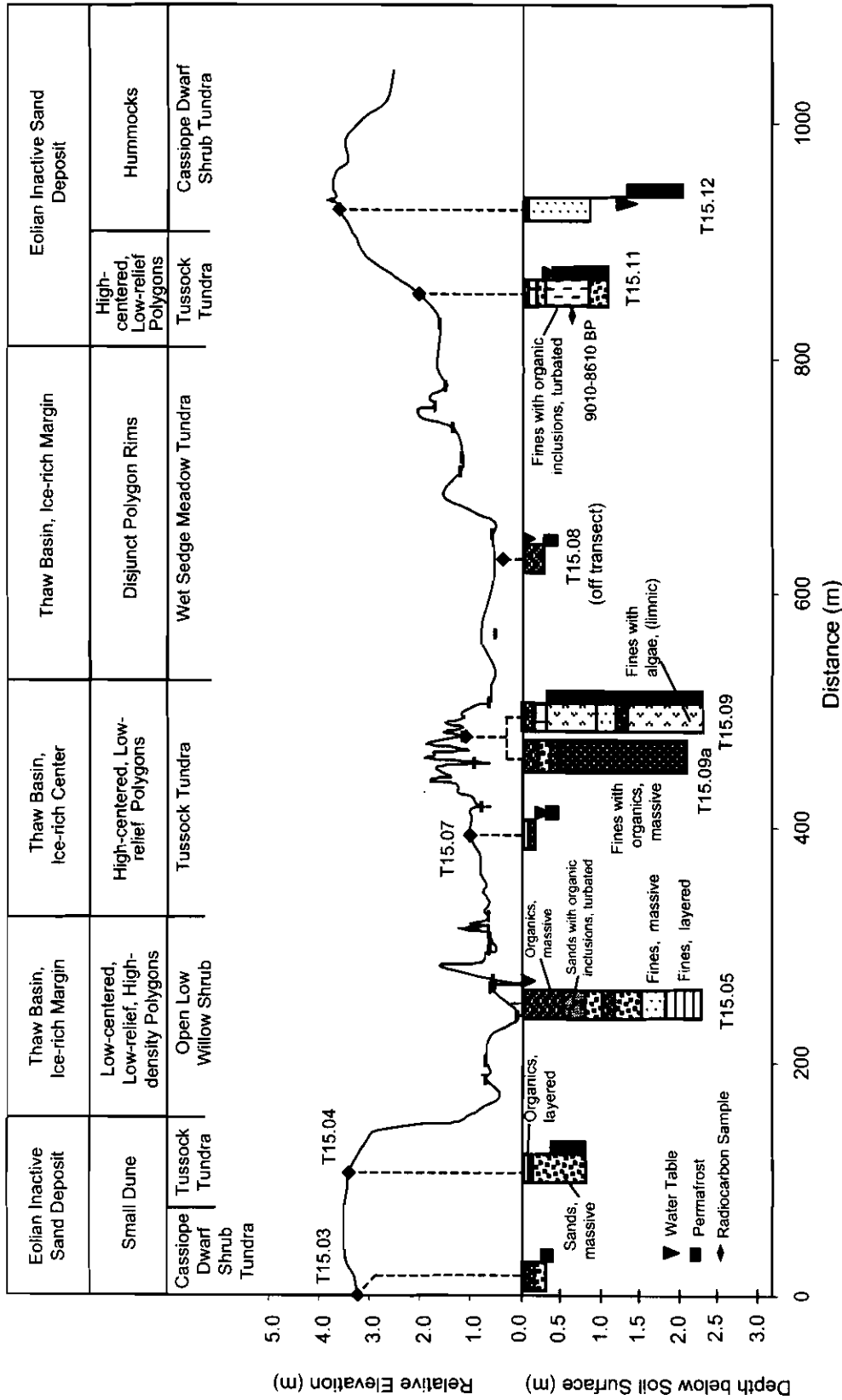


Figure 8. Soil stratigraphy along a terrain sequence (Transect 15) in the western portion of the Northeast Planning Area, NPRA, 2002.

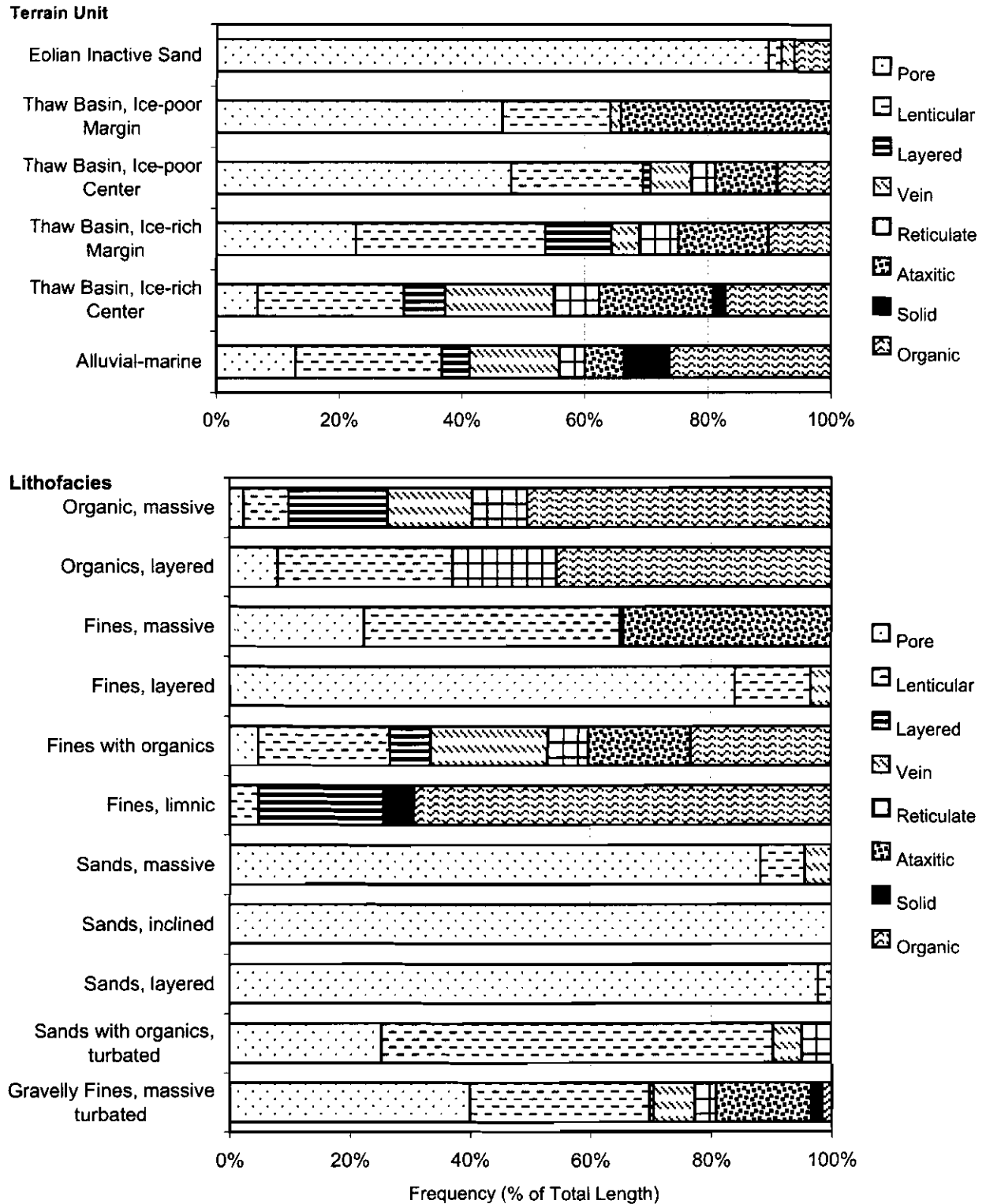


Figure 9. Frequency of occurrence (% of total core length) of ice structures by lithofacies (top) and by surface terrain unit (bottom) for profiles in the Northeast Planning Area, NPRA, 2002.

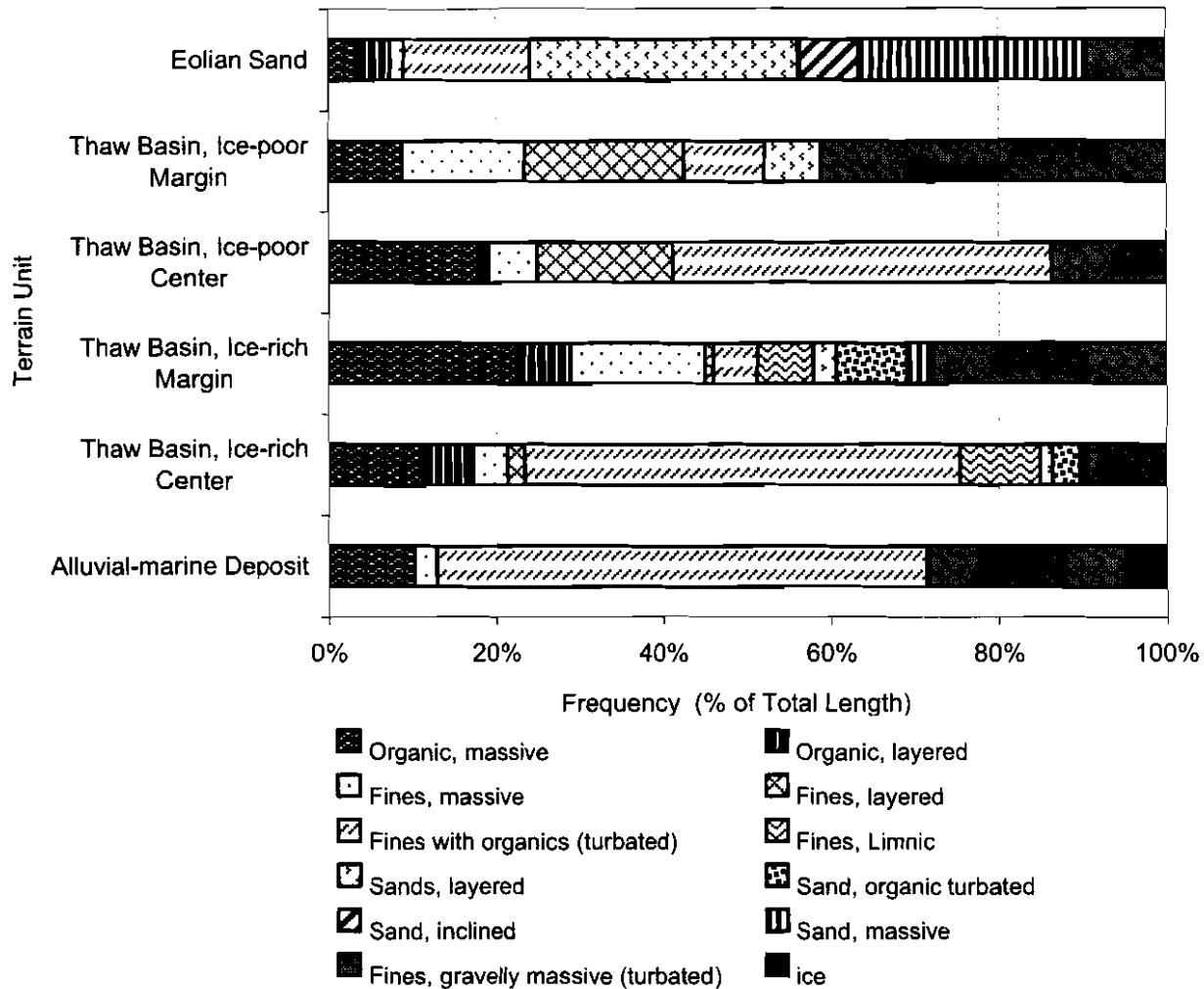


Figure 10. Frequency of occurrence (% of total core length) of lithofacies by surface terrain unit for profiles in the Northeast Planning Area, NPRA, 2002.

were dominated by turbated fines with organics as a result of extensive ice wedge development and the associated cryoturbation. Lithofacies associations were more complex in thaw basin deposits, reflecting thaw-lake and ice aggradation processes.

#### Particle Size

Particle size analysis was performed on the six most common mineral-dominated lithofacies classes: massive fines, layered fines, massive turbated gravelly fines, massive fines with organics, massive sands, and layered sands (Figure 11). Nearly all samples were composed mainly of sand, most of which were characterized in the field

as fine or very fine. Medium sand was present in a few samples. The predominance of sand within the study area is likely due to eolian processes associated with the formation of thin loess deposits, sand sheets, distinct sand dunes, and scattered thin loess deposits.

#### Electrical Conductivity and pH

Salinity, as measured by electrical conductivity (EC), can be used to assess whether the soil material is of marine origin. For all soils near the surface, EC was low (<500  $\mu\text{S}/\text{cm}$ ) indicating no current marine influence and suggesting that soluble cations may have been leached from the soil by precipitation and drainage.

Results and Discussion

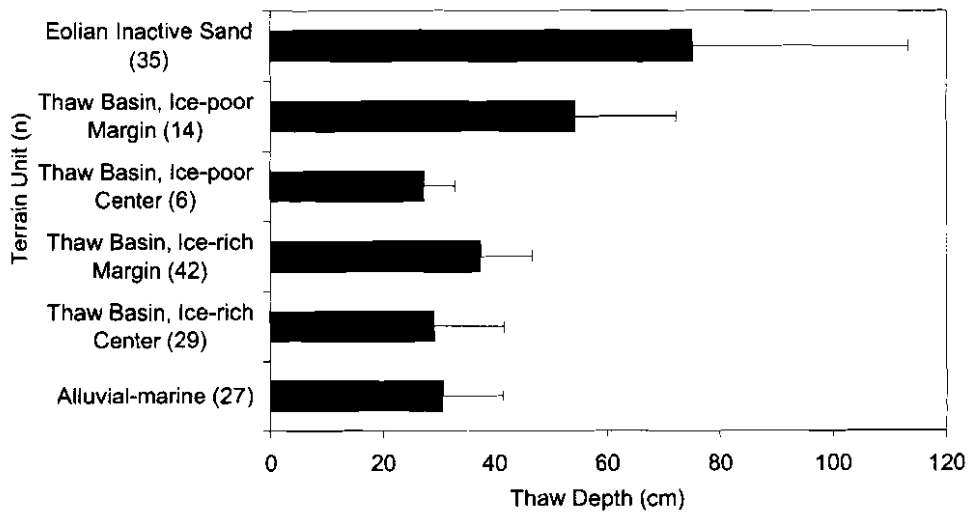
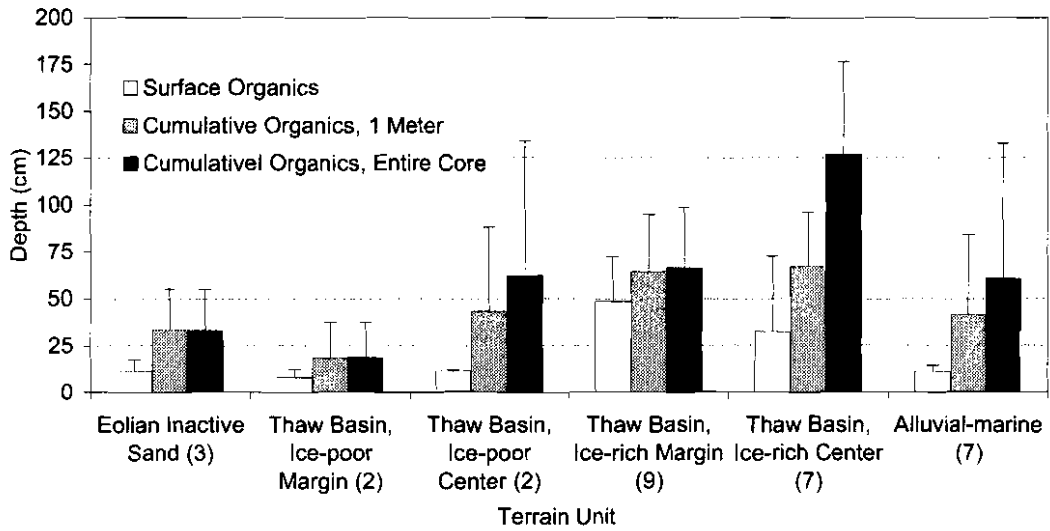
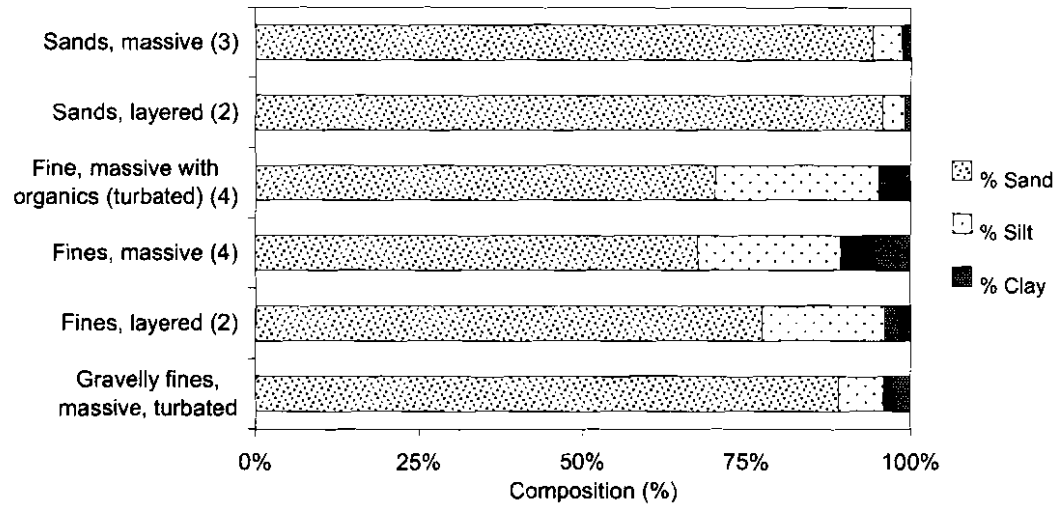


Figure 11. Particle-size characteristics of dominant lithofacies (top), thickness of surface organics and cumulative organics by surface terrain unit (middle), and thaw depths within the soil profiles (bottom), Northeast Planning Area, NPRA, 2002.

EC generally increased with depth in eolian inactive sands and alluvial-marine deposits, with a maximum value around 5000  $\mu\text{S}/\text{cm}$  at depths greater than 1.5 m. The highest observed EC value was 7900  $\mu\text{S}/\text{cm}$  (1.8 m) in a sample from an ice-rich thaw basin center. Elevated EC values ( $>1000$   $\mu\text{S}/\text{cm}$ ) were seen in cores that penetrated the underlying massive turbated gravelly fines (Fgmt) and were most common in areas with thin surficial deposits (Figure 12).

We attribute the lack of a salinity gradient in the thaw basins to the leaching of soluble cations and redistribution of materials during lake-basin development. The few elevated EC values in the ice-rich thaw basin centers may be related to carbonate deposition in the centers, although the data are insufficient to support a stronger conclusion. We speculate that in deep lakes calcium carbonate is excluded from the ice during winter freezing of the lake surface and precipitated in the sediments. In several cores, we observed yellowish granular carbonate materials in thin layers indicative of annual deposition.

Soil pH ranged from 4.0 at the surface of an ice-rich thaw basin center to 7.8 in the mineral soils of an ice-poor thaw basin and generally increased with depth in all terrain units (Figure 12). We attribute the lower pH values at the surface to leaching of cations and production of organic acids in the organic-rich surface layers.

#### Organic Matter Accumulation

Accumulation of surface organic material was least in ice-poor thaw basin margins (8.0 cm), eolian inactive sands (11.3 cm), and alluvial-marine deposits (11.1 cm), and greatest in ice-rich thaw basin centers (32.2 cm) and margins (48.8 cm) (Figure 11).

Subsurface organic horizons within the cores were summed to provide a cumulative measure of thickness, because most cores had discontinuous organic matter disrupted by cryoturbation and thermokarst processes (Figure 2). The mean cumulative thickness of organic matter within the top 1 m of the cores was double in the ice-rich thaw basin centers (66.8 cm) and somewhat higher in the ice-rich thaw basin margins (64.5 cm). In eolian inactive sand, ice-poor thaw basin margin, and ice-rich thaw basin margin, nearly all the organic deposits occur within the top 1 m of soil (Figure

11). Cumulative organic thickness continued to increase as organic layers were summed along the entire length of the core in thaw basin centers and on alluvial-marine deposits. Profiles of total carbon (%) and carbon density ( $\text{g}/\text{cm}^3$ ) show that organic matter is more evenly distributed with depth in these terrain types (Figure 13). The comparison of organic material by total core length should be interpreted with caution, however, as cores varied in length. For example, some cores in ice-rich thaw basin centers did not reach the maximum depth at which organic layers occurred, so the cumulative thickness of all organic layers was underestimated for this terrain unit.

Carbon stocks were greatest in alluvial-marine deposits and thaw basin centers, and lowest in eolian inactive sands and basin margins (Figure 14). Mean ( $\pm$  s.d.) carbon stocks in the top 1 meter of soil were lowest in eolian inactive sand ( $35.2 \pm 9.2$   $\text{kg C}/\text{m}^2$ ) and ice-poor and ice-rich basin margins ( $41.8 \pm 1.7$   $\text{kg C}/\text{m}^2$  and  $48.4 \pm 8.0$   $\text{kg C}/\text{m}^2$ , respectively) intermediate in ice-poor and ice-rich thaw basin centers ( $60.3 \pm 6.0$   $\text{kg}/\text{m}^2$  and  $52.0 \pm 14.6$   $\text{kg C}/\text{m}^2$ ) and highest in alluvial marine ( $63.5 \pm 12.8$   $\text{kg C}/\text{m}^2$ ). When calculated in the top 2 meters, large increases in carbon stocks were seen in thaw basin centers and alluvial marine terrain (Figure 14). These data represent conservative estimates of total soil carbon stocks because additional soil carbon may be present beyond our sampling depths, especially in ice-rich thaw basin centers and alluvial-marine terrains (Figure 13). Our estimates of carbon stocks agree with other published accounts (Ping, et al. 2002) that have reported carbon stocks ranging from 36–94  $\text{kg}/\text{m}^2$  in the top meter of soil on the arctic coastal plain.

#### Thaw Depth

Comparisons of thaw depths are important for evaluating how various landscape surfaces equilibrate thermally with respect to topographical conditions and provides a baseline for predicting how the terrain may respond to disturbance. Mean  $\pm$  SD thaw depths were greatest in eolian inactive sands ( $74.8 \pm 38.5$  cm), intermediate in ice-poor thaw basin margins ( $54.0 \pm 18.0$  cm) and ice-rich thaw basin margins ( $37.3 \pm 9.4$  cm), and least in alluvial-marine deposits ( $30.7 \pm 10.7$  cm), ice-rich

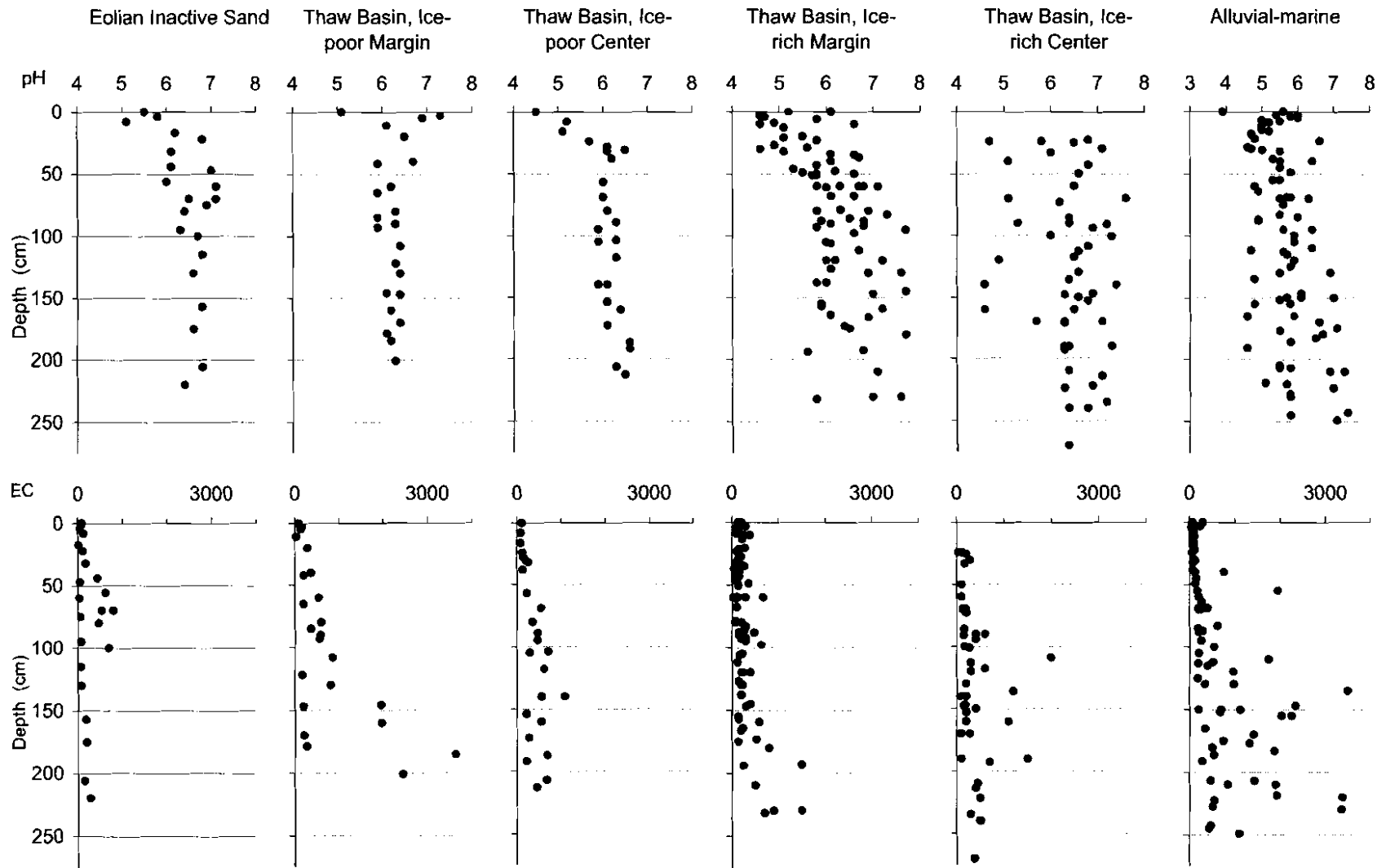


Figure 12. Depth profiles of electrical conductivity (EC) and pH by surface terrain unit, Northeast Planning Area, NPRA, 2002.

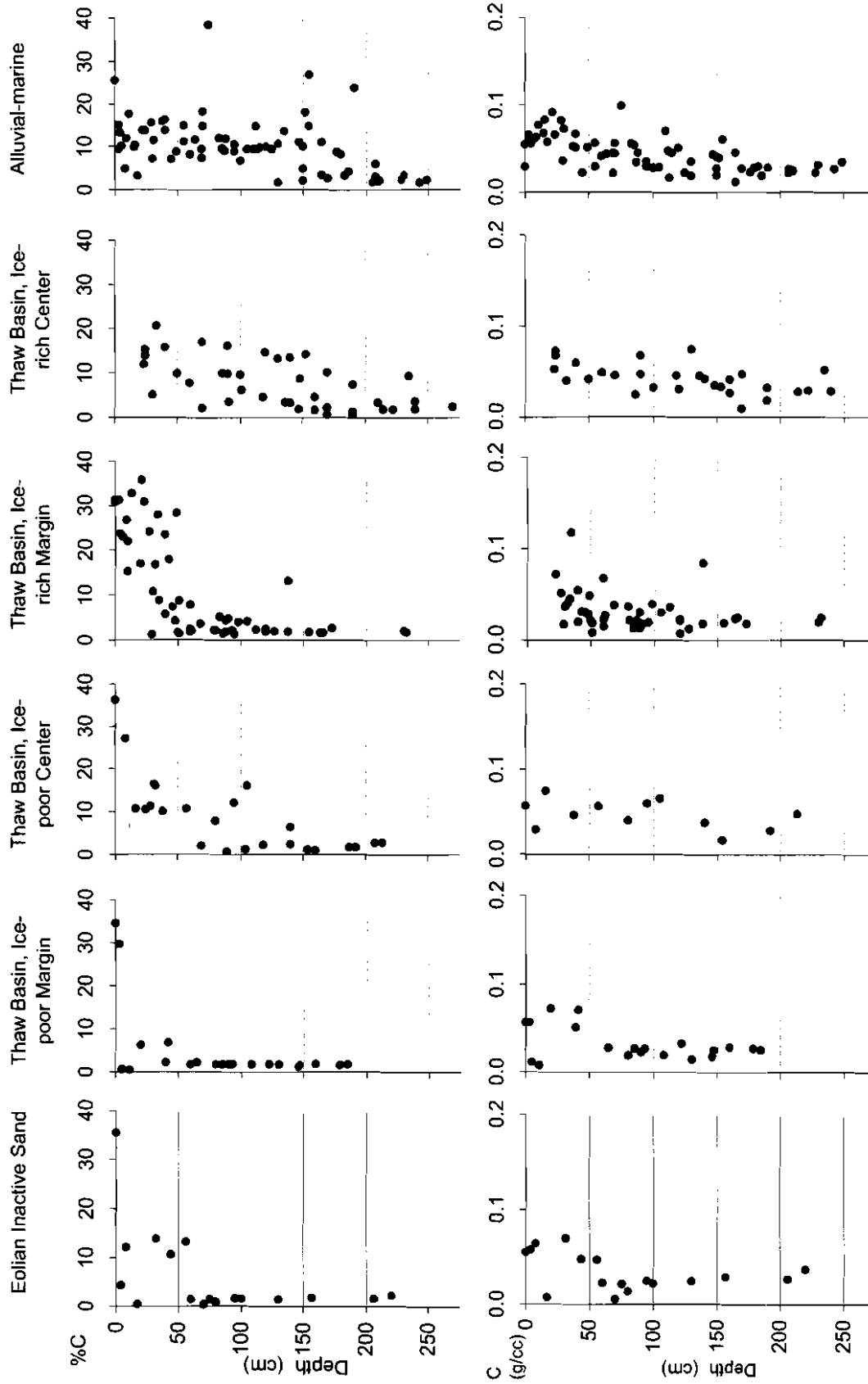


Figure 13. Depth profiles of % carbon and carbon density by surface terrain unit, Northeast Planning Area, NPRA, 2002.

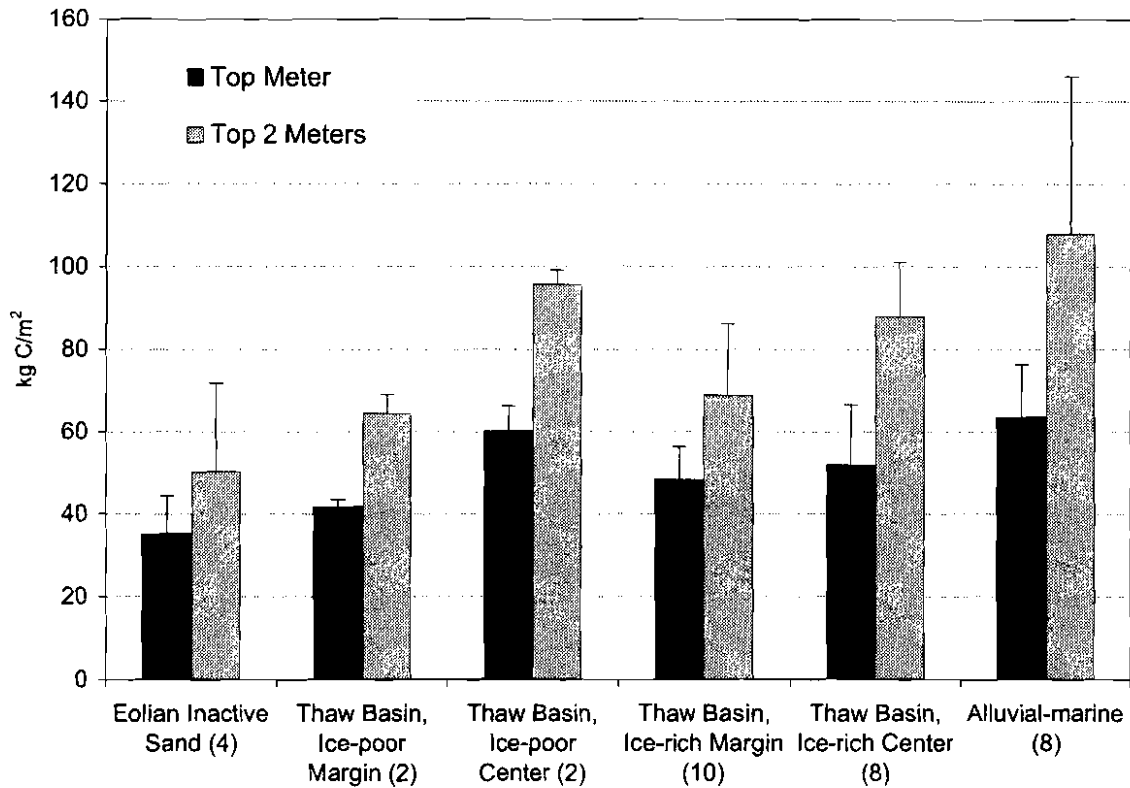


Figure 14. Mean carbon stocks by surface terrain unit, Northeast Planning Area, NPRA, 2002.

thaw basin centers ( $29.0 \pm 12.7$  cm), and ice-poor thaw basin centers ( $27.2 \pm 12.7$ ).

We attribute the greater thaw depths in the eolian inactive sands to soil thermal properties, particularly low moisture contents, the associated low latent heat of fusion, and higher heat conductivity due to low soil organic contents. Thaw depths in inactive sands occasionally exceeded the length of our thaw probe (130cm) and were set to 150 cm for the purpose of calculating a mean thaw depth value. In comparison, thaw depths in active sands were measured up to 172 cm. Moderate thaw depths in the ice-poor and ice-rich thaw basin margins, despite thick surface organic layers, presumably were due to the presence of standing water at the surface that increases absorption of solar radiation and increases thermal conductivity of material. The relatively low thaw depths in ice-rich thaw basin centers and alluvial-marine deposits presumably were due to their elevated, relatively well-drained, surfaces with abundant vegetation and litter, which

reduces heat conduction during the summer months.

#### Ice Volume

To evaluate the distribution of ground ice, we compared the volumes of segregated ice among ice structures, lithofacies (texture/structure classes), and surface terrain units. Among ice structures, mean ice volumes determined from laboratory analysis were highest for layered ice (77%) and organic-matrix ice (73%), intermediate for reticulate ice (71%), ataxitic ice (70%), and veined ice (69%), and lowest for lenticular ice (59%) and pore ice (45%) (Figure 15).

These data show that ice volume is closely related to ice structure and that the ice structure classification alone is valuable for estimating ice volumes. Indeed, the classification is better than visual assessments for estimating ice because we found a poor correlation between our visual estimates and laboratory values. Mean ice volumes in this study were similar to results obtained for the coastal plain near Prudhoe Bay

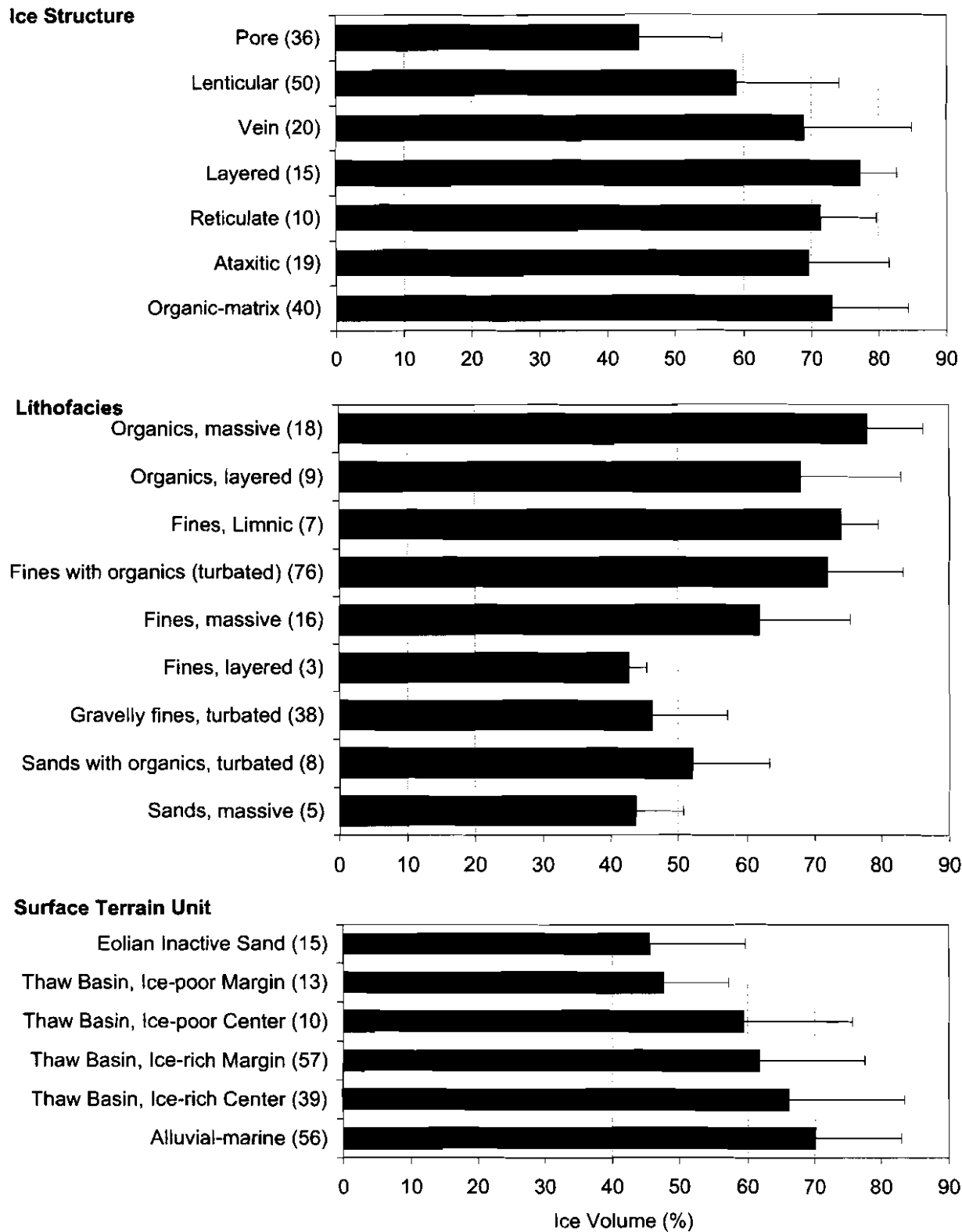


Figure 15. Mean ( $\pm$  SD) volumetric ice contents grouped by primary ice structure (top), lithofacies (middle), and surface terrain unit (bottom), Northeast Planning Area, NPRA, 2002.

and Kuparuk for organic matrix ice (84%), layered ice (81%), reticulate ice (74%), vein ice (70%), lenticular ice (65%), and pore ice (50%), but were somewhat lower than the value for ataxitic ice (83%) there (Burgess et al. 1999).

Among lithofacies, the mean volume of segregated ice was highest in massive organics (78%), intermediate in fines with organics (72%) and layered organics (68%), and lowest in massive sands (43%), layered fines (43%), and layered sands (40%) (Figure 15). Ice volumes at saturation for pure mineral soils were assumed to be in the range of 40–48%, based on porosity of the silts and fine sands. Thus, volumes above this range represent excess ice (above what the soil would contain at saturation). The large differences in ice content among lithofacies demonstrate that particle size and organic content exert large effects on ice development, although the small sample size resulted in large standard deviations in ice content.

Among terrain units, mean ice volumes were highest in alluvial-marine deposits (71%) and ice-rich thaw basin centers (66%), intermediate in ice-rich thaw basin margins (62%) and ice-poor thaw basin centers (59%), and lowest in ice-poor thaw basin margins (48%) and eolian inactive sand (45%) (Figure 15). These values do not include massive ice deposits (ice wedges were avoided during sampling) in near-surface sediments (1–3 m). Mean ice volumes in this study were similar to results obtained for the coastal plain near Prudhoe Bay and Kuparuk for alluvial plain (76%), ice-rich thaw basins (74%), and ice-poor thaw basins (58%) (Burgess et al. 1999).

Soil ice volumes generally decrease with depth as soils become dominated by massive sands and massive turbated gravelly fines (Figure 16). Ice volumes decrease rapidly with depth in terrain units with thin layers of surface material over the underlying sand sheet (ice-poor and ice-rich thaw basin margins and eolian inactive sand). In other terrain types, ice volumes are high throughout the top 1.5–2 m of the profile. In deeper coring, Lawson (1983) found ice-rich sediments generally were limited to the upper 3–5 m of coastal plain deposits in the Fish Creek area.

#### Accretion Rates

The rates of accumulation (accretion) of materials were determined using radiocarbon

samples obtained from the base of the surface organic deposits (Figure 17). Dates for basal peat were the oldest in alluvial-marine deposits (mean calibrated age range 9580–16,225 BP,  $n = 3$ ) and eolian inactive sands (8810 BP,  $n = 1$ ). Accretion rates (organic and mineral materials) were lowest in the eolian inactive sands, (0.06 mm/yr) and alluvial-marine deposits ( $0.12 \pm 0.05$  mm/yr). In the ice-rich thaw basin centers, basal peat dates were variable (5075–8315 BP,  $n = 2$ ) and accretion rates were  $0.26 \pm 0.04$  mm/yr. In ice-poor thaw basin centers, one core was sampled and yielded a basal carbon date of 10,310 BP at 195 cm and 4670 BP at 19 cm (the bottom of the organic horizon in the active layer). The accretion rate calculated from this interval was 0.26 mm/yr. At this particular site, much of the accreted material was mineral soil that may have been deposited by overbank flooding from a nearby abandoned stream channel. Dates from ice-rich thaw basin margins were younger than other terrain types (840–5435 BP), and estimated accretion rates were the highest of the five terrain types sampled ( $0.43 \pm 0.26$  mm/yr). We attributed the higher accretion rate to higher organic matter accumulation.

## LANDSCAPE CHANGE

### LAKESHORE EROSION

Shoreline erosion and waterbody contraction in three small study areas (1450 ha) during the 46–56 year period from 1945–1955 to 2001 were evaluated using photogrammetric analysis (Figure 18). Shoreline erosion rates were greatest in large, deep lakes. These lakes were more prevalent across the landscape and covered a mean of 26.6% of the three study areas (range 14.6–40.4%). Shallow lakes covered a mean of 6.2% (range 5.0–7.8%) in the three map areas (Figure 19) and typically were small (<5 ha). Overall, 0.7% (range 0.4–0.9%) of the land in the three study areas was lost to shoreline erosion. The average annual erosion rate for the three study areas ranged from 0.008–0.017 %/yr of total land area (mean = 0.013 %/yr).

Shoreline erosion was evident in both deep and shallow lakes. Preliminary observations indicated that the amount of erosion depended on type of deposit encountered along the shoreline, and that erosion was most prevalent in ice-rich

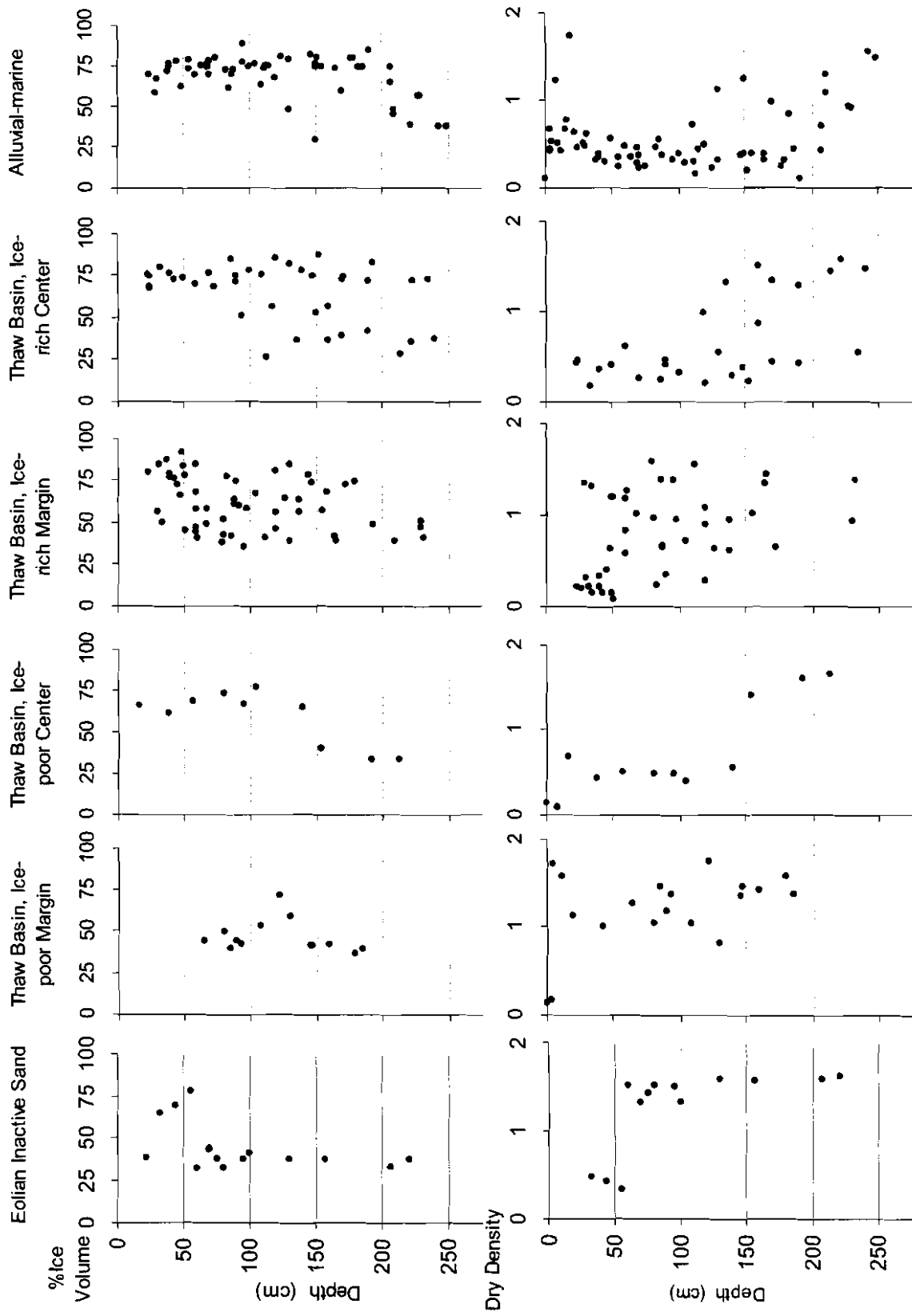


Figure 16. Depth profiles of volumetric ice and dry density by surface terrain unit, Northeast Planning Area, NPRA, 2002.

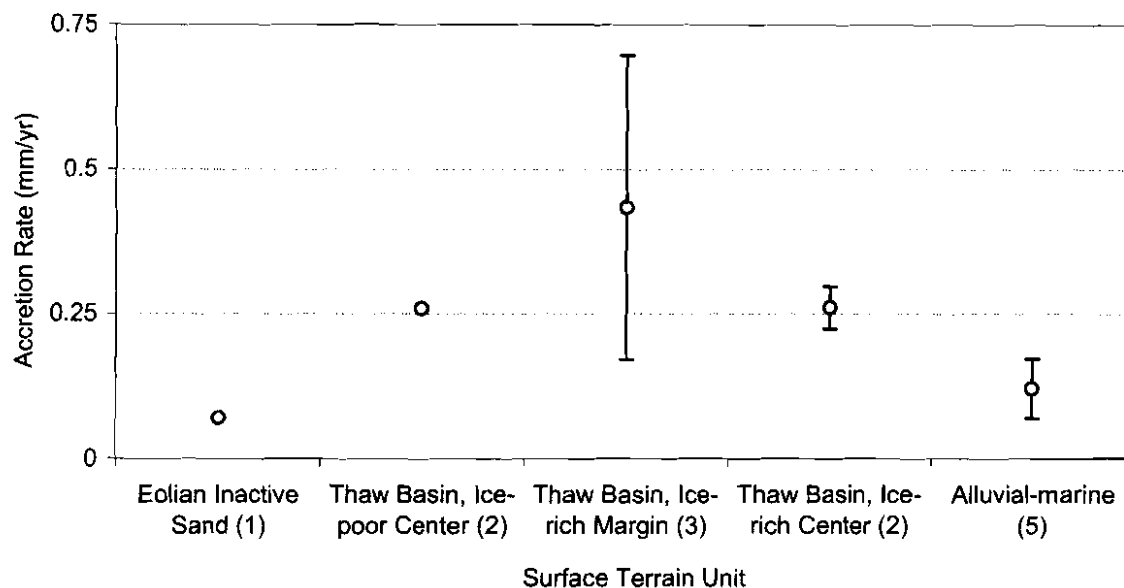


Figure 17. Mean accretion rates (mm/yr) of surface materials (organic, mineral, ice) by surface terrain unit, Northeast Planning Area, NPRA, 2002. Accretion rates were calculated by dividing depth by calibrated radiocarbon age.

thaw basin deposits. This results because most shorelines were comprised of ice-rich thaw basin deposits. However, erosion also was observed in coastal plain deposits (alluvial-marine, alluvial terrace, and eolian inactive sand). The maximum observed erosion rate was 0.8 m/yr, but in most areas erosion rates were much lower (Figure 18).

A striking feature of the change analysis was the decrease in size of many small, shallow lakes. We attribute this size change to high water levels in 1945 and to difficulties in interpreting shorelines due to the poor quality of the 1945 photography. Close examination of the photographs revealed that much more water was in tundra polygons and flooded tundra areas in 1945 than in 2001. Low quality of the 1945 photography also was a factor; photo-interpretation of shorelines was reliable for deep water bodies where contrast was high, but was difficult in areas where the shoreline was indistinct or gradational onto flooded tundra. We concluded that the apparent decrease in waterbody size was due primarily to water level changes and limitations of the mapping procedures, rather than contraction of waterbodies due to infilling or heaving of the surface by ice aggradation.

The erosion rates we observed can be used to estimate the ages of the lakes, based on the

assumption that the rate of erosion was constant over both time and space. Using the recent rates of erosion, and assuming the lakes eroded out from a central point, the waterbodies would have required 2466 years (range 1995–2875 years) to reach their present sizes. Extrapolated into the future, it would take an additional 5895 years (range 3068–9897 years) to erode all the remaining land. Thus, over a period of 8361 years (range 5961–12,427) the landscape could be completely reworked from 100% terrestrial to 100% water. Of course, this process does not occur in a linear fashion and numerous factors exist that cause erosion rates to vary in both time and space. Our data suggest that erosion rates increase in proportion to lake area. As a result, this simplistic approach tends to overestimate the age of the lakes and underestimate the time to complete the erosion. Nevertheless, the results provide a rough guide to the age of the lakes, and the rate at which erosion can affect the remaining land.

To evaluate the precision of our shoreline change measurements, we calculated the precision of the co-registration of the old and recent photographs. Mean ( $\pm$  SD) positional errors between photographs were  $2.6 \pm 1.8$  m in the west,  $1.7 \pm 1.7$  m in the central, and  $2.5 \pm 1.8$  m in the

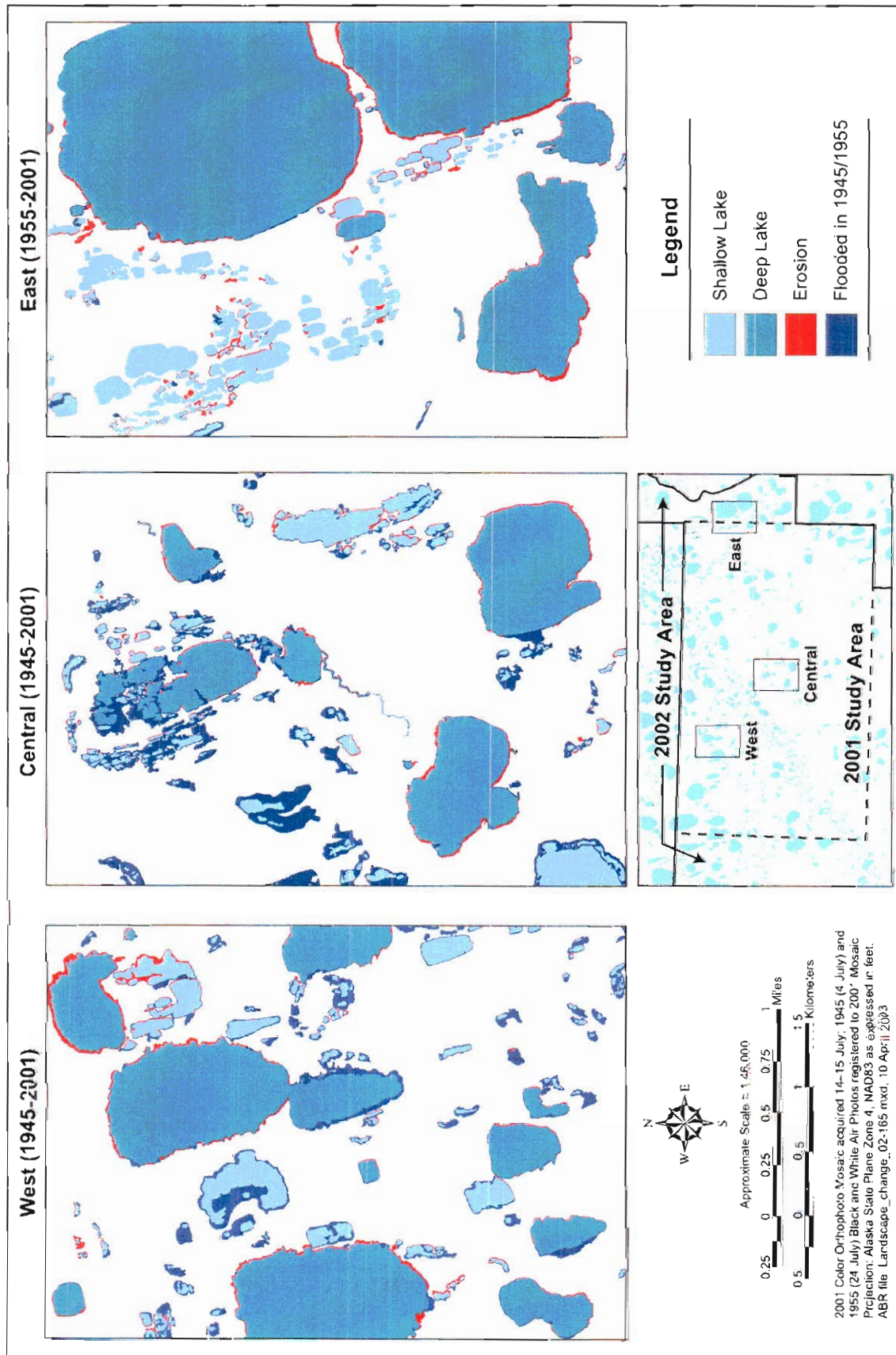


Figure 18. Map of changes in lake shorelines from 1948 to 2001, Northeast Planning Area, NPRA, 2002.

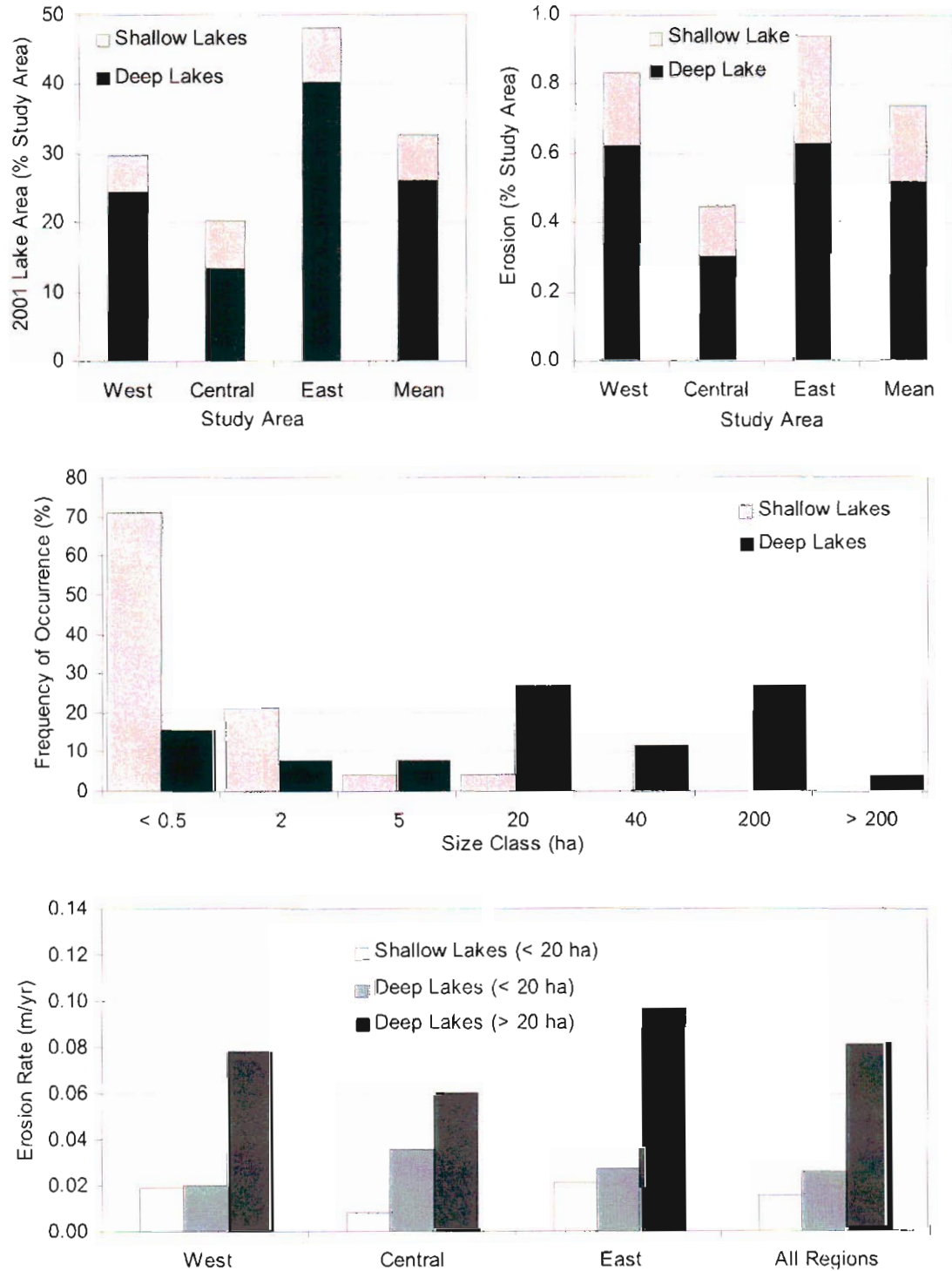


Figure 19. Waterbody characteristics of eroding lakes in the Northeast Planning Area, NPRA, 2002. Percentage of deep and shallow lakes (top) and their frequency by size class (second from top) are for the year 2001. The percentage of area eroded (second from bottom) and the mean annual rate of shoreline retreat (bottom) are based on changes over 56 years for the western and central areas and 46 years for the eastern area.

east regions of the study area. While these errors are small, a substantial portion of the shoreline changes was within our measurement precision.

In summary, the measurements of shoreline change indicated that erosion is still an active process and continues to alter the landscape. Examination of the distribution of indicators indicates that reworking of the surface by erosion is mostly confined to the pre-existing basins.

#### ICE WEDGE DEGRADATION

The degradation of ice wedges was evaluated using four approaches. First, we documented ice-wedge and active-layer characteristics at several exposures to assess potential for thermokarst. Second, we examined surface conditions at nine locations to look for vegetative and microtopographic indicators of subsidence. Third, we examined soil cores over degrading ice wedges at the same nine locations to determine whether the thawing front had encountered wedge ice. Fourth, we performed photogrammetric and spectral analyses using photography from 1945 and 2001 to evaluate the changes in surface-water distribution as an indicator of thermokarst development along the polygonal network of ice wedges.

Ice wedges in old upland terrain (alluvial-marine deposit, old alluvial terrace) typically were 2.5–3 m across at the top (Figure 20). Depths of the ice-wedges were not determined, but we estimated the wedges extended 3–4 m deep. The ice wedges were capped by 35–45 cm of organic and mineral soil. Thaw depths in the active layer above the wedges typically were 30–40 cm, leaving 5–10 cm of frozen soil above the wedge ice. Based on the stratigraphy at these exposures, we expect that ice wedges can remain stable under modest thermal changes because there is a small amount of additional soil that can be incorporated into the active layer to protect the wedge ice if thawing is increased in the active layer. There is, however, only a limited ability to readjust to large thermal changes or surface disturbance before the thawing front encounters wedge and degradation and thaw settlement is initiated.

Surface indicators of recent thermokarst at nine locations included: (1) increased greenness of tussocks in shallow troughs indicating changing

nutrient regimes, (2) presence of recently killed tussocks in deeper troughs, (3) changes in vegetation to hydrophytic graminoids and mosses, (4) presence of surface cracks along the margins of the troughs indicating slumping, and (5) ponding of water (Figure 21). Of particular interest was the occurrence of recently drowned tussocks in a few of the troughs that we examined. Tussocks can be centuries old (Fletcher and Shaver 1983) and typically develop on surfaces that are at least 1500 yrs old (Jorgenson et al. 1998). Similarly, formation of large ice wedges takes 1500–3000 years (Jorgenson et al. 1998). This evidence indicates that the partial thermokarst we observed is a recent phenomenon and that the ground surface was for the most part stable (allowing readjustment to minor changes) for >1000 yrs prior to the recent degradation. The surface characteristics in the degrading troughs also provided an indication of how fast settlement is occurring. We interpreted areas that had standing water over dead tussocks to be rapidly degrading. In contrast, some troughs had vigorous stands of sedges (*Carex aquatilis* and *Eriophorum angustifolium*) that were colonizing soils normally associated with tussock tundra, indicating slow degradation and successional change. Water was evident in only a small proportion of the troughs that we interpreted to be degrading.

Shallow soil cores (<1 m) were obtained at nine locations that spanned a range of thermokarst development from initial stages of settlement that were barely perceptible to deep (1.2 m) thermokarst pits at the intersections of ice-wedge polygons (Figure 21). The thickness of unfrozen and frozen layers of the soils over the wedge ice averaged 36.2 cm and 43.8 cm, respectively. The mean thickness ( $\pm$ SD) of the frozen soil over the ice wedges was  $7.7 \pm 3.4$  cm. The minimum amount of frozen soil above the wedge ice was 3 cm. Ice structures in the frozen soil above the wedge ice were dominated by fine, wavy lenticular ice, with lesser amounts of medium thick (3–5 mm) layered ice and organic-matrix ice.

The occurrence of a thin layer of ice-rich, frozen soil above the ice wedges indicates that degradation of the ice wedges did not occur in 2001 (at least by mid-August) and that the degradation must have occurred during other recent years. Because the active layer completely

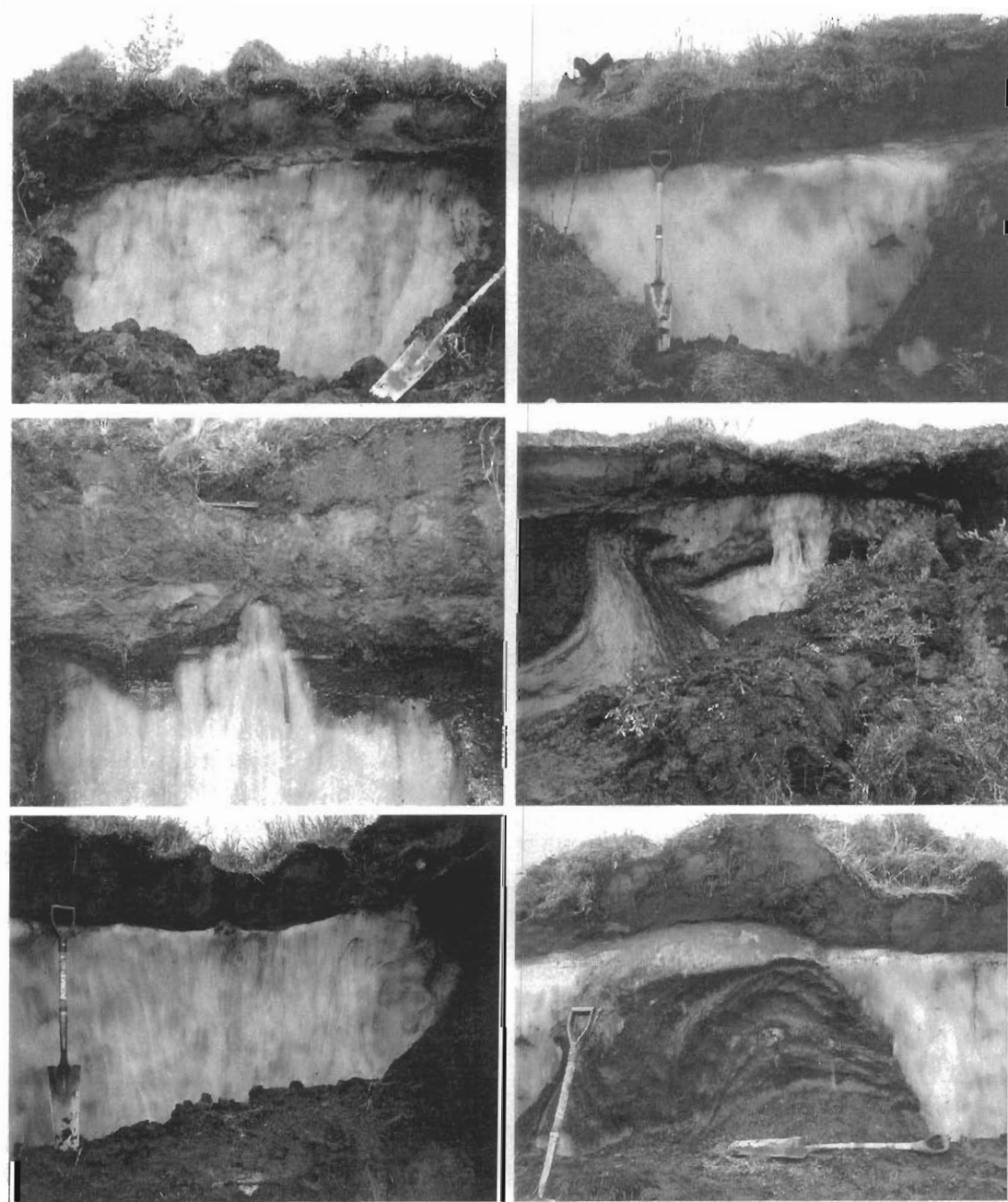


Figure 20. Views of ice wedges at bank exposures illustrating the thin layer of organic and mineral material over massive ice, and sediment deformation between ice wedges, Northeast Planning Area, NPRA, 2002.

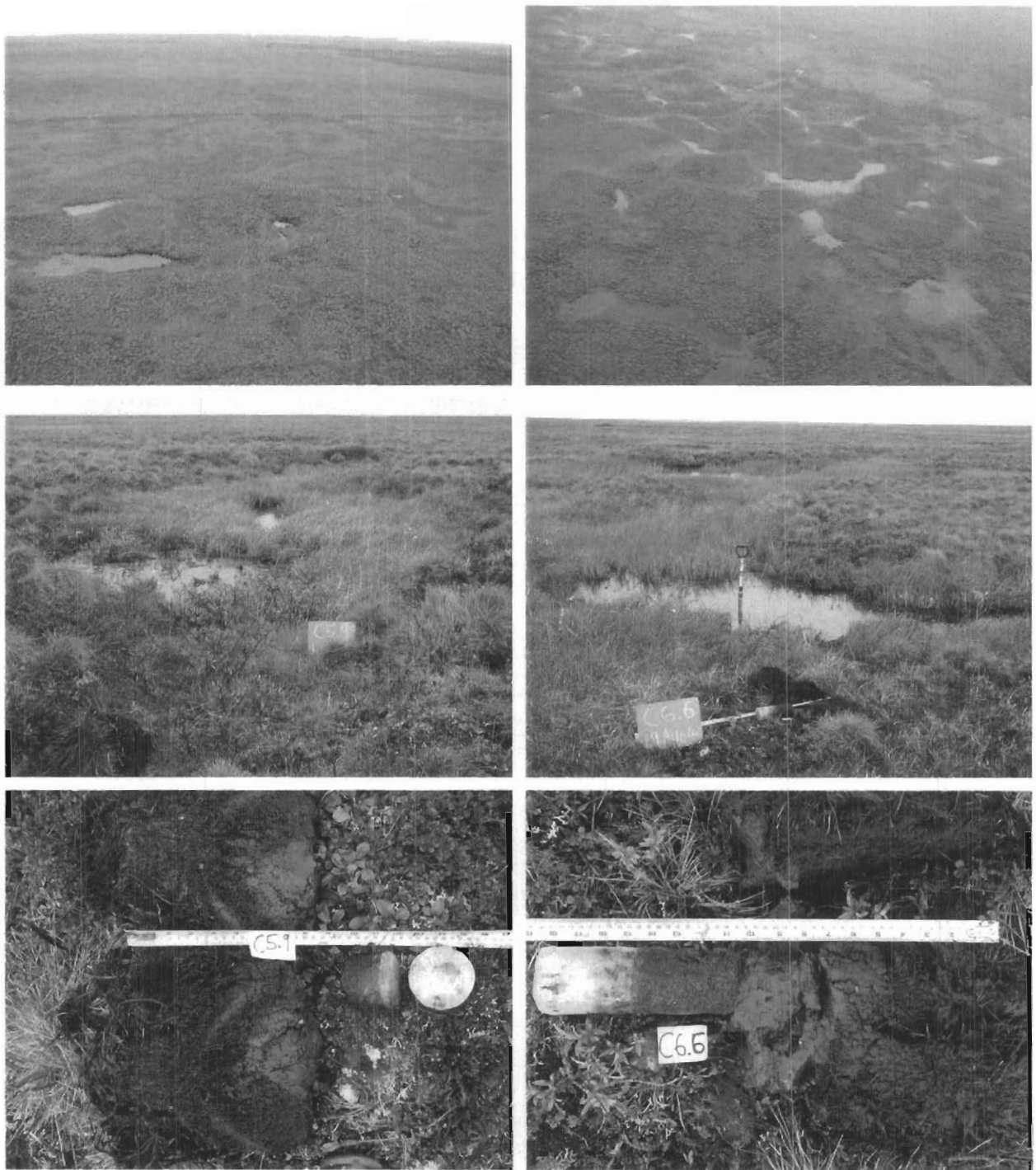


Figure 21. Oblique aerial views and ground views at two sites (T6 and T5) illustrating degradation of ice wedges. Photographs of soil stratigraphy illustrate the presence of a thin layer of frozen soil above the massive ice, Northeast Planning Area, NPRA, 2002.

refreezes during the winter, degradation is not a continuous process but occurs only during relatively warm years. While the observations indicate ice wedge thawing is sensitive to short-term variations in climate (temperature and snow depth), stratigraphic evidence also indicates that organic matter accumulation at the surface over a longer-term may help stabilize wedges where thaw settlement is slow. Several troughs had robust wet sedge meadow vegetation and thick accumulations of sedge peat indicating that vigorous plant growth and organic accumulation at the surface may have been sufficient to stabilize the surface. Thus, there are counteracting microclimatic processes of increased water impoundment that increases soil heat gain and increased sedge and moss growth that decreases soil heat gain, making the process unpredictable. Consequently, we are not able to conclude whether the observed changes are the initial stages of catastrophic degradation or an evolutionary stage of ice wedge development where the surface undergoes continual hydrologic, pedologic, and vegetative readjustment to moderate climatic changes.

To assess the extent of ice wedge degradation we performed a spectral classification of small waterbodies (excluding permanent deep lakes and ponds delineated by the ITU mapping) to quantify the areal extent of "terrestrial" terrain that was flooded only in 1945, only in 2001, and in both years (Figures 22 and 23). Terrestrial terrain covered 20.2% of the area in the central map area (1450 ha) and 30.0% in the western map area (1450 ha), for a combined total of 25.1% for both map areas. In the central map area, 14.1% of the terrestrial terrain was flooded only in 1945, 3.5% only in 2001, and 1.9% in both years. In the western map area, 13.2% of the terrestrial terrain was flooded only in 1945, 4.3% only in 2001, and 2.5% in both years.

Larger-scale views of the photography reveal dramatic changes in the distribution of flooded tundra that are associated with the changes in areal extent of flooding. In upland areas (typically having high-centered, high-relief polygons and mixed polygons and pits), most isolated, flooded low-centered polygons visible in 1945 were not flooded in 2001 (Figure 24). The 2001 photos also revealed numerous new linear waterbodies that

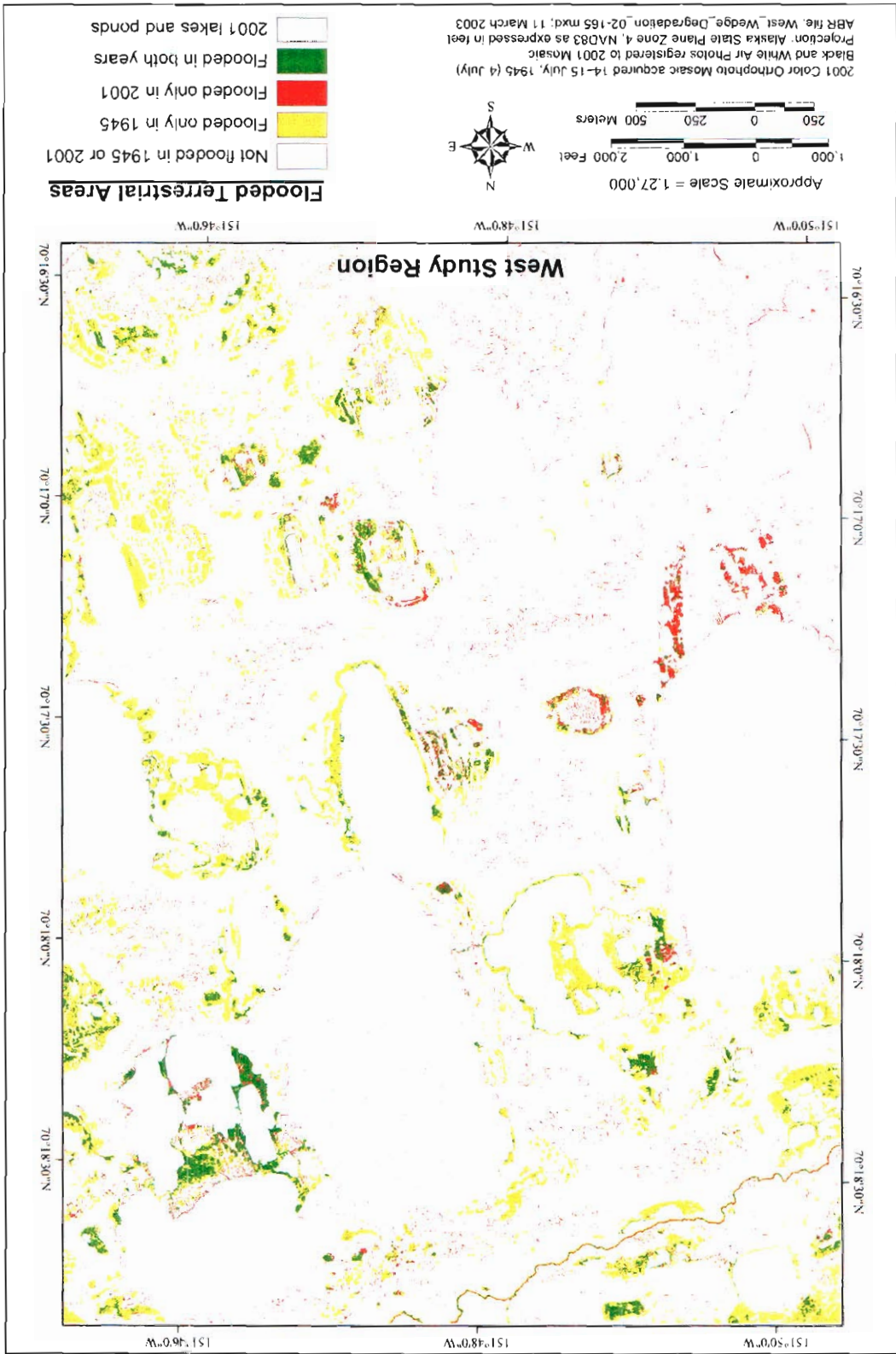
have primarily formed at the intersection of polygonal troughs. In lowland, ice-rich terrain (usually having low- and high-centered polygons), similar differences between 1945 and 2001 were apparent (Figure 25). Flooding of polygon centers was much less extensive in 2001, while the polygonal trough network appeared to be extensively flooded compared to conditions in 1945.

To better understand changes in flooding and to link the flooding to ice-wedge degradation, the extent of flooding was analyzed by terrain unit and then grouped by upland and lowland terrain (Figure 26). In the central and western map areas, flooding of higher upland areas on alluvial-marine deposits and domed ice-rich centers of drained basins was much less than for low-lying areas in the margins of ice-rich and ice-poor basins. When both map areas were combined, the extent of flooding in upland areas was 1.7% in 1945 only, 4.3% in 2001 only, and 0.1% in both years. In lowland areas, flooding covered 16.2% of the terrestrial area in 1945 only, 3.5% in 2001 only, and 2.7% in both years. Overall, flooding covered 13.7% of the terrestrial area (larger waterbodies excluded) in 1945 only, 3.8% in 2001 only, and 2.2% in both years.

Results from both ground observations and photogrammetric analysis indicate that there has been extensive degradation of the surfaces of ice wedges along the polygon trough network over a 57-year period. Assuming that the new linear-shaped waterbodies that were prevalent during a relatively dry year in 2001 were due to ice-wedge degradation, the degradation has affected at least 3.8% of the terrestrial landscape. The waterbody coverage provides only a minimum estimate, however, because ground observations indicated that many polygonal troughs over ice-wedges had indications of subsidence, yet were not sufficiently low to be covered by water. Assuming that ice wedges occupy 10–20% of the volume of near surface terrestrial deposits, the analysis indicates that at least 20–40% of the ice wedges have undergone partial degradation.

This analysis also has revealed that degradation has caused a substantial redistribution of surface water from the centers of low-centered polygon to the adjacent trough network. This redistribution of water which presumably lowers

Figure 22 Changes in flooded areas in the west change study region 1945 and 2001 used to differentiate areas of thermokarst, Northeast Planning Area, NPRA, 2002.



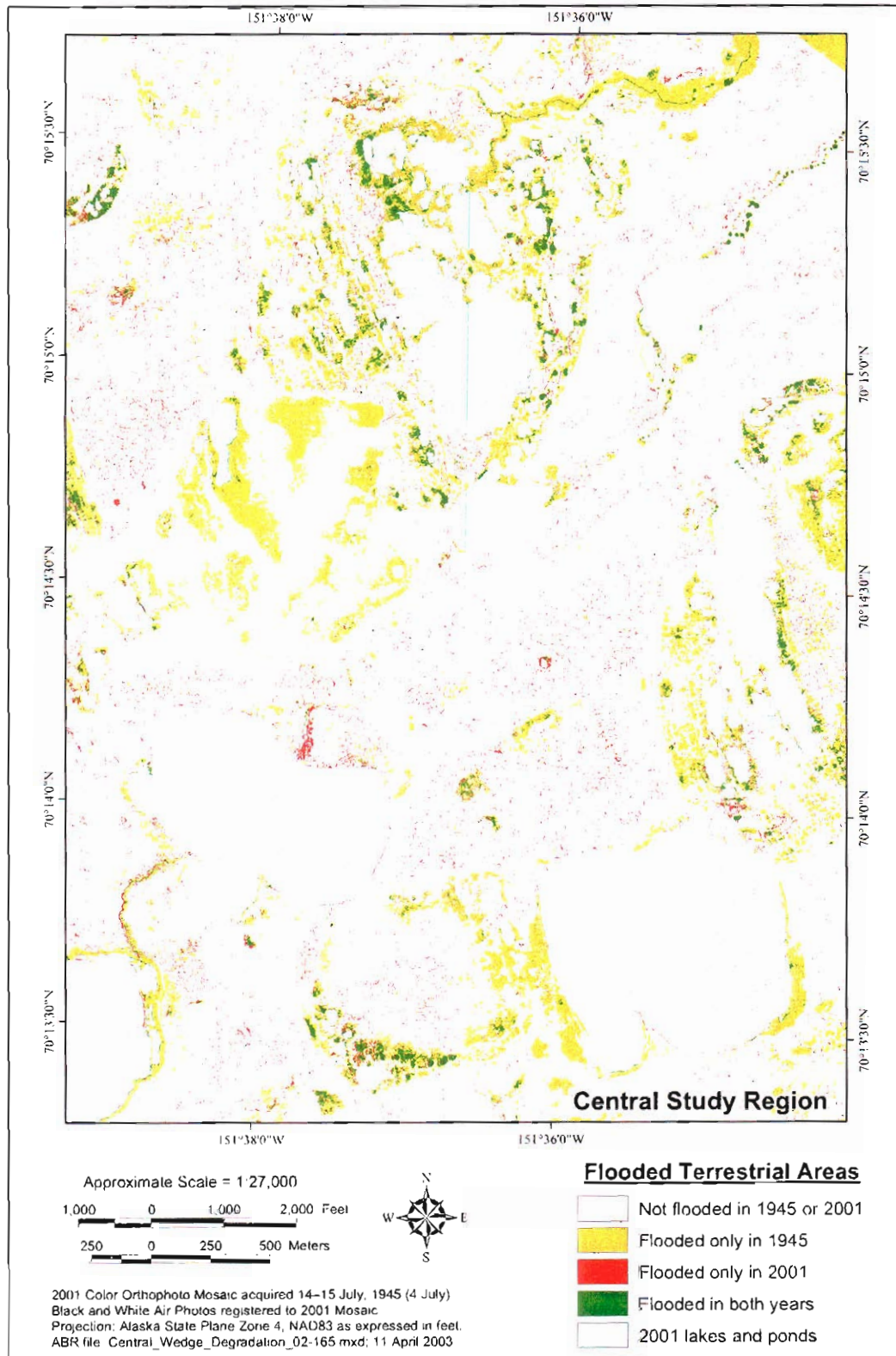


Figure 23. Changes in flooded areas in the central change study region between 1945 and 2001 used to differentiate areas of thermokarst, Northeast Planning Area, NPRA, 2002.

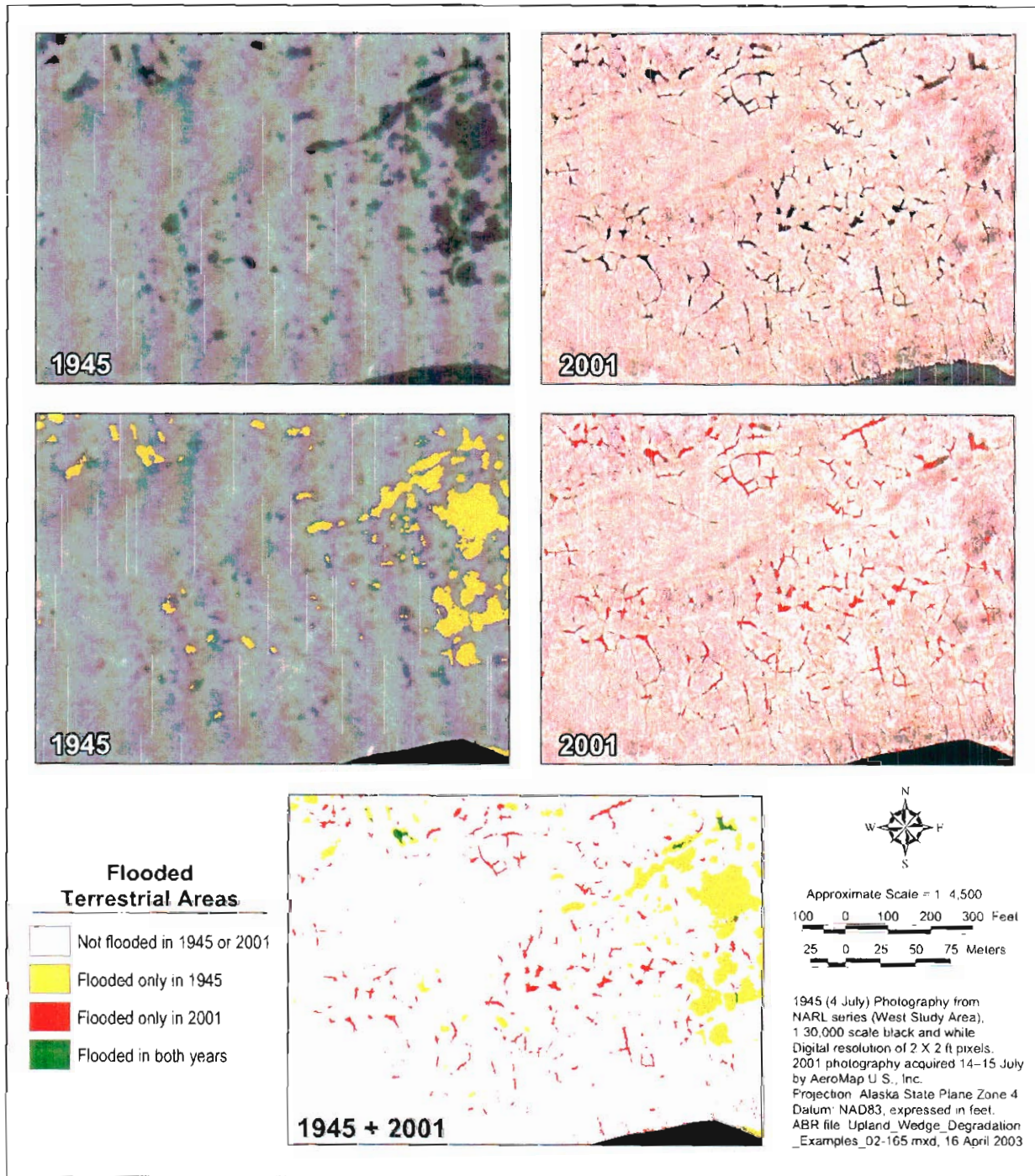


Figure 24. Aerial photographs from 1945 and 2001 (top), maps of waterbodies classified by spectral classification (middle), and a map of waterbody change (bottom) for uplands in the west study region, Northeast Planning Area, NPR, 2002.

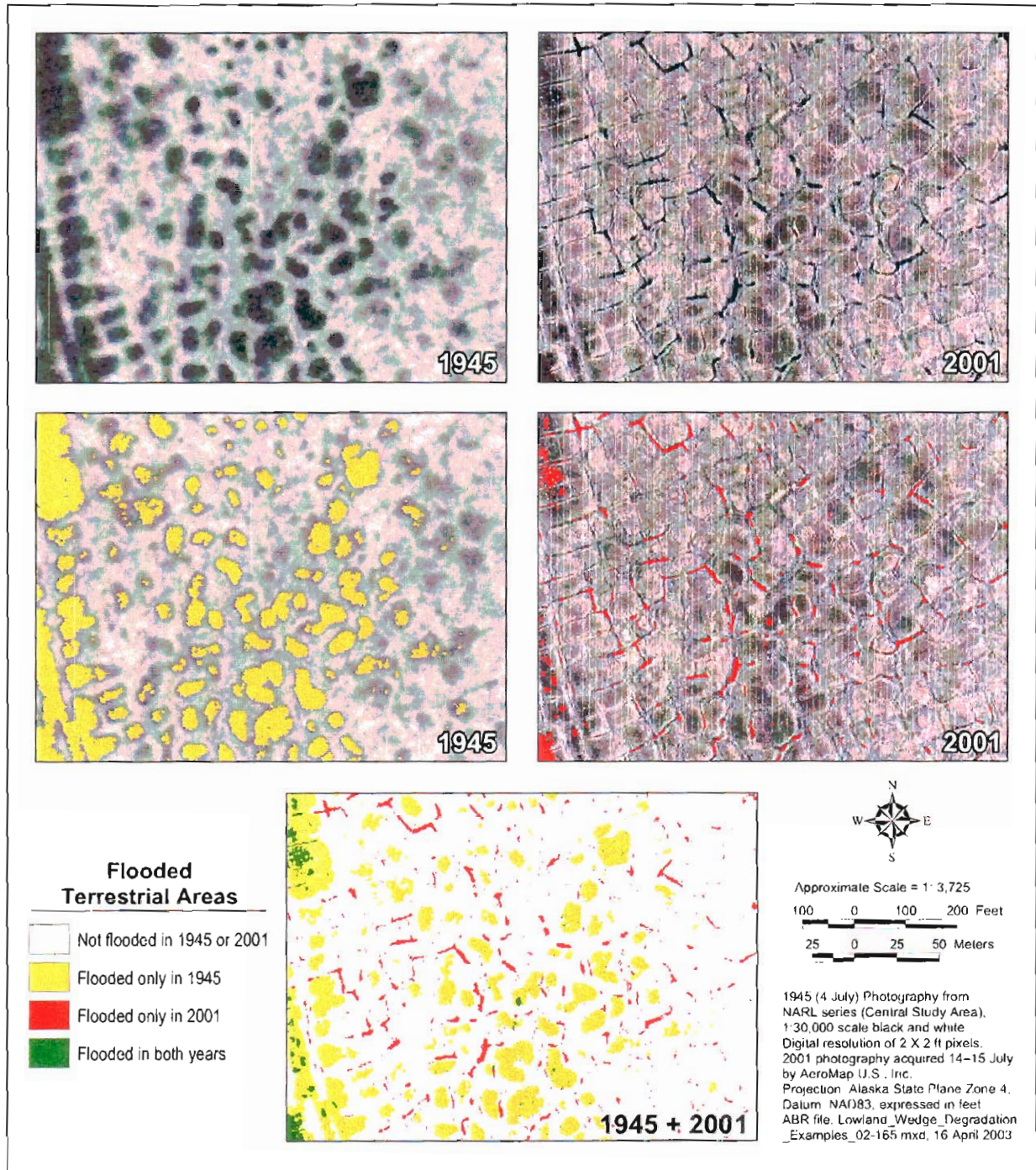


Figure 25. Aerial photographs from 1945 and 2001 (top), maps of waterbodies classified by spectral classification (middle), and a map of waterbody change (bottom) for lowlands in the central study region, Northeast Planning Area, NPRA, 2002.

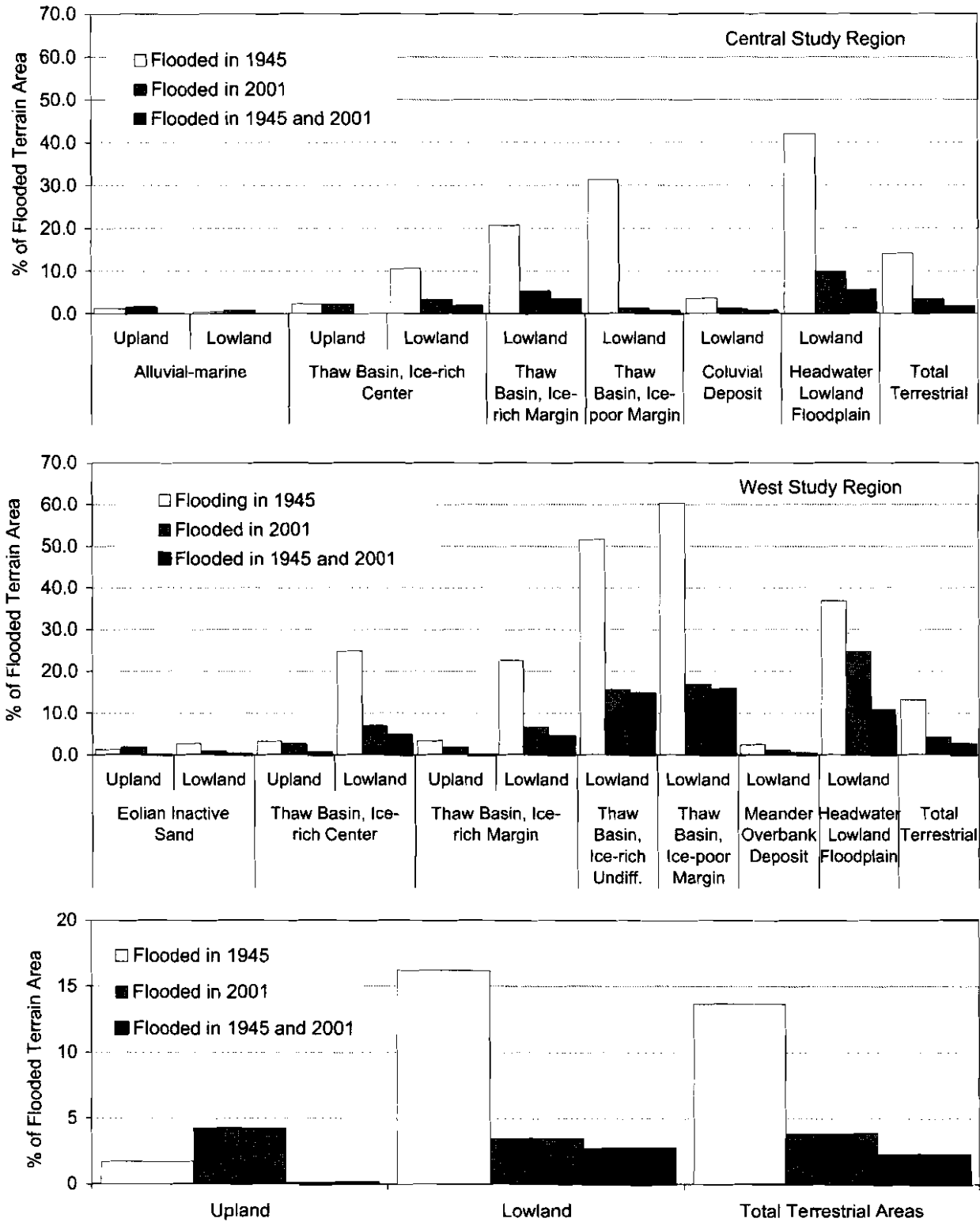


Figure 26. Summary of changes in flooded areas by terrain unit grouped by upland and lowland terrain unit, for the central and western map areas, Northeast Planning Area, NPRA, 2002.

the water table in the tundra adjacent to the troughs has important implications for plant community changes, soil respiration, and release of trace gases.

We attribute the degradation of ice wedges to warm temperatures during 1989–1998. Climatic records for Barrow indicate that mean annual temperatures were substantially warmer in 1989 (-10.2 °C), 1993 (-10.2 °C), and 1995–1998 (-8.4 to -10.9 °C) than the long-term (1921–2002) average (-12.3 °C). Indeed, four of the five highest mean annual temperatures in the historical record occurred during this period (Figure 27). On a decadal basis, the ten-year running average had an initial peak of -11.2 °C centered around 1939, decreased during the mid-1950s to mid-1970s to a low of -13.2 °C around 1973, and increased to -10.5 °C around 1997. Thus, the ten-year running average indicates a general warming trend of nearly 2 °C from the mid-1950s to mid-1970s to the 1990s. Similarly, permafrost temperatures along the Arctic Coastal Plain near Prudhoe Bay indicate that permafrost has warmed by 2–3 °C since the mid-1980's (Romanovsky and Osterkamp 1997, Osterkamp 2002). Over the whole recorded period, however, regression analysis indicates mean annual air temperatures have only increased at a rate of 0.6 °C/80 yr (1921–2002). Based on qualitative examination of other aerial photography obtained in 1979 (this area) and 1984 (Kuparuk oilfield) that lacked the prominent waterbodies along the ice-wedge polygon network and the substantial increase in recent air and ground temperatures, we conclude that most of the degradation we have observed occurred during 1989–1998, when mean annual air temperatures were frequently 2–4 °C above the long-term average. In contrast, in 2001, when the mean annual air temperature was -12.0 °C and near the long-term average, stratigraphic evidence indicates no degradation occurred.

The long-term outcome of the ice wedge degradation, however, remains uncertain. While we have documented partial degradation of the surface of the ice wedges, minor thaw settlement, and hydrologic changes, we believe the surfaces above ice wedges have a limited ability to readjust to changing conditions through increased vegetation production and organic matter accumulation at the surface. Thus, there are counteracting microclimatic processes of increased

water impoundment that increases soil heat gain, and increased sedge and moss growth that decreases soil heat gain, making the process unpredictable. Furthermore, soil coring in 2001 revealed the presence of a thin layer of frozen soil above the ice wedges indicating no ice wedge degradation occurred in 2001 and that degradation is not a continuous process. Given that the ice wedges have persisted for thousands of years under only a thin soil cover, ice wedges appear to be able to adjust to modest climatic changes. On the other hand, if the degradation we observed was directly linked to the warm years during 1989–1998, when mean annual air temperatures frequently were 2–4 °C above the long-term average, then ice wedge degradation likely will increase during the next century if arctic air temperatures increase by 3–8 °C as expected.

#### CONCEPTUAL MODEL OF THE EVOLUTION OF LAKES AND DRAINED BASINS

The oriented lakes of the Arctic Coastal Plain of Alaska have long fascinated scientists because of their importance to ecological processes (Hobbie 1984) and permafrost dynamics (Hopkins 1949, Sellman et al. 1975), their striking pattern (Cabot 1947, Black and Barksdale 1949, Livingstone 1954), apparent cyclic occurrence (Cabot 1949, Britton 1957), and uncertainty about their origins (Carson 1968). While a thermokarst origin for the majority of lakes has been frequently postulated, the specific mechanisms of ice aggradation and degradation and of lake orientation remain controversial.

Numerous concepts of a “lake cycle” have been proposed, but most lack complete descriptions of the processes by which the surface returns to original conditions. A “lake cycle” was first proposed by Cabot (1947) based on interpretation of lake patterns evident on aerial photographs; this concept emphasized thaw pond formation and drainage and omitted ice aggradation in drained basins. Britton (1957) articulated a more complete “thaw lake cycle” that involved (1) initial flooding of basins, (2) lake expansion and coalescence through lateral mechanical erosion and thawing accompanied by material sorting, (3) drainage, (4) ice-wedge development in drained basins, and (5) secondary development of thaw ponds from ice-wedge

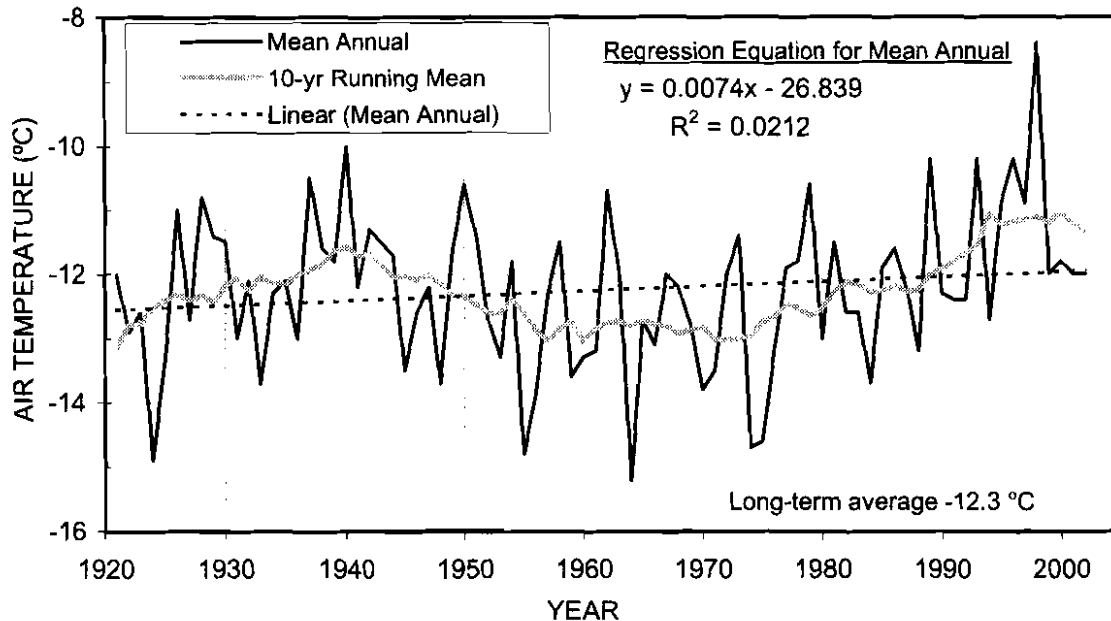


Figure 27. Mean annual air temperatures for Barrow Alaska, 1921–2002.

degradation. This concept provided little detail on the ice-aggradation process and does not complete the cycle by recreating the original upland surface. Carson (1968) described a “lacustrine cycle” that included (1) initial development of thaw ponds, (2) expansion and deepening of ponds through lateral erosion and subsurface thawing in a “youthful stage”, (3) basin elongation perpendicular to the wind due to long shore currents and thawing at the ends in a north-south direction during the “mature stage”, (3) drainage by stream migration, and (4) a secondary cycle of ponds on shelves behind barrier beaches and strands with persistence of the deeper central lake at the “old stage”. The role of ice-aggradation and the processes involved in return to the original surface are not included in his cycle. Everett (1980) defined a more complete cycle beginning with an ice-rich raised surface that includes (1) climate change or surface disturbance that initiates permafrost degradation, (2) degradation of ice wedges and development of small thaw ponds, (3) expansion of the thaw pond by surface and subsurface thaw, (4) expansion into large lakes by bank erosion and subsurface thawing accompanied by material sorting, (5) partial or complete drainage by stream capture or breaching, (6) and reestablishment of ice-wedges and surface

polygon patterns. Finally, Billings and Peterson (1980) described a “thaw-lake cycle” with 10 stages that is similar to Everett’s, but emphasizes the role of ice-wedge aggradation and degradation within basins.

While similar, the concepts vary in their explanations of lake formation, in the roles attributed to ice aggradation and degradation, and in their treatments of the return of surfaces to near-original conditions to complete the “cycle”. They all assumed that initial conditions had substantial ground ice and were favorable for thermokarst, an assumption that is problematic. Most authors recognized that sediments are sorted and redistributed during lake expansion, yet the importance of this redistribution to ground-ice dynamics has not been generally acknowledged. While attention has focused on ice-wedges, the nature and distribution of other types of ground ice have been overlooked. Finally, previous investigators have hypothesized that the surface returns to near-original conditions, thus creating a “cycle”, but have provided little stratigraphic evidence to support that concept. Consequently, the primary reason a consensus has not emerged on the concepts underlying the “thaw lake cycle” is that these studies have not been supported by the

quantitative data on topographic changes, soil stratigraphy, and ice volumes necessary to evaluate the physical processes associated with thaw-lake development.

In this report, we reevaluate the concept of the "thaw-lake cycle" based on detailed terrain analysis, field surveys, and photogrammetry. First, we used a terrain-unit approach to relate surficial materials to landform patterns (see section on Classification and Mapping). Second, we used results of our field surveys to compare differences in elevation and microtopography, sediment characteristics, and ice structure and volume among the terrain units (see section on Nature and Distribution of Ground Ice). Third, we quantified changes in waterbodies over time by comparing aerial photography from 1945–1955 and 2001 to help evaluate rates and patterns of lake development (see section on Lakeshore Erosion). We then synthesized this information to develop a modified conceptual model of the lake-basin evolution that incorporates information on both patterns and processes. While orientation is a prominent characteristic of lakes on the Beaufort Coastal Plain (Cabot 1947, Black and Barksdale 1949, Carson and Hussey 1962, Sellman et al. 1975), it is discussed only briefly here. The specific causes of lake orientation remain controversial, and orientation is not central to understanding of the evolution of lakes and drained basins across the coastal plain landscape.

We have revised the earlier conceptual models of lake-basin development to include six main stages of development (Figure 28): (1) initial flooding of primary lakes, (2) lateral expansion and sorting and redistribution of lacustrine sediments, (3) lake drainage, (4) differential ice aggradation in silty centers and sandy margins, (5) secondary development of thermokarst lakes in the centers and infilling ponds along the margins, and (6) lake stabilization. This conceptual model applies to most of the Beaufort Coastal Plain, where sand sheets blanket the surface. In the following discussion of the various developmental stages, we evaluate the stages in terms of topographic changes, soil stratigraphy, ice content, and relative ages.

We recognize that true thaw lakes can develop from degradation of older, upland surfaces, in areas with thick, extremely ice-rich deposits of eolian,

fluvial, or marine silt, but these areas are limited in extent in arctic Alaska. Examples of such arctic areas include the Colville River Delta (Jorgenson et al. 1998), the narrow coastal plain extending from Barrow to Cape Halkett that is underlain by marine silts and clays, the Seward Peninsula (Hopkins 1949) where loess during deglaciation has buried Pleistocene ice deposits. In addition, there are extensive areas of thermokarst in the Siberian Lowlands that also have thick accumulations of Pleistocene massive ice. For most of the Beaufort Coastal Plain, including most of the NPRA, Prudhoe Bay and Kuparuk region, and the Arctic National Wildlife Refuge, we propose an alternative conceptual model that is supported by extensive photogrammetric and soil stratigraphic data.

#### Initial Flooding of Low-lying Basins

Radiocarbon dating of lake sediments indicates that lakes have existed on the coastal plain only since about 12,000 years ago, when the climate became warmer and wetter after glacial conditions ameliorated at end of the Pleistocene (Hopkins et al. 1981; Rawlinson 1983, 1993). Most of the lakes appear to be less than 9000 years old (Rawlinson 1993). The lack of older lakes is attributed to cold, arid, and windy conditions and active eolian deposition near the end of the Pleistocene Era (Carter et al. 1987, Rawlinson 1993).

Eolian sediments are nearly ubiquitous across the Beaufort Coastal Plain; in most areas eolian deposition ceased and the ground surface was stabilized about 8000 years ago (Carter et al. 1984). In our study, basal peat from the oldest upland surfaces (alluvial-marine, old alluvial terrace, and eolian inactive sand deposits) yielded calibrated radiocarbon ages of 9460–9700, 10,260–10,690, and 15,870–16,580 BP. These dates are in agreement with the earlier studies indicating that surfaces stabilized near the beginning of the Holocene.

The onset of the earliest lake formation in our study is indicated by calibrated radiocarbon ages for basal organic material from the centers of two old, deep lakes that were 4850–5300 BP and 8200–8430 BP (Figures 6 and 7). This material is rich in algal remains and provides an age range for lacustrine material associated with initial lake

## LAKE BASIN EVOLUTION ON THE BEAUFORT COASTAL PLAN

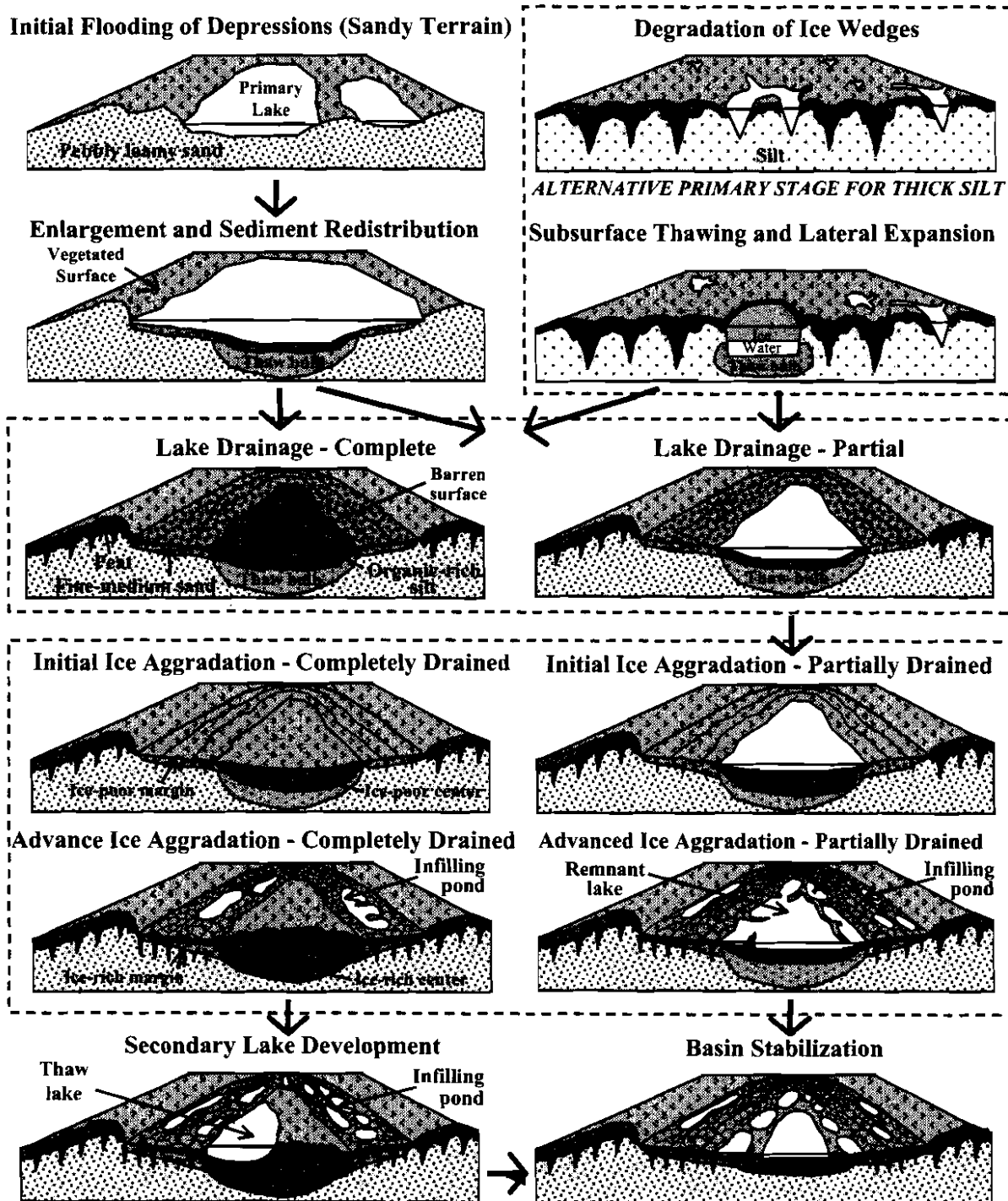


Figure 28. A conceptual model of lake-basin development on the Arctic Coastal Plain in the Northeast Planning Area, NPRA, 2002.

development. While the sampling is limited, the older dates indicate that the primary lakes formed soon after stabilization of the land surface during the early Holocene.

During the period when the sand sheets were stabilizing, ground ice content presumably was low because (1) the material was recently deposited, or there would not have been sufficient time to develop much ice; (2) the cold, dry landscape lacked water for ice-wedge development; and (3) the sandy sediments had low potential for development of both segregated and wedge ice. In our field surveys, sandy lithofacies typically had pore ice structures and the amount of excess ice was low. Therefore, the first lakes to develop during the early Holocene could not have been formed by degradation of ground ice. Rather, these lakes formed simply by the accumulation of water in depressions across the undulating surface. This mode of development of the first lakes is consistent with the initial basin flooding concept of Britton (1957), Gravis (1978), and Shur (1977), and alluded to by Billings and Peterson (1980), but absent from Everett (1980). Many of the deep lakes that exist today simply are remnants of these old primary lakes.

In the classical concept of thaw-lake development (alternatively primary stage in thick silt, Figure 28), the formation of waterbodies begins with the degradation of ice wedges in ice-rich upland terrain (Shumskiy and Vturin 1963, Tomirdiaro and Ryabchun 1978, Everett 1980). Degradation is most intense at the intersections of ice wedges, and deepening of the water in the troughs leads to the formation of small, deep (>1.5 m) ponds. A thaw bulb then develops under the deep water and the thaw lake expands laterally through both mechanical and thermal erosion. While this process is evident in extremely ice-rich, silty sediments, such as those on the Colville River Delta (Jorgenson et al. 1997, 1998) and the Seward Peninsula (Hopkins 1949), this stage of thaw-lake development is not evident on the sandy coastal plain to the east and west of the Colville. Generally, the surficial deposits in this area do not have the volume of excess ice to allow sufficient thaw settlement for large lake development. Even after years of intensive field surveys and mapping, we have not yet been able to identify any small, deep ponds on upland surfaces within the study

area that appear characteristic of this stage of development. Even severe disturbances in the region, such as the "peat roads" bladed during early oil exploration, have created only discontinuous deep thermokarst pits and high-centered polygons, not deep thaw ponds.

#### Lateral Expansion and Sediment Redistribution

After initial flooding, lake levels would have fluctuated in response to changes in precipitation and other components of the water balance, and shorelines would have expanded as a result of wave erosion. In the study area, we observed that the older and higher alluvial-marine deposits (capped with thin eolian silt) were eroding principally through mechanical erosion, leaving characteristic wave-cut benches. In these locations (i.e., G15.02, T12.10, T13.01, T13.08), the banks were 1.5–2 m high and comprised mostly of fine sands that typically had pore ice with low ice content. At these locations, the thawed portion of the bank had slumped only 0.2–0.3 m due to thaw settlement, indicating that thawing of ground ice contributes slightly to the loss of volume but was insufficient to account for lake formation.

Another indication that erosion was dominated by physical processes (vs. thermal erosion) was the presence of a shallow, sandy wave-cut bench at the foot of the eroding bluffs. Water depths increase slowly from <0.1 m near the bank to 0.3–0.5 m at a distance of tens of meters. Sediments near the wave-cut bank are dominated by fine to medium sands. In contrast, bank morphology that typically results from thermal erosion, such as thermal niches that develop from melting of ice rich layers, was uncommon and observed only in association with erosion of ice-rich materials in the centers of drained basins. Thus, the soil stratigraphy, shoreline morphology, and sediment composition all indicate that wave-dominated erosion and sediment transport are the dominant processes, not settlement of ice-rich terrain. In contrast, true thaw lakes in ice-rich terrain, such as the Colville River Delta, have steep shore profiles and water depths of 3–4 m within 10 m of the banks (Jorgenson et al. 1997).

Redistribution of sediments during early lake formation and expansion, with concomitant accumulation of fines and organics in the deepest

portions of the lakes, is key to the dynamics of later ice aggradation and degradation. Numerous investigators have observed the prominence of sandy sediments along the margins of large lakes and the accumulation of fine-grained sediments and organic material in the centers (Britton 1957, Carlson and Hussey 1962, Carson 1968, Tedrow 1969, Hunter and Carter 1985). In our study, sediments near the margins of ice-rich thaw basins were dominated by massive and layered sands (fine and medium sands), whereas the sediments of the ice-rich thaw basin centers were dominated by massive fines with organics, turbated fines with organics, and limnic fines (algal rich) (Figure 10). Also of interest is the fate of organic material from the eroding bluffs. Our sampling, as well as other studies (Britton 1957, Kidd 1990), revealed a continuum of peat block sizes away from the eroding bluff, apparently due to incorporation of organic material into the lake sediments. Peat sod mats may be incorporated into the adjacent sandy sediments or may roll and float along the shore, decompose, and become incorporated into bottom sediments in the basin center. Drifting ice also can redistribute peat toward deeper water (Shur 1977). Peat-rich sandy sediment was classified as turbated sand with organics and frequently was observed in the stratigraphic profiles of ice-poor basins (Figure 10). Most of the organic-rich silt that was observed appeared to contain algal material and small amounts of vascular plant parts, such as shredded leaves and seeds. This sorting of materials during the primary lake stage establishes the conditions for later differential ice segregation and development of ice wedges because particle size is fundamental to the development of ice (Figure 9). Shoreline erosion, lake expansion, and redistribution of sediments were partially recognized in the thaw-lake concept of Britton (1957), but are absent from the concepts of Billings and Peterson (1980) and Everett (1980).

#### Lake Drainage

The partial or complete drainage of lakes by stream capture, shoreline breaching, or coastal erosion is a dramatic and frequently observed phenomenon in some regions of the coastal plain (Cabot 1947, Hopkins 1949, Britton 1957, Carlson and Hussey 1962, Carson 1968, Tedrow 1969, Everett 1980). While the process of lake drainage

appears straightforward, differences in the extent and rate of drainage result in a wide range of subsequent basin water-levels and surface conditions. In addition, lakes levels can fluctuate over time due to climatic changes, or be drawn down slowly as the outlet channels progressively erode and lower the base levels of the lakes. The multiple processes causing water-level changes thus create a range of surface ages from initial exposure. This stage of basin development is incorporated in all conceptual models, although substantial uncertainty remains about the relative importance of tapping versus climatic change in causing lowered water levels in the lake basins.

Calibrated radiocarbon dates for two basal peat samples from *in-situ* peat layers on ice-rich thaw basin margins were 690–990, 1420–1720, and 5290–5580 BP. This fibrous sedge peat formed after drainage of the basin and, therefore, provides approximate dates for the drainage of the basin margins. These dates are consistent with dates of partially drained lakes near Barrow (Carson 1968), where most old basins have sequences of two to four ancient strands. Radiocarbon dating of these strands revealed that most are between 700 and 3500 years old. The radiocarbon dates for both our study area and Barrow, combined with the low numbers of recently drained lakes (thaw basins with bare or partially vegetated surfaces) in both our NPRA Study Area and on the coastal plain east of the Colville River (Jorgenson et al. 1997), indicates that lake drainage was most active 1000–4000 BP. The ages also indicate that it took considerable time from when the surface stabilized in the early Holocene to develop a drainage network with sufficient integration to tap the isolated lakes.

The extent of early primary lakes before drainage can be estimated from distribution of lacustrine deposits. Terrain unit mapping indicates that exposed lacustrine deposits cover 39.4% and freshwater lakes (deep and shallow lakes combined) currently cover 15.3% of the mapped area. Taken together they indicate that primary lakes once covered or affected 54.7% of the area.

Once drainage has occurred in the initial primary lakes, however, further drainage of the remaining lake is uncommon because the elevations of the current water surface and the bottoms of lakes are much lower. Further draining

of the isolated lakes would require much deeper incision of channels across the landscape and gradients are too low for such scouring. Currently, deep open lakes cover 8.9% of the mapped area. We believe that most of the deep lakes are the central remnants of the larger primary lakes after partial drainage.

The lack of drained lakes in our area compared with other areas of the coastal plain also suggests that drainage was more active in the past. No recently drained lakes (basins with bare sediments) were present in any of the small study areas, or anywhere in the entire NPRA Study Area. Similarly, mapping of the coastal plain east of the Colville River Delta (Jorgenson et al. 1997) revealed that lacustrine barrens (recently drained lakes with barren sediments) also were uncommon there (<0.1% of area). Drained lakes are more prevalent in some other areas, such as near the coast at Barrow (Sellman et al. 1975) and in the Colville River Delta (Jorgenson et al. 1997), presumably because stream gradients are higher or channel migration is more active. The lack of recently drained lakes in our study areas indicates that the drainage process was more active in the past and that once the surface water elevation has been lowered in the basins by the initial drainage, further drainage of the lower-lying lakes is much less likely.

#### Differential Ice Aggradation

Differences in sediment textures between the organic-rich silts in the deep centers of the lakes and the sandy sediments along the shallow margins provide the conditions for widely varying patterns and processes of ice development across the drained basins. The dynamics of the original active layer along the margins, and development of a thaw bulb in the centers of deep lakes, also greatly affect ice development.

Fundamental to the aggradation of ice in the centers of drained lakes is the size of the thaw bulb, which can develop where water depths are greater than 1.5–1.8 m on the Beaufort Coastal Plain. The size of the thaw bulb depends on both water depth and lake area and, therefore, can be highly variable. The size and sediment composition of the thaw bulb then determines the volume and structure of ground ice development after drainage and the subsequent extent of surface heaving of the

basin center. After drainage, frost can penetrate about 2–3 m deep the first year. After that, the ice aggrades downward into the unfrozen talik (thaw bulb) and an active layer is maintained at the surface. Because the freezing is downward into the talik, free water is able to migrate to the freezing front, and there is a large volume of material to refreeze, the volume of ice can be much larger than in basin margins where there is no thaw bulb. While organic-matrix, ataxitic, and reticulate ice structures are abundant, layered and vein ice often are associated with the downward freezing and heaving. Ataxitic, reticulate, and layered ice usually were associated with high (70–80%) ice contents (Figure 16). Mean ice volumes in the ice-rich centers in our study generally were in the 70–80% range throughout the 2–2.5 m cores, although volumes were highly variable.

This refreezing within the lake basin creates large, heaving forces that raise the surface. Most of the uplift probably occurs within the first 100 years following drainage. In addition to this uplift from ice segregation formed at the downward freezing front in the underlying thaw bulb, segregated ice formed during upward freezing associated with readjustment of the active layer and epigenetic wedge ice formed by thermal contraction at the surface also contribute to the volume expansion. Along our three surveyed transects, the tops of the ice-rich centers were 1.5–4 m above the bottoms of the ponds along the margins of the basin (Figures 6–8).

Under certain circumstances, pingo ice can form during freezing of water in coarse sediments within the closed talik that forms under the deep-water zone in a lake. This excess water is injected under pressure into the weakest sediments, where it freezes. During freezing, heaving forces create large ice-cored hills termed “pingos”. The domed surface is characterized by radial tension cracks, which result from the stretching of the surface sediments, and by abundance of large ice wedges that can form in the easily deformed organic-rich sediments. At one exposure that we sampled where the pingo was 4.5 m above the surrounding surface, the surface of the pingo had 3.5 m of organic-rich lacustrine sediments. The ice structures were dominated by organic matrix and layered ice, with prevalent vertical veins, presumably formed during heaving and

deformation of the sediments. Pingo ice was encountered at a depth of 3.5 m. We have not included pingos in our simplified conceptual model of lake-basin evolution, however, because they are uncommon features that develop under special circumstances related to thaw bulb size and hydraulic conductivity of the soil materials.

Along the margins of drained basins, ice aggradation is affected by the thickness of the original active layer below the shallow margins of the lake, the sandy sediments, and surface organic accumulation. Where water is shallower than 1.5–1.8 m, pond sediments will have a thin (0.6–0.8 m) layer that thaws during the summer. This active layer is important because it constrains the volume of material where new segregated ice can develop by upward freezing. After drainage, initial freezing and readjustment of the active layer occurs within a winter or two after drainage. Thereafter, the active layer slowly thins as the thermal regime readjusts to increased vegetation development and organic accumulation. During this readjustment, thin layers of ataxitic and reticulate ice are prevalent, but the volume of segregated ice is limited by the thickness of the original active layer under the lakes, and the presence of sandy sediments near to the surface. The accumulation of organic material at the surface adds to the soil volume and affects the structure and volume of ice that develops. In our sampling, the cumulative thickness of organics near the surface averaged 0.66 m in the ice-rich margins of basins. Ice structures in massive organics are dominated by organic-matrix and layered ice (Figure 9), and mean ice volume in massive organics was 78% (Figure 16). The underlying massive and layered sand (very fine to medium sands) usually had predominantly pore ice (Figure 9), and mean ice volume was 44% (Figure 16). Our limited surveys revealed that the ice-rich margins of basins were only 0.7 to 1.5 m higher than the bottoms of shallow ponds in adjacent ice-poor basins (Figures 6–8). Because the heaving of the soils in these sandy margins is low, they persist as areas of low-lying and usually flooded terrain.

The development of ice wedges in newly exposed sediments, or under shallow water that freezes to the bottom during winter, makes an important contribution to ice volume and greatly

affects surface water movement. Development of the wedges follows a progression of micro-topographic changes that includes (1) nonpatterned ground, (2) disjunct low rims, (3) low density, low-centered polygons, (4) high density, low-centered polygons, and finally (5) mixed high- and low-centered polygons. Analyses of floodplain development on the Colville River indicates that disjunct rims take ~300–500 years to develop, low density, low-centered polygons take ~500–1500 years, and complete development of high density low-centered polygons can take 1500–3000 years (Jorgenson et al. 1998). At the last stage, the syngenetic ice wedges typically occupy ~20% of the volume of the top 2 m of soil (Jorgenson et al. 1998). On some old and unusual surfaces on sand sheets with thin (<1 m) loess caps near Prudhoe Bay and Kuparuk, wedge ice volumes as high as 40% have been estimated for locations (Burgess et al. 1999). Development of this wedge ice deforms the adjacent sediments and contributes to heaving of the land surface. While wedge ice can develop in both the sandy margins and organic-rich centers, they probably develop larger volumes in the centers because of the more easily deformed organic-rich sediments. We used the amount of polygon development as the key characteristic for differentiating ice-poor basins (nonpatterned and disjunct polygons) from ice-rich basins (low density, low-centered polygons; high density low-centered polygons, and mixed high- and low-centered polygons).

#### Secondary Development of Lakes within Basins

While the secondary development of waterbodies within the ice-rich basins is complicated by the large variation in sediment and ground ice, we have identified two main types of waterbodies that can reoccupy the drained basins: (1) small shallow infilling ponds caused by impoundment of water in the low-lying margins of the basin and (2) deeper, larger lakes created by thawing of the organic- and ice-rich materials in the center. These differences, based on the evaluation of sediment characteristics, photogrammetric analysis of lakeshore erosion, and photo-interpretation of waterbody characteristics, are discussed below.

We attribute the formation of numerous small, shallow ponds around the margins of the drained

basins primarily to impoundment of water in the lowest portions of the basins. Because of ice aggradation in the organic-rich silts and heaving of the basin centers, the margins of the basins usually become the lowest portion of the landscape and, therefore, collect water. Initially, the water that collects in these low-lying areas can form large ponds, but over time accumulation of organic matter and ice aggradation in the surrounding tundra cause the ponds to become subdivided and reduced in size. During this stage, organic material is added both as algal material in diatomaceous benthic mats within the shallow ponds and as fibrous sedge peat in the wet tundra surrounding to the ponds. At the later stages of development, these ponds become shallow because of thick accumulations of diatomaceous benthic algae at the bottom, and tend to have round-to-polygonized margins and abrupt vegetated margins.

This concept of pond paludification, or infilling, is supported by evidence from soil stratigraphy and photogrammetric analysis of 1945 and 2001 photography. First, soil stratigraphy of adjacent soils frequently revealed buried layers of well-preserved, olive-green limnic material, indicating that the ponds have been infilling and shrinking. Second, the thickness of the tundra organic mat (mean = 0.66 m in ice-rich basins) is similar to the difference in the elevation between the pond bottom and the adjacent wet tundra surface (Figure 6–8). This accumulation of organic matter helps elevate the surface, creates surface conditions favorable for plant growth and development of wet and moist tundra vegetation, and helps create the abrupt peat margins along most small ponds. Continued accumulation of both benthic algal mats and sedge peat helps transform the ponds from aquatic sedge marsh along the margins to wet sedge meadow tundra and causes the pond area to shrink. During the accumulation of this organic matter, the depth of the active layer decreases so that some of this organic material becomes incorporated into the permafrost. Reinforcing this process is aggradation of both segregated and wedge ice. Ice volumes in ice-rich basins are highly variable (ranging from 40 to 80%) in the top 2 m, but decrease to 40–50% below 2 m (Figure 15). In addition, at an intermediate stage of ice-wedge polygon development, wedge ice associated with

low-centered, low-relief polygons contribute ~10% to the volume of materials near the surface. Our limited data indicates surface accretion (through organic matter and ice accumulation) averages 0.4 m/1000 yr (Figure 17) and, therefore, is sufficiently rapid to help modify the shoreline configuration. Finally, photogrammetric analysis of 1945 and 2001 photography indicates that the pond margins are remarkably stable and erosion is minimal. The lack of evidence of thermokarst processes further supports the conclusion for the paludification process. If the ponds were of thermokarst or erosional origin, they would have measurable rates of retreat (particularly if due to thermokarst), organic mat fragments would be scattered across sandy bottom sediments from erosion, and algal remains would not be present in the adjacent soils.

In contrast to the shallow, infilling ponds formed through basin impoundment and paludification, some of the deep lakes in the centers of the basins are true thaw lakes formed from the degradation of ice-rich materials in the centers. In some situations, ponds that have developed near the ice-rich centers can cause lateral thermokarst of the basin centers. Evidence for this thermokarst includes the occurrence of (1) abundant excess ice in the degrading soils at the eroding front, (2) an abrupt face (0.7–1.0 m) where the shoreline is eroding, (3) organic mats slumping over the eroding shoreline that indicate material is being lost by thawing of ice and not by mechanical erosion of organic and inorganic material, (4) abundant fragments of organic mat strewn across the sandy lake sediments, and (5) scalloped shorelines created by more rapid degradation of wedge ice that leaves the rounded polygon centers protruding into the lake.

These true thaw lakes are constrained to the centers of old basins. Based on photogrammetric analysis of erosion rates, we estimated the larger, secondary thaw lakes to be 2000–3000 years old. While secondary thaw lakes resemble primary catchment lakes, because they both can be large with deep centers, the remnant primary lakes typically have shorelines with multiple fringes of beach ridges and old shorelines that indicate drainage and not expansion, or have wide sandy wave-cut benches with gradual water depths.

The formation of new thaw lakes developing in the original deep portion of the primary lakes (ice-rich centers) does form a one-time cycle, in the sense that a primary lake was drained, formed ice-rich material, and returned to a thaw lake. Once the lakes form from thermokarst in the centers, however, the surface water elevations are low relative to the surrounding older surfaces. Thus, future drainage and continuation of the cycle is unlikely. In addition, this "cycle" is different from the traditional concept where old, higher terrain outside the basins degrades to form lakes, the lakes drain and return to an elevated surface by ice aggradation in a continual march of basins across the landscape.

#### Basin Stabilization

In the final stage of basin development, the shallow, infilling ponds and deeper thermokarst lakes that have developed in the former ice-rich centers are persistent features. The infilling ponds are too small, and the shorelines have too much thick fibrous peat, to be susceptible to wave erosion. They continue to accrue diatomaceous benthic material in the bottoms and peat along the shores. While the surface around the ponds can be susceptible to minor ice wedge degradation, ice wedge degradation results only in high-centered polygons. Thermokarst is insufficient to initiate large ponds because of the low thaw settlement properties of the organic and sandy material in the basin margins. The large abundance of old, indistinct basins with numerous small, rounded ponds indicates that this stage is very stable (Figure 4).

The deep thermokarst lakes that have reoccupied the basin centers also are persistent features. Because the lakes have reoccupied the lower centers, and the sandy margins have developed thick organic accumulations that have low thaw settlement properties, the possibility of further tapping and drainage is low. While basins adjacent to large, meandering rivers are susceptible to tapping and complete drainage, most thermokarst lakes in the basin centers away from the larger floodplains have little likelihood of further lowering because elevational gradients are too low.

The ice-rich centers of basins do not all degrade into ponds, however. Many basins have

persistent, domed centers surrounded by the small, shallow, infilling ponds. At the oldest recognizable stage, the domed centers become indistinct and the infilling ponds are reduced to tiny round remnants. While some ice-rich centers have degrading ice wedges, the resulting high-centered polygons appear to have sufficient peat accumulation to resist degradation into larger ponds.

#### Summary

Our examination of the development of lake basins, based on topographic profiles, stratigraphic analysis, radiocarbon dating, and photogrammetric analysis, reveals that the evolution of lakes and basins on the coastal plain is more complex and less cyclic than previous investigators have envisioned. In our interpretation, lakes over most of the Beaufort Coastal Plain were formed initially by flooding of low-lying catchments during the beginning of the Holocene, when the surface stabilized and climate ameliorated from the cold and dry conditions of the late Pleistocene. Radiocarbon dating of basal peat on upland surfaces indicates that stabilization of the sand sheet that is ubiquitous across the region mostly occurred 8000–10,000 years ago. Undulations of the surface formed the conditions for the creation of primary lakes as water collected in low-lying, isolated catchments. Radiocarbon dating of basal organic-rich sediments in basin centers indicates most lake basins are <9000 years old. Mechanical shoreline erosion and differential transport of sediments in the lakes lead to the accumulation of sandy sediments around the margins and organic-rich silts (disseminated peat and algae) in the centers. This reworking of the original sandy deposits and sediment redistribution is required to allow sufficient development of ground ice and the subsequent development of thaw lakes. In contrast, the old upland surfaces do not have sufficient ice volumes to support formation of large thermokarst lakes; instead degradation leads only to the formation of thermokarst troughs and high-centered polygons.

Drainage of the lakes, through the development of a drainage network over a lengthy period, creates the conditions for permafrost expansion in newly exposed sediments. Radiocarbon dating of basal peat in drained basins and lacustrine strands indicates most basins

drained 1000–4000 years ago. After drainage, the nature and volume of ground ice that develops in the newly exposed sediments are highly variable across the basins, depending on the texture of the redistributed sediments and on thaw bulb development in the former lakes. The general trend, however, has been for little ice aggradation in the sandy sediments along the margins where thaw bulbs did not develop, and abundant ice aggradation in the organic-rich centers where thaw bulbs had developed under deep water. This differential ice accumulation controls the pattern of the secondary development of waterbodies within the drained basins.

Secondary development of waterbodies within the basins is associated with two distinct processes: (1) impoundment of water in the low-lying margins of the basins and subsequent modification of waterbodies through paludification or infilling, and (2) thermokarst of ice-rich materials in the centers of the basins. The shallow infilling ponds around the margins are caused by large-scale hydrologic changes that have resulted from the doming of the ice-rich centers by up to 4 m. As a result, previously drained margins become the lowest portions of the landscape and thus catchments for standing water. These ponds are then reinforced and modified by the accumulation of fibrous sedge peat in the saturated soil surrounding the ponds, and ice aggradation under the thinning active layers, which raise the vegetated surface around the pond margins by 0.5–1.5 m. Over time, paludification of the surface through the accumulation of peat in the wet tundra and diatomaceous benthic material in the ponds causes the ponds to become dissected and reduced in size. The common occurrence of buried limnic layers at the base of the sedge peat around the margins of the old basins provides strong evidence for this process. Because these shallow infilling ponds result from paludification, and not thermokarst, they are stable and persistent features of the landscape.

In contrast to this paludification and pond development around the margins, true thaw lakes can develop in the centers of old basins where the sediments are organic silts and particularly ice-rich. These sediments have 20 to 30% excess ice extending below 2.5 m (and probably are much more ice rich below the limit of our coring), and

thus have sufficient thaw settlement to allow thaw ponds to develop. Photogrammetric analysis indicates erosion rates along these ice-rich center are relatively high compared with other terrain units. Based on the rate of erosion, the thaw lakes may be as much as 2000–3000 years old and, in many instances, are continuing to erode into the remaining ice-rich centers of the basins. Eventually, these thaw lakes reoccupy the former centers of the primary catchment lakes. Once the lakes have thawed the ice-rich centers, however, expansion greatly slows because the soils in the surrounding basin margins have thick surface organic layers and are underlain by sandy sediments with little excess ice. While the ice-rich centers have degraded in many basins, in others the domed centers have remained stable because of thick surface organic accumulations.

In the final stage of basin development, the basins become highly stable and persistent features of the landscape. The small ponds continue to infill and shrink, but at slow rates. The larger thaw ponds, when present, expand rapidly only as far as the ice-rich centers, then stabilize and become prone to paludification. Because these thaw lakes reoccupy the original centers, they form at the lowest elevations on the landscape and additional tapping and drainage is unlikely. At the latest stage of development, these basins become indistinct and are recognizable only as concentrations of tiny, shallow ponds with thick diatomaceous benthic mats encircled by low, indistinct basin rims.

The concept that thaw lakes continually migrate across the surface of the coastal plain and that soil materials go through a complete cycle from old upland surfaces, to thaw lakes, and then back to conditions similar to the original is not consistent with our analysis of surficial materials and patterns of ground-ice development. Furthermore, the rates at which lakes erode and drain, and at which ground ice develops, are too slow for the entire landscape to have been reworked by multiple cycles during the Holocene. Instead, we conceptualize a landscape that is altered by climatic changes, formation of large primary lakes in low-lying catchments, reworking of surficial materials in the primary lakes, development of integrated drainage networks, drainage, and differential development of ground ice within the drained basins. This sequential

development of unique circumstances formed the conditions for the secondary development of small infilling ponds along the sandy margins of the basins and occasional thaw lakes in the ice-rich silty centers within the large lacustrine basins that currently are widespread across the landscape today.

## THAW SETTLEMENT AND TERRAIN SENSITIVITY

### THAW SETTLEMENT

We developed estimates of potential thaw settlement based on (1) the amount of excess segregated ice, (2) the amount of wedge ice, and (3) the depth of soil incorporated into the active layer to achieve a new thermal equilibrium following disturbance (Figure 29). Although ice distribution was highly variable both vertically and horizontally, there were some clear differences in potential for thaw settlement among terrain units. These differences allowed us to make some generalizations that should be useful for assessing the sensitivity of the terrain to disturbance and for predicting surface responses during future rehabilitation of oilfield facilities. In the following section, we present (1) the assumptions used in the developing estimates of potential thaw settlement, and (2) estimates of thaw settlement associated with segregated ground ice obtained from field samples, followed by (3) conceptual models of the overall potential for thaw settlement in the different terrain units.

We assumed a maximum thaw depth of 1.1 m, after re-establishment of thermal equilibrium in the active layer following a severe surface disturbance (removal of the vegetated surface). This assumption was based on the maximum thaw depths observed at scraped reserve pits in the Kuparuk Oilfield (Burgess et al. 1999). However, substantially lower thaw depths (mean  $\pm$  1 SD) were observed at other disturbed sites, including the S.E. Eileen Exploratory Well Site ( $80 \pm 16$  cm, 8 years after scraping to the tundra surface [Bishop et al. 1999]); the 2U oil spill ( $46 \pm 7$  cm, 7 years after scraping to the tundra surface [Cater et al. 1999]), and the DS-30 overburden caps ( $60\text{--}70$  cm, 7 years after capping [Cater and Jorgenson 1996]). In addition, the mean thaw depth in sediments underlying shallow ponds in the

Kuparuk Oilfield was  $60 \pm 31$  cm (Burgess et al. 1999). Given this range of values, we believe that 1.1 m represents the maximum likely extent of settlement that could occur after severe surface disturbance. For comparison, we also calculated thaw settlement using an expected thaw depth of 0.8 m, which is more typical for disturbed sites without impounded surface water.

Assuming an equilibrium active layer depth of 1.1 m, the maximum thaw settlement from the thermal degradation of segregated ice is calculated to be  $0.77 \pm 0.42$  m in alluvial-marine deposits,  $0.37 \pm 0.41$  m in ice-rich thaw basin centers,  $0.34 \pm 0.38$  m in ice-rich thaw basin margins, 0.28 m in ice-poor thaw basin centers,  $0.09 \pm 0.10$  m in ice-poor thaw basin margins, and  $0.12 \pm 0.05$  m in eolian inactive sand (Figure 29). Based on an active-layer readjustment to 0.8 m, which is more typical of non-flooded highly disturbed surfaces, thaw settlement is expected to be  $0.51 \pm 0.40$  m in alluvial-marine deposits (includes alluvial terraces),  $0.27 \pm 0.29$  m in ice-rich thaw basin centers,  $0.19 \pm 0.23$  m in ice-rich thaw basin margins, 0.22 m in ice-poor thaw basin centers,  $0.05 \pm 0.05$  m in ice-poor thaw basin margins, and  $0.10 \pm 0.07$  m in eolian inactive sand. The relatively low predicted thaw settlement for the ice-rich centers appears at first to be inconsistent with our concept that this is the most ice-rich terrain unit. The thaw basin centers are unusual, however, in that they usually contain accumulations of sand within the top 1.5 m that help stabilize the active layer. In addition, organic soils have smaller thaw strain values without heavy loading. Substantial uncertainty is associated with some of the estimates, particularly for ice-rich thaw basin centers, because of high organic content and spatial variability in the volume of segregated ice.

The relative abundance of ice wedges is of particular importance to the progression of thermokarst. Although we did not make a systematic assessment of ice wedge volumes across terrain types in the NPRA, we were able to rely on estimates based on an exposure at Mine Site F (M. T. Jorgenson, pers. obs.), trenching studies (Everett 1980), and air photo analysis of the Kuparuk Oilfield (Burgess et al. 1999). While there usually is a thin layer of frozen soil between the active layer and the ice wedges that helps

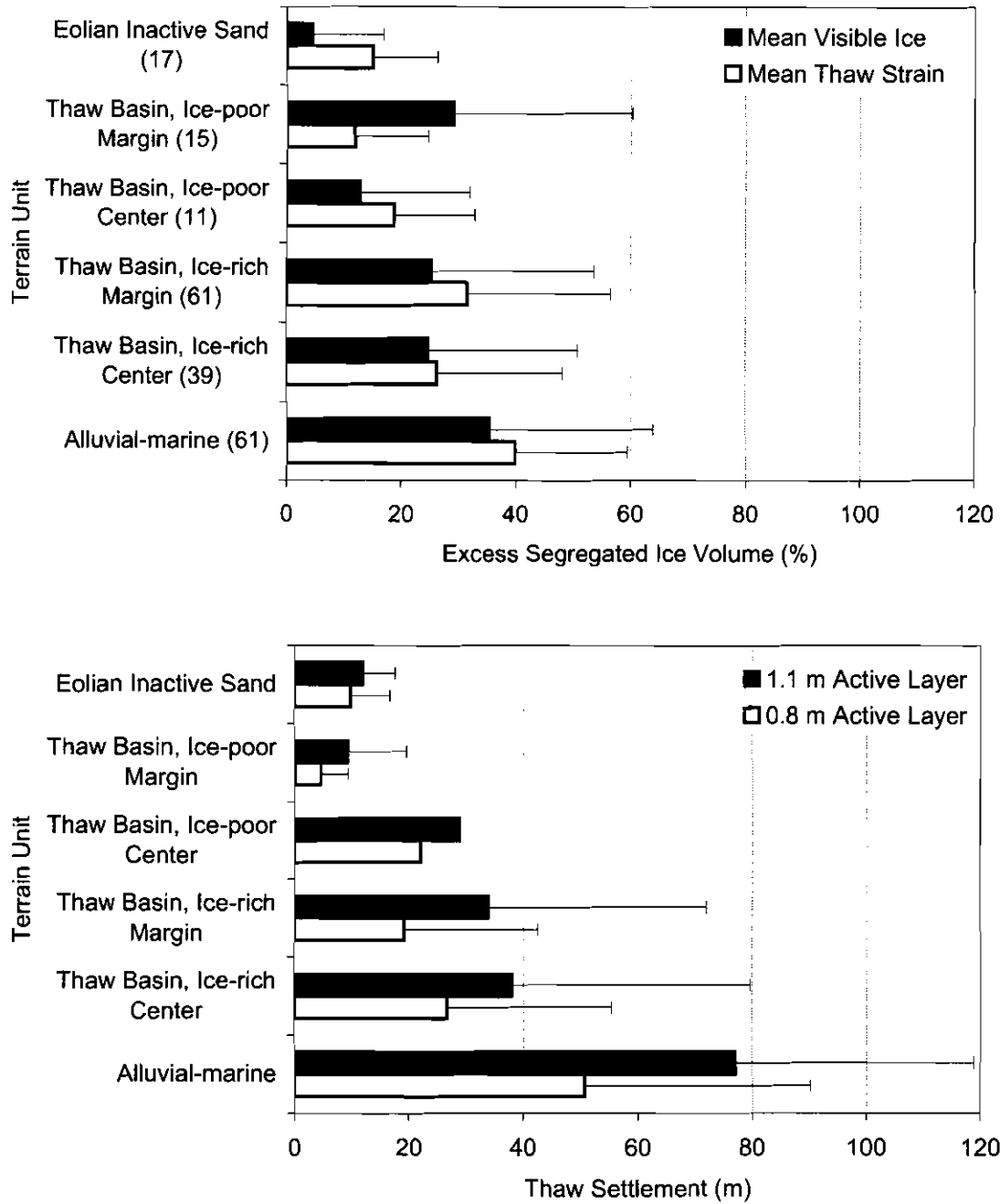


Figure 29. Estimates of mean excess segregated ice volume ( $\pm$ SD) and potential thaw settlement due to melting of segregated ice ( $\pm$ SD) in each of six terrain units in the Northeast Planning Area, NPRA, 2002.

protect ice wedges from small disturbances or climatic fluctuations, disturbances that removes most of the vegetation or exposes substantial soil usually cause ice wedges to degrade. Large increases in heat flux associated with severe disturbance lead immediately to thaw settlement, leading to impoundment of water, which in turn leads to increased soil heat flux and additional thermokarst. These processes are likely to cause complete or nearly complete loss of the ice within months to years. The degradation can be further accelerated if surface water movement is channelized through the degrading trough network. Based on a compilation of the available data, we predict that all wedge ice in the top 2 m would be lost, leaving a highly polygonized surface. We predict that the loss of volume due to thawing of ice wedges will be about 20% for old alluvial-marine deposits, 15% for ice-rich thaw basin centers with well-developed, low-centered polygons, and negligible for ice-poor thaw basins.

Observations based on aerial photographs, exposure on lakeshores, and soil cores suggest that thaw settlement potential in ice-rich thaw basin centers may have been underestimated in this analysis. At a number of core sample sites (4 of 7), we did not encounter the underlying sand sheet due to the depth of lake deposits and ice present in the soil column. The development of secondary thaw lakes and subsequent thermal erosion of ice-rich thaw basin centers observed on aerial photograph and in the field suggest that a total subsidence of 2 to 4 meters is possible follow a severe surface disturbance.

#### CONCEPTUAL MODEL OF THERMOKARST DEVELOPMENT

Based on the differences in potential thaw settlement among terrain units, we developed a simple conceptual model of terrain response to severe disturbances, such as scraping of the surface or complete removal of the vegetative cover. In this model, the degradation of both segregated and wedge ice results in a mosaic of polygonal troughs and high-centered polygons, depending on terrain type (Figure 30). In alluvial-marine deposits, which have the highest volumes of both segregated ice and wedge ice, the thermokarst micro-topography will be highly irregular, with deep and shallow troughs and prominent

high-centered polygons. Because these terrain units occupy slopes and gently rolling uplands between thaw basins, some surface drainage and lowering of the water table are likely. In most cases, these changes will result in most of the polygon centers being above the water table. In ice-poor thaw basins, where segregated ice volumes are much lower and wedge ice is negligible, the thermokarst topography is likely to be relatively uniform after only a moderate amount of thaw settlement. However, the surface will remain flooded because this terrain unit occurs in the lowest portions of the basins. Thus, even minor thermokarst will result in the development of large, shallow ponds.

This conceptual model is consistent with thermokarst we have observed at numerous sites. At sites on alluvial plains, such as Sinclair Exploratory Well Site (Bishop 1998) and N.W. Eileen State No. 1 (Jorgenson and Cater 1993), thermokarst, settlement and partial drainage have resulted in a highly prominent relief mosaic with deep and shallow water in troughs and patches of wet and moist tundra on the tops of the polygon centers. At a site in an ice-rich thaw basin near the Prudhoe Bay Operations Center, where ~20 cm of gravel was left after gravel removal in 1988, thermokarst has resulted in shallow water over the tops of polygon centers and deep water in the troughs (Kidd and Rossow 1998). At the S.E. Eileen Exploratory Well Site (Bishop 1999), on an inactive floodplain of the Kuparuk River, thermokarst has resulted in mostly moist and wet high-centered polygons with only limited occurrences of shallow water in troughs. This site is somewhat unusual in being located next to the riverbank, so drainage is better than on most flat inactive floodplains. At sites in ice-poor thaw basins, such as the abandoned access road to Drill Site 3K in the Kuparuk Oilfield (Cater and Jorgenson 1993) and the abandoned access road to the Operations Storage Pad in Prudhoe Bay (Kidd and Rossow 1998), where thick gravel was removed from the tundra surface, thermokarst has resulted in level flooded topography with shallow ponds or wet meadows, depending on water depth.

While the estimated potential thaw settlement differs substantially among terrain units, the high variability in the estimates indicates that predicting the amount of settlement at a specific location is

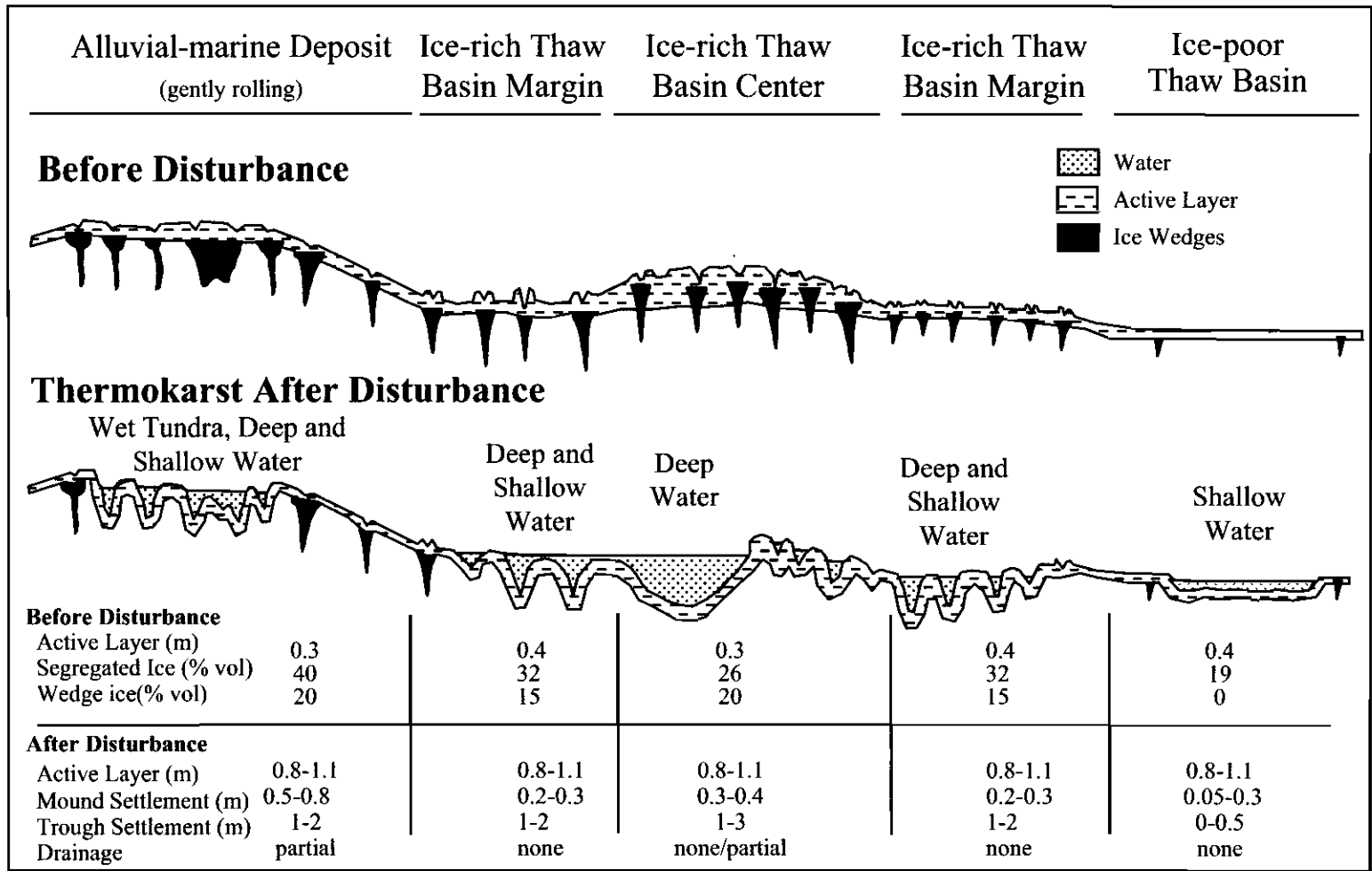


Figure 30. Conceptual model of thermokarst development after disturbance of ice-rich permafrost on the dominant terrain units in the Northeast Planning Area, NPRA, 2002. Typical values are given for active layer depths before and after severe disturbance, volume of excess segregated and wedge ice before disturbance, estimated thaw settlement of mounds or flat surfaces from degradation of segregated ice and settlement in troughs due to degradation of wedge ice, and potential for drainage.

difficult. Furthermore, the amount of settlement is sensitive to the amount of thaw that occurs as the active layer reaches a new thermal equilibrium and to the extent of surface disturbance. The value of 0.8 m for the equilibrium thaw depth was based on thaw depths found at some of the more highly disturbed sites, however, the actual increase in thaw depth is likely to vary considerably among sites. While assumptions can be made to parameterize thermal models for predicting initial adjustment of the active layer to disturbance, long-term predictions of equilibrium conditions are more tenuous because numerous factors associated with the energy balance interact during changes in vegetation, soil moisture, and hydrology as the surface settles (Hinzman et al. 1997). While these factors make modeling and prediction difficult, we believe our conceptual model based on knowledge of the complexity of ground ice characteristics and simple assumptions of active layer behavior provides reasonable predictions of surface change after severe disturbance. The concepts are consistent with observations at a number of disturbed sites, helping to validate use of the model for land management decisions on the Beaufort Coastal Plain.

#### IMPLICATIONS FOR LAND MANAGEMENT

Differences in thermokarst potential in the various terrain units have important implications for land management, facility planning, and the development of site-specific rehabilitation strategies appropriate to changing site conditions after abandonment. However, evaluation of probable surface responses to specific management decisions must also consider the nature and extent of water impoundment after thaw settlement, as affected by slope position on the landscape. Some management implications are discussed below.

Appropriate siting of facilities, roads, and cross-drainage structures in relation to thaw stability of the terrain can greatly reduce potential problems with both thermokarst and roadbed performance. While the thaw settlement estimates indicate eolian inactive sand sheets and ice-poor thaw basins have the most thaw stable conditions for development activities, the evaluation is complicated by landscape position. For example, ice-poor thaw basins have low potential for thaw settlement, but even with little settlement these

areas can become uniformly flooded after severe disturbance because of their position in basins. In contrast, thaw settlement estimates are high for upland alluvial-marine deposits, but these are probably better surfaces for road and pad placement because they are better drained. Good drainage reduces the need for cross-drainage structures, with their associated impacts. Culverts on this type of terrain can cause localized ice-wedge degradation, but the relatively good off-site drainage tends to minimize propagation of the disturbance. Siting facilities on crests, which lack much water movement, is preferable to siting facilities on slopes because alteration of drainage can have substantial affect on surface water channelization and subsequent degradation of ice wedges. Perhaps the least favorable terrain for siting facilities is ice-rich thaw basin centers. While estimates indicate that thaw settlement should be small because of the thick organic accumulations at the surface, this terrain is susceptible to severe degradation as indicated by the prevalence of deep thaw ponds in these deposits.

Estimates of potential thaw subsidence (along with other landscape characteristics) also are crucial for directing oil spill response and cleanup operations. Oil spill cleanup often requires weighing the potential risk of thermokarst against the cost and efficiency of the oil recovery techniques. Knowledge of the thaw stability can reduce the risk of thermokarst in ice-rich terrain if appropriate precautions are taken during cleanup operations. In addition, cleanup efficiency can be enhanced in thaw-stable terrain by the use of more aggressive techniques.

Knowledge of the thermokarst potential of a site can help to ensure the long-term success of rehabilitation efforts and enhance the functional relevance of the rehabilitation plan. Thermokarst is a natural process that is integral to development of the landscape on the Beaufort Coastal Plain (Britton 1967, Billings and Peterson 1980, Walker et al. 1980), increases the terrain diversity, and can provide useful wildlife habitat (Murphy and Anderson 1993). Thus, thermokarst can be incorporated into the rehabilitation strategies as a natural phenomenon that can increase habitat diversity and productivity. However, minimization

of thermokarst propagation beyond the disturbed site should remain an important objective.

When evaluating revegetation options, thermokarst must be recognized as a critical factor because it fundamentally alters soil and hydrologic conditions. If the goal is a moist, well-drained site that is thermally stable, thermokarst can be prevented by adding overburden material (typically about ~0.6 m fines and organics) (Jorgenson 1986). If a patchy mosaic with varying soil and hydrologic conditions is desired, then thermokarst can be allowed to proceed. Plant materials adapted to aquatic, wet, or moist conditions can then be selected depending on the rehabilitation strategy and the amount of thermokarst expected.

If gravel removal is selected as a rehabilitation technique, thermokarst will greatly affect the outcome of the effort. Areas on eolian inactive sand and alluvial-marine deposits will likely become diverse mosaics of well-drained, high-centered polygons and flooded troughs. Over time, areas in ice-rich thaw basin margins probably would become large shallow ponds, while areas in ice-rich thaw basin centers would likely become large deep ponds. Areas in ice-poor thaw basins would likely become shallow ponds in wet areas, or uniform wet or moist meadows in better-drained areas.

## CONCLUSIONS

Data on ice structures, lithofacies, and terrain units from 31 cores (2–3 m deep) and 7 exposures, revealed strong relationships that can be used to partition the variability in ice distribution across the landscape based on the surface terrain classification. Large differences were found in the frequency of occurrence of the various ice structures among lithofacies: pore ice was nearly always associated with massive, inclined, and layered sands; lenticular and ataxitic ice were most frequently associated with massive and layered fines, and organic matrix ice was usually found in massive and layered organics and limnic fines. Reticulate ice was broadly distributed among fine and organic lithofacies. Among surface terrain units, mean ice volumes were highest in alluvial-marine deposits (71%), intermediate in ice-rich thaw basin margins (64%) and ice-rich thaw basin centers (64%), and lowest in ice-poor

thaw basin margins (60%) and eolian inactive sand (54%).

Geomorphic processes associated with lake-basin development primarily control the spatial distribution of ground ice in the region. Evaluating terrain stability in the study area required both assessing the volume and distribution of different forms of ground ice, and estimating the rates of landscape change due to lakeshore erosion. Photogrammetric analysis of waterbody changes in three small study areas was used to evaluate shoreline erosion during a 46–56 year period from 1945–1955 to 2001. For the three areas combined, 0.74% of the total land area was lost to shoreline erosion over 46–56 years. The mean annual erosion rate for the three areas, expressed as a percentage of total area, was 0.04%/yr. Mean rates of shoreline retreat were slow (0.02 m/yr), even for large, deep lakes (0.08 m/yr). The maximum rate of shoreline retreat we observed was 0.8 m/yr. Deep lakes (mean = 26.1% of area) were much more common than shallow lakes (mean = 6.6%), and shallow lakes typically were small (<5 ha).

Recent degradation of ice wedges was evident from both field observations and photogrammetric analysis. Field observations at nine polygonal troughs found indicators (e.g. water in pits, drowned tussocks) that indicate the degradation has been recent, although coring indicated that degradation did not occur in 2001. Photogrammetric analysis of waterbody characteristics found the extent of flooding in upland areas was 1.7% in 1945 only, 4.3% in 2001 only, and 0.1% in both years. In lowland areas, flooding covered 16.2% of the terrestrial area in 1945 only, 3.5% in 2001 only, and 2.7% in both years. Overall, flooding covered 13.7% of the terrestrial area (larger waterbodies excluded) in 1945 only, 3.8% in 2001 only, and 2.2% in both years. We attributed the increase in newly flooded areas (3.8%) in 2001 (a dry year) not present in 1945 (wet year) to be the result of thermokarst. The low percent of areas flooded in both years indicates the thermokarst has caused a redistribution of water from round flooded polygon centers to linear degrading troughs.

We developed a conceptual model of lake-basin evolution that enhances our understanding of landscape stability. The model is based on interpretation of aerial photographs and

data collected during the 2001 and 2002 field seasons, including topographic profiles, stratigraphic analysis, ice structure studies, radiocarbon dating, and regional comparisons. Our analysis revealed that the process of lake development on the coastal plain is more complex and less cyclic than previous investigators believed. Our revised conceptual model for the portion of the Beaufort Coastal Plain underlain by extensive sand sheets includes (1) initial flooding of primary lakes, (2) lateral expansion and sorting and redistribution of lacustrine sediments, (3) lake drainage, (4) differential ice aggradation in silty centers and sandy margins, (5) formation of secondary thaw lakes in the centers and infilling of small ponds along the margins, and (6) basin stabilization. While we still used the term "thaw basins" for our terrain unit mapping to be consistent with earlier mapping efforts, our revised conceptual models indicates these are better termed lacustrine or drained-lake deposits and not thaw-lake deposits.

Effective land management on permafrost-dominated terrain requires terrain-specific estimates of the potential for thermokarst following disturbance. Knowledge of the likely extent of thaw settlement across the landscape is essential for evaluating facility locations and effective rehabilitation planning, including surface treatments and selection of appropriate plant materials. This information also is valuable in planning and directing effective and efficient oil spill cleanup and remediation activities. We developed estimates of the amount of thaw settlement likely to occur in various terrain types after severe disturbance. Based on an active-layer readjustment to 0.8 m, which is typical of non-flooded highly disturbed surfaces, mean ( $\pm$  SD) thaw settlement is expected to be  $0.51 \pm 0.40$  m in alluvial-marine deposits,  $0.27 \pm 0.29$  m in ice-rich thaw basins centers,  $0.19 \pm 0.23$  m in ice-rich thaw basin margins, 0.22 in ice-poor thaw basin centers,  $0.05 \pm 0.05$  m in ice-poor thaw basin margins, and  $0.10 \pm 0.07$  m in eolian inactive sand. Based on data from the literature and our field observations, we estimated that all wedge ice in the top 2 m would be lost, leaving a highly polygonized surface. The expected loss of volume due to thawing of ice wedges is about 20% for old alluvial-marine deposits, 15% for ice-rich thaw

basins with well-developed, low-centered polygons, and negligible for ice-poor thaw basins.

#### LITERATURE CITED

- Billings, W. D., and K. M. Peterson. 1980. Vegetational change and ice-wedge polygons through the thaw lake cycle in Arctic Alaska. *Arctic and Alpine Research* 12: 413-432.
- Bishop, S. C., J. G. Kidd, T. C. Cater, L. J. Rossow, and M. T. Jorgenson. 1998. Land rehabilitation studies in the Kuparuk Oilfield, Alaska, 1997. Twelfth annual report prepared for ARCO Alaska, Inc., Anchorage, AK, by ABR, Inc., Fairbanks, AK. 66 pp.
- Bishop, S. C., J. G. Kidd, T. C. Cater, L. J. Rossow, and M. T. Jorgenson. 1999. Land rehabilitation studies in the Kuparuk Oilfield, Alaska, 1998. Thirteenth annual report prepared for ARCO Alaska, Inc., Anchorage, AK, by ABR, Inc., Fairbanks, AK. 72 pp.
- Black, R. F., and W. L. Barksdale. 1949. Oriented lakes of northern Alaska. *Journal of Geology* 57: 105-118.
- Brierley, G. J. 1991. Floodplain sedimentology of the Squamish River, British Columbia: relevance of element analysis. *Sedimentology* 38: 735-750.
- Britton, M. E. 1957. Vegetation of the Arctic tundra. Pages 67-113 in H. P. Hansen, ed. *Arctic Biology: 18th Biology Colloquium*. Oregon State University Press, Corvallis.
- Brown, J. 1968. An estimation of the volume of ground ice, Coastal Plain, Northern Alaska. U. S. Army Cold Regions Research and Engineering Laboratory, Hanover, NH.
- Brown, J., and N. A. Grave. 1979. Physical and thermal disturbance and protection of permafrost. U.S. Army Cold Regions Research and Engineering Laboratory, Hanover, NH. Special Report 79-5. 42 pp.
- Burgess, R. M., E. R. Pullman, T. C. Cater, and M. T. Jorgenson. 1999. Rehabilitation of salt-affected land after close-out of reserve pits. Third Annual Report prepared for ARCO Alaska, Inc., Anchorage, AK, by ABR, Inc., Fairbanks, AK. 48 pp.

*Literature Cited*

- Cabot, E. C. 1947. The northern Alaskan coastal plain interpreted from aerial photographs. *Geographical Review* 37: 639–648.
- Carson, C. E. 1968. Radiocarbon dating of lacustrine strands in arctic Alaska. *Arctic* 21: 12–26.
- Carson, C. E., and K. M. Hussey. 1962. The oriented lakes of arctic Alaska. *Journal of Geology* 70: 417–439.
- Carter, L. D., R. M. Forester, and R. E. Nelson. 1984. Mid-Wisconsin through early Holocene changes in seasonal climate in northern Alaska. Pages 20-22 in American Quaternary Association, Eighth Biennial Meeting, Program and Abstracts. Boulder, CO.
- Carter, L. D., and J. P. Galloway. 1985. Engineering-geologic maps of northern Alaska, Harrison Bay quadrangle. Pages 85–256 in U.S. Geological Survey, Open File Report 85-256
- Carter, L. D., J. A. Heginbottom, and M. Woo. 1987. Arctic Lowlands. Pages 583-628 in *Geomorphic Systems of North America. Centennial Special Volume, 2 ed.*, U.S. Geological Society of America, Boulder, CO.
- Cater, T. C., and M. T. Jorgenson. 1993. Land rehabilitation studies in the Kuparuk Oil Field, Alaska, 1992. Seventh annual report prepared for ARCO Alaska, Inc., and Kuparuk River Unit, Anchorage, AK, by Alaska Biological Research, Fairbanks, AK. 38 pp.
- Cater, T. C., and M. T. Jorgenson. 1996. Land rehabilitation studies in the Kuparuk Oilfield, Alaska, 1995. Tenth annual report prepared for ARCO Alaska, Inc., and the Kuparuk River Unit, Anchorage, AK, by ABR, Inc., Fairbanks, AK. 72 pp.
- Cater, T. C., and M. T. Jorgenson. 1999. Assessing damage from hydrocarbons and cleanup operations after crude oil spills in Arctic Alaska. Final report prepared for ARCO Alaska, Inc., and Kuparuk River Unit, Anchorage, AK, by ABR, Inc., Fairbanks, AK. 80 pp.
- Crory, F. E. 1973. Settlement associated with the thawing of permafrost. Pages 599-607 in *Proceedings 2nd International Conference on Permafrost, Yakutsk, U.S.S.R., North American Contribution*. National Academy of Sciences, Washington, D.C.
- Emers, M., and J. C. Jorgenson. 1997. Effects of winter seismic exploration on tundra vegetation and the soil thermal regime on the Arctic National Wildlife Refuge, Alaska. Pages 443-456 in R. M. M. Crawford, ed. *Disturbance and Recovery in Arctic Lands, An Ecological Perspective*. Kluwer Academic Publishers, Dordrecht, Netherlands.
- Everett, K. R. 1980. Landforms. Pages 14-19 in D. A. Walker, K. R. Everett, P. J. Webber, and J. Brown, eds. *Geobotanical atlas of the Prudhoe Bay region, Alaska*. U.S. Army Cold Regions Research and Engineering Laboratory, Hanover, NH. Report 80-14.
- Fetcher, N. and Shaver, G. R. 1983. Life histories of tillers of *Eriophorum vaginatum* in relation to tundra disturbance. *Journal of Applied Ecology* 71:131-148.
- Gravis, G. F. 1978. Cyclic nature of thermokarst on the Marine Plain in the Upper Pleistocene and Holocene. Pages 282-287 in *Proceedings of the 3rd International Permafrost Conference*. National Research Council of Canada, Ottawa, ON.
- Hinkel, K. M., F. E. Nelson, Y. Shur, J. Brown, and K. R. Everett. 1996. Temporal changes in moisture content of the active layer and near-surface permafrost at Barrow, Alaska, U.S.A.: 1962–1994. *Arctic and Alpine Research* 28: 300–310.
- Hinzman, L. D.; Goering, D. J.; Kinney, T. C., and Li, S. 1997. Numeric simulation of thermokarst formation during disturbance. Pages 191-212 in Crawford, R. M. M., ed., *Disturbance and Recovery in Arctic Lands, An Ecological Perspective*. Kluwer Academic Publishers, Dordrecht, Netherlands.

- Hobbie, J. E. 1984. E. Pendleton, Project Officer, National Coastal Ecosystems Team, Div. Bio. Services, R. and D., USFWS/USDI, Wash. DC.20240. The ecology of tundra ponds of the arctic coastal plain: a community profile. USFWS/OBS, FWS/OBS-83/25. 52 pp. Plastic-spiral bound.
- Hopkins, D. M. 1949. Thaw lakes and thaw sinks in the Imuruk Lake area, Seward Peninsula, Alaska. *Journal of Geology* 57: 119-131.
- Hopkins, D. M., K. McDougall, and E. M. Brouwers. 1981. Microfossil studies of Pelukian and Flaxman deposits, Alaska coast of the Beafort Sea. Appendix G, Pages 230-239 in P. A. Smith, R. W. Hartz, and D. M. Hopkins, eds. Offshore permafrost studies and shoreline history as an aid to predicting offshore permafrost conditions: National Oceanic and Atmospheric Administration, Environmental Assessment of the Alaskan Continental Shelf, Annual Reports of Principal Investigators, April 1979-March 1980. Volume 4.
- Johnson, G. H. 1981. Permafrost Engineering Design and Construction. National Research Council of Canada, Ottawa, Canada. 540 pp.
- Johnson, L. A. 1981. Revegetation and selected terrain disturbances along the Trans-Alaska Pipeline, 1975-1979. U. S. Army Cold Regions Research and Engineering Laboratory, Hanover, CRREL Report 81-12. 115 pp.
- Jorgenson, M. T. 1986. Biophysical factors affecting the geographic variability of soil heat flux. M.S. Thesis, Univ. of Alaska, Fairbanks, 109 pp.
- Jorgenson, M. T. 1986. Revegetation of gravel pads: ARCO 3 Pad and 3K Spur Road, Kuparuk Oilfield, Alaska. Annual report prepared for ARCO Alaska, Inc., Anchorage, AK, by Alaska Biological Research, Fairbanks, AK. 29 pp.
- Jorgenson, M. T., and T. C. Cater. 1993. Site assessments and remedial planning for five exploratory well sites on the Arctic Coastal Plain. Final report prepared for ARCO Alaska, Inc., Anchorage, AK, by Alaska Biological Research, Inc., Fairbanks, AK. 82 pp.
- Jorgenson, M. T., and J. G. Kidd. 1991. Land rehabilitation studies in the Prudhoe Bay Oilfield, Alaska, 1990. Annual report prepared for ARCO Alaska, Inc., Anchorage, AK, by Alaska Biological Research, Inc., Fairbanks, AK. 57 pp.
- Jorgenson, M. T., K. Kielland, B. S. Schepert, and J. B. Hyzy. 1991. Bioremediation and tundra restoration after a crude-oil spill near Drill Site 2U, Kuparuk oilfield, Alaska, 1990. Annual report prepared for ARCO Alaska, Inc., Anchorage, AK, by Alaska Biological Research, Inc., Fairbanks, AK. 82 pp.
- Jorgenson, M. T., L. W. Krizan, and M. R. Joyce. 1991. Bioremediation and tundra restoration after an oil spill in the Kuparuk Oilfield, Alaska, 1990. Pages 149-154 in Proceedings of the 14th Annual Arctic and Marine Oil Spill Technical Program. Environ. Canada, Ottawa, ON.
- Jorgenson, M. T., E. R. Pullman, T. Zimmer, Y. Shur, A. A. Stickney, and S. Li. 1997. Geomorphology and hydrology of the Colville River Delta, Alaska, 1996. Final report prepared for ARCO Alaska, Inc., Anchorage, AK, by ABR, Inc., Fairbanks, AK. 148 pp.
- Jorgenson, M. T.; Roth, J. E.; Emers, M.; Schlentner, S.; Swanson, D. K.; Pullman, E.; Mitchell, J., and Stickney, A. A. 2003. An ecological land survey for the Northeast Planning Area of the National Petroleum Reserve - Alaska, 2002. Final Report prepared for ConocoPhillips, Alaska, Inc., Anchorage, AK by ABR, Inc., Fairbanks, AK. 128 pp.
- Jorgenson, M. T., and Y. Shur. 1999. An integrated terrain unit approach to analyzing landscape change on the Colville Delta, northern Alaska, U.S.A. Page 13 in J.

- Brown, ed., An International Workshop on Arctic Coastal Dynamics. Marine Biological Laboratory, Woods Hole, MA. 31 pp. (abstract).
- Jorgenson, M. T., Y. Shur, and H. J. Walker. 1998. Factors affecting evolution of a permafrost dominated landscape on the Colville River Delta, northern Alaska. Pages 523-530 in A. G. Lewkowicz, and M. Allard, eds. Proceedings of Seventh International Permafrost Conference. Universite Laval, Sainte-Foy, Quebec. Collection Nordicana, No. 57.
- Jorgenson, M. T., T. Zimmer, E. R. Pullman, Y. Shur, and J. E. Roth. 1998. Evolution of soils on the permafrost-dominated landscape of the Colville River Delta, northern Alaska. Page 103 in Proceedings of Society of Wetland Scientists, 19th Annual Meeting. Society of Wetland Scientists, (abstract)
- Kidd, J. G. 1990. The effect of thaw-lake development on the deposition and preservation of plant macrofossils—a comparison with the local vegetation. M. S. Thesis, Univ. of Alaska, Fairbanks. 48 pp.
- Kidd, J. G., L. L. Jacobs, T. C. Cater, and M. T. Jorgenson. 1997. Ecological restoration of the North Prudhoe Bay State No. 2 exploratory drill site, Prudhoe Bay Oilfield, Alaska, 1995. Final Report prepared for ARCO Alaska, Inc., Anchorage, AK, by ABR, Inc., Fairbanks, AK. 36 pp.
- Kidd, J. G., and L. J. Rossow. 1998. Land rehabilitation studies in the Prudhoe Bay Oilfield, Alaska 1997. Final report prepared for ARCO Alaska, Inc., Anchorage, AK, by ABR, Inc., Fairbanks, AK. 51 pp.
- Kreig, R. A., and R. D. Reger. 1982. Air-photo analysis and summary of landform soil properties along the route of the Trans-Alaska Pipeline System. Alaska Division of Geological and Geophysical Surveys, Fairbanks, AK. Geologic Report 66. 149 pp.
- Kudryavtsev, V. A. 1977. Fundamentals of frost forecasting in geological engineering investigations. U.S. Army Cold Regions Research and Engineering Laboratory, Hanover, NH. Draft Translation 606.
- Lawson, D. E. 1986. Response of permafrost terrain to disturbance: a synthesis of observations from northern Alaska, U.S.A. Arctic and Alpine Research 18: 1-17.
- Livingstone, D. A. 1954. On the orientation of lake basins. American Journal of Science 252: 547-554.
- McFadden, T. T., and F. L. Bennet. 1991. Construction in Cold Regions—A Guide for Planners, Engineers, Contractors, and Managers. John Wiley and Sons, Inc., New York, NY.
- Miall, A. D. 1978. Lithofacies types and vertical profile models in braided river deposits: a summary. Fluvial Sedimentology 5: 597-604.
- Miall, A. D. 1985. Architectural-element analysis: a new method of facies analysis applied to fluvial deposits. Earth Sciences Review 22: 261-308.
- Murphy, S. M., and B. A. Anderson. 1993. Lisburne terrestrial monitoring program: the effects of the Lisburne development project on geese and swans, 1985-1989. Final report prepared for ARCO Alaska, Inc., Anchorage, AK, by Alaska Biological Research, Inc., Fairbanks, AK. 202 pp.
- Murton, J. B., and H. M. French. 1994. Cryostructures in permafrost, Tuktoyaktuk coastlands, western arctic Canada. Canadian Journal Earth Science 31: 737-747.
- Osterkamp, T. E. 2003. A thermal history of permafrost in Alaska. Proceedings of Eighth International Conference on Permafrost. Zurich, Switzerland. In Press.
- Osterkamp, T.E., V.E. Romanovsky. 1996. Characteristics of changing permafrost temperatures in the Alaskan Arctic, U.S.A. Arctic and Alpine Research 28: 267-273.

- Ping, C. L., G.J. Michaelson, J.M. Kimble, and L.R. Everett. 2002. Organic carbon stores in Alaska Soils. *in* J.M. Kimble, R. Lal, and R.F. Follett. *Agricultural Practices and Policies for Carbon Sequestration in Soil*, CRC Press, New York.
- Pollard, W. H., and H. M. French. 1980. A first approximation of the volume of ground ice, Richards Island, Pleistocene Mackenzie Delta, Northwest Territories, Canada. *Canadian Journal of Earth Sciences* 17: 509–516.
- Rawlinson, S. E., ed. 1983. Guidebook to permafrost and related features, Prudhoe Bay, Alaska. Guidebook 5, Fourth International Conference on Permafrost. Alaska Division of Geological and Geophysical Surveys, Fairbanks, AK. 177 pp.
- Rawlinson, S. E., ed. 1993. Surficial geology and morphology of the Alaskan Central Arctic Coastal Plain. Alaska Division of Geological and Geophysical Surveys, Fairbanks, AK. Report of Investigations 93-1. 172 p.
- Romanovsky, V.E., T.E. Osterkamp, G.S. Tipenko, D.O. Sergueev 2002. Influence of Climate and Environmental Factors on the Thermal and Moisture Regimes of the Active Layer and Permafrost. Unpublished data available at [http://www.gi.alaska.edu/snowice/Permafrost-lab/proj\\_influ/pr\\_influ.html](http://www.gi.alaska.edu/snowice/Permafrost-lab/proj_influ/pr_influ.html).
- Sellman, P. V., J. Brown, R. I. Lewellen, H. McKim, and C. Merry. 1975. The classification and geomorphic implications of thaw lakes on the Arctic Coastal Plain, Alaska. U.S. Army Cold Regions Research and Engineering Laboratory, Hanover, NH. Research Report 344. 21 pp.
- Shumskiy, P. A., and B. I. Vturin. 1963. Underground Ice. Proceedings Permafrost International Conference. National Academy of Sciences. Washington, D.C.
- Shur, Y. L. 1977. Thermokarst (on thermal-physical fundamentals of process). Moscow, "Nedra", 98 pp. (In Russian)
- Shur, Y. L. 1988. Upper permafrost and thermokarst. Moscow, "Nauka", 210 pp. (In Russian)
- Soil Survey Division Staff (SSDS). 1993. Soil survey manual. U.S. Dept. Agriculture, Washington, D.C. Handbook No. 18. 437 pp.
- Tedrow, J. C. F. 1969. Thaw lakes, thaw sinks, and soils in northern Alaska. *Biuletyn Peryglacjalny* v. 20: 337–345.
- Tomirdiaro, S. V., and Ryabchun, V. K. 1973. Lake thermokarst on the Lower Anadysr Lowland. Pages 100–104 *in* Proceedings 2nd International Conference on Permafrost, USSR Contributions. National Academy of Sciences, Washington, D.C.
- Walker, D. A. 1981. The vegetation and environmental gradients of the Prudhoe Bay region, Alaska. Unpublished report by University of Colorado, Boulder.
- Walker, D. A., D. Cate, J. Brown, and C. Racine. 1987. Disturbance and recovery of arctic Alaskan tundra terrain: a review of investigations. U.S. Army Cold Regions Research and Engineering Laboratory, Hanover, NH. CRREL Rep. 87-11.
- Webber, P. J., and J. D. Ives. 1978. Damage and recovery of tundra vegetation. *Environmental Conservation* 5: 171–182.
- Webber, P. J., P. C. Miller., F. S. Chapin III, and B. H. McCown. 1980. The vegetation: pattern and succession. Pages 186-218 *in* J. Brown, P. C. Miller, L. L. Tieszen, and F. L. Bunnell, eds. *An arctic ecosystem, the coastal tundra at Barrow, Alaska*. Dowden, Hutchinson, and Ross, Stroudsburg, PA.
- Weller, G. E., and B. Holmgren. 1974. The microclimates of the Arctic tundra. *Journal of Applied Meteorology*. 13: 854–862.

